DOE Hydrogen Program
2022 Annual Merit Review and Peer Evaluation Meeting
June 6 – 8, 2022

ElectroCat 2.0
(Electrocatalysis Consortium)

Piotr Zelenay
Los Alamos National Laboratory

Deborah Myers
Argonne National Laboratory

Project ID: FC160

This presentation does not contain any proprietary, confidential, or otherwise restricted information

Overview

Timeline

- **Start date**: Oct 1, 2020
- **End date**: Sep 30, 2023

Budget

- **FY22 funding total planned:** $3M
- **Planned FY23 funding:** $3M

Barriers

- **A. Cost** (catalyst)
- **D. Activity** (catalyst; MEA)
- **B. Durability** (catalyst; MEA)
- **C. Power density** (MEA)

Laboratory – PI

Los Alamos National Laboratory

Los Alamos NATIONAL LABORATORY – Piotr Zelenay

Argonne National Laboratory

Argonne NATIONAL LABORATORY – Deborah Myers

National Renewable Energy Laboratory

NREL NATIONAL RENEWABLE ENERGY LABORATORY – Derek Vigil-Fowler

Oak Ridge National Laboratory

OAK RIDGE National Laboratory – David Cullen

Relevance and Goals

Heavy-Duty Transportation Fuel Cell Targets (2025)

- Durability: 25,000 hour lifetime
- 68% peak efficiency
- $80/kW fuel cell system cost
- **Overall Target:** 2.5 kW/g_{PGM} power (1.07 A cm^{-2} current density at 0.7 V after 25,000 hour-equivalent accelerated durability test)

Electrolyzer Stack Goals (2025)

- Durability: 80,000 hour lifetime
- 70% efficiency at 3 A cm^{-2}
- $100/kW
- **Overall Target:** $2/kg H_2 over 80,000 hour lifetime

End-of-consortium Goals:

Fuel Cell: H_2-air performance of ≥ 100 mA/cm^2 at 0.8 V and ≥ 500 mA/cm^2 at 0.675 V at beginning of test (BOT) and ≥ 80 mA/cm^2 and ≥ 400 mA/cm^2 after 30,000 AST cycles (0.6 V to OCV, 3 s each, H_2-air), respectively, under integral conditions for a PEMFC with a PGM-free oxygen reduction catalyst

Electrolyzer: 2.5-fold increase, from 0.2 A/cm^2 to 0.5 A/cm^2 at 1.8 V and reduction in the voltage loss at a reference current density of 0.2 A/cm^2 from 0.2 mV/h to 0.1 mV/h with alkaline-exchange membrane electrolyzer using a PGM-free oxygen evolution catalyst

Approach: FY21 ElectroCat Milestones

FY21 Milestone Name/Description	End Date	Type	Status
Initiate ElectroCat 2.0 consortium and establish baseline durability of most active national lab core-team catalyst, e.g., LANL's CM-PANI-Fe-C(Zn), (AD)Fe-N-C, or ANL's Fe(N-C), using differential cell and ElectroCat AST protocol.	12/31/2020	Quarterly Progress Measure (Regular)	**Completed**, see 2021 AMR
Apply machine-learning techniques to develop surrogate regression models of ANL high-throughput data for metal loading and ratio of two different carbon-nitrogen precursors and propose 12 validation experiments. After synthesis and activity evaluation of the 12 suggested catalysts using high-throughput methodology, update surrogate regression model and provide a 'Design of Experiments' suggesting 6 additional, optimized "next-step" experiments for optimizing catalyst activity.	3/30/2021	Quarterly Progress Measure (Regular)	**Completed**, see 2021 AMR
Demonstrate H_2-air performance with PGM-free cathode MEA of ≥ 60 mA/cm^2 at 0.8 V and ≥ 300 mA/cm^2 at 0.675 V at beginning-of-test and ≤ 50% and ≤ 40% loss in current density at 0.8 V and 0.675 V, respectively, after 30,000 AST cycles under differential conditions.	06/30/2021	Quarterly Progress Measure (Regular)	**Completed** see slide #6
LTE: Achieve 0.7 A cm^{-2} with LTE electrolyzer PGM-free anode at 1.85 V and degradation rate ≤ 0.15 mV/h with pure water reactant.	09/30/2021	Annual Milestone (Regular)	**Completed** see slides #32, #33, #58
PEFC: Hydrogen-oxygen performance: Achieve PGM-free cathode MEA performance in an H_2-O_2 fuel cell of 35 mA cm^{-2} at 0.90 V (*iR*-corrected) at 1.0 bar partial pressure of O_2 and cell temperature 80 °C.	09/30/2021	Annual Milestone (Regular) GPRA	**Exceeded**, 38 mA cm^{-2}; see 2021 AMR

FY21 Q3 ORR QPM: 'Single-Zone' Fe-N-C Catalyst

Cathode: *ca.* 4.0 mg cm^{-2}, 'single-zone' Fe-N-C catalyst, 1700 sccm, 1.0 bar air partial pressure, 100% RH; **Anode:** 0.3 mg_{Pt} cm^{-2} Pt/C, H_2, 700 sccm, 1.0 bar H_2 partial pressure, 100% RH; **Membrane:** Nafion® 211; **Cell:** differential, 5 cm^2, **Temperature:** 80 °C. **Durability Testing:** square-wave cycle from (OCV-0.01) V to 0.60 V

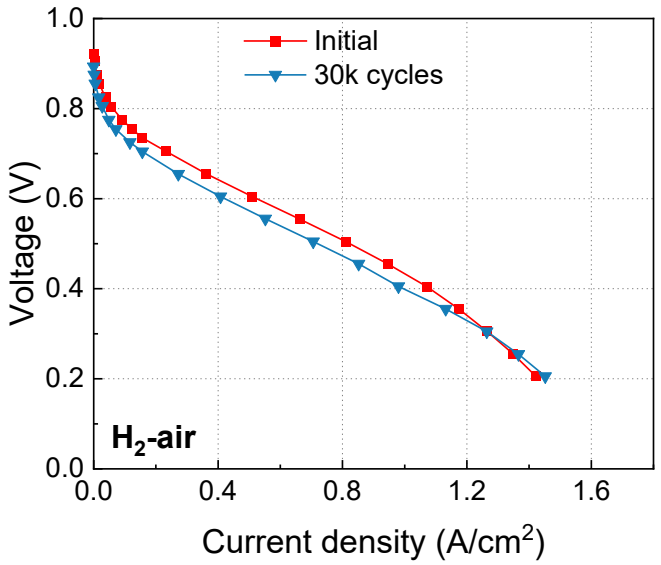

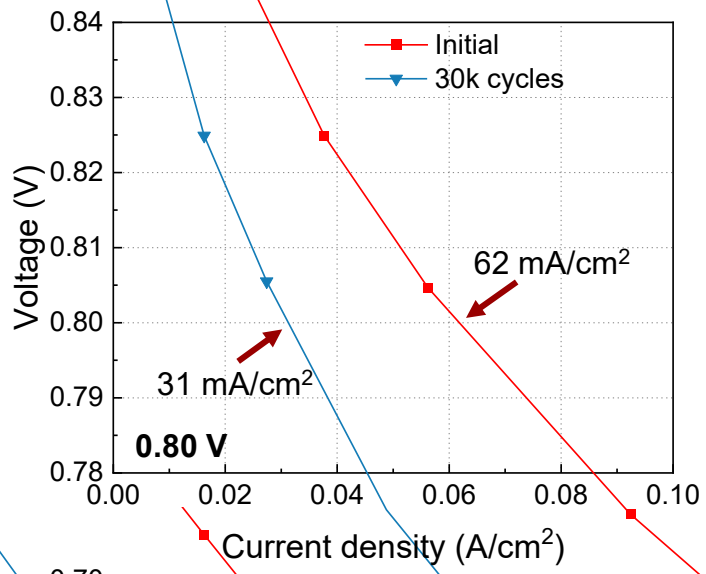

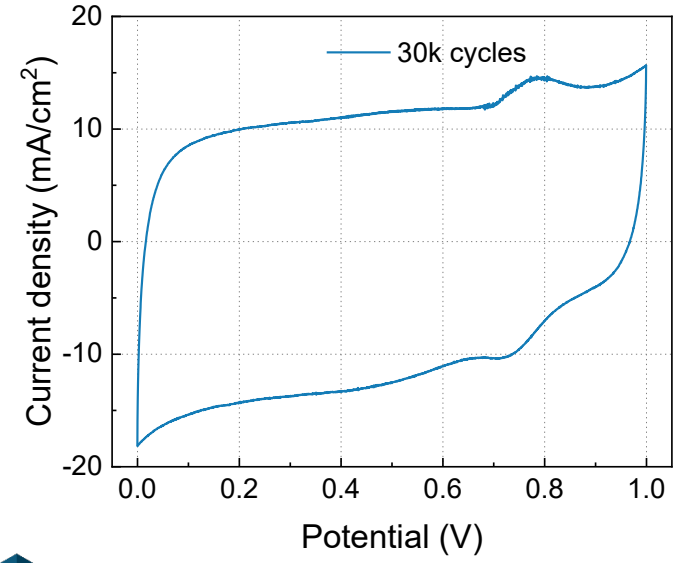

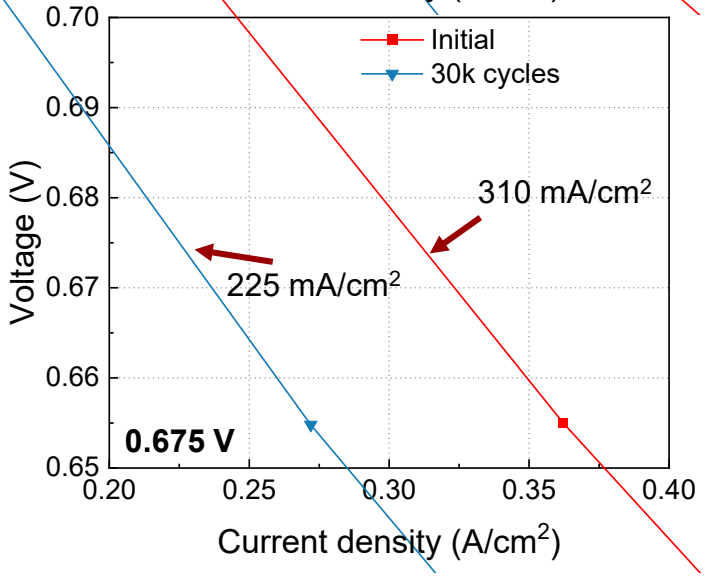

Voltage (V)	i (mA/cm²) Initial	i (mA/cm²) 30k	Loss (%)
0.80	62	31	49
0.675	310	225	27

- Test interrupted after 100, 1k, 2k, 3k, 6k, 10k, 15k and 23k cycles to adjust cycling upper voltage limit
- **49%** and **27%** loss of initial current density at 0.80 V and 0.675 V, respectively
- **Highlight:** Have met the first ever milestone that combines PGM-free catalyst activity and durability targets at two fuel cell voltages (performance controlled by either the ORR kinetics or O_2 mass transport)

Approach: FY22 ElectroCat Milestones

Milestone Name/Description	Criteria	End Date	Type	Status
Multi-objective optimization scoring for combining four DFT-based activity and stability descriptors	Develop and apply Pareto-optimization scoring approach for DFT-derived activity (1) and stability descriptors (3) to existing library to show currently calculated “Pareto front”. (LANL)	12/31/2020	Quarterly Progress Measure (Regular)	**Completed** see slide #19
ORR catalyst performance in H_2-air fuel cell	Current density of ≥ 65 mA cm^{-2} at 0.80 V and ≤ 50 mV voltage loss at 0.80 A cm^{-2} after 30,000 catalyst AST cycles. (LANL, ANL)	3/31/2022	Quarterly Progress Measure (Regular)	**Completed** see slide #8
Synthetic route for high-throughput synthesis to achieve improved ORR activity and durability	Provide ‘Design of Experiment’ surrogate model for higher-dimensional high-throughput experimental data by identifying two “next-step” experiments based on available activity/durability data; synthesize and test ORR activity and stability of materials suggested by ML task. (LANL, ANL)	6/30/2022	Quarterly Progress Measure (Regular)	**On track** see slides #16, #17, #18
ORR catalyst performance in H_2-air fuel cell	Current density of ≥ 75 mA cm^{-2} at 0.80 V and ≤ 50 mV voltage loss at 0.80 A cm^{-2} after 30,000 catalyst AST cycles. (LANL, ANL)	9/30/2022	Annual Milestone (Regular)	**Completed** see slide #8
OER performance of Ni-based mixed metal oxide in liquid electrolyte	OER current density in an aqueous alkaline electrolyte of 10 mA cm^{-2} at a potential of ≤ 1.55 V *vs*. RHE (*iR*-free) and no more than 1.0 mV/h potential loss during ≥ 48 h durability test at 10 mA cm^{-2}. (LANL, ANL)	9/30/2022	Annual Milestone (Regular)	**Completed** see slide #40

Approach: FY22 ElectroCat Go/No-Go Decisions

Name	Description	Criteria	Date	Status
ElectroCat Go/No-Go	PGM-free catalyst performance and durability in H_2-air fuel cell.	Current density of ≥ 65 mA cm^{-2} at 0.80 V at beginning of test and ≤ 50 mV voltage loss at 0.80 A cm^{-2} after 30,000 catalyst AST cycles.	12/31/2020	**Go** see slide #8
AEM LTE testing of multi-transition-metal oxides	Go/no-go on multi-transition-metal oxides for next-quarter AEM LTE testing; selection based on performance in alkaline liquid electrolyte (three-electrode electrochemical cell).	OER activity of ≤ 1.60 V vs. RHE (*iR*-free) at 10 mA cm^{-2} at beginning of test in liquid alkaline electrolyte (three-electrode electrochemical cell).	3/31/2022	**Go** see slide #30
Theory: Multi-objective optimization	Go/no-go on Me-N-C active site structures without the OH ligand based on Pareto-optimization scoring approach.	New active site structures found with Pareto-optimization score superior to that of HO-FeN_4 zig-zag edge structure.	6/30/2022	**On track** see slide #19

FY22 ElectroCat ORR Milestone: 'Dual Zone' Catalyst Synthesized in H_2

Cathode: *ca.* 4.0 mg cm^{-2}, H_2-synthesized'dual-zone' Fe-N-C catalyst, 1700 sccm, 1.0 bar air partial pressure, 100% RH; **Anode:** 0.3 mg_{Pt} cm^{-2} Pt/C, H_2, 700 sccm, 1.0 bar H_2 partial pressure, 100% RH; **Membrane:** Nafion® 211; **Cell:** differential, 5 cm^2, **Temperature:** 80 °C. **Durability Testing:** square-wave cycle from (OCV-0.01) V to 0.60 V

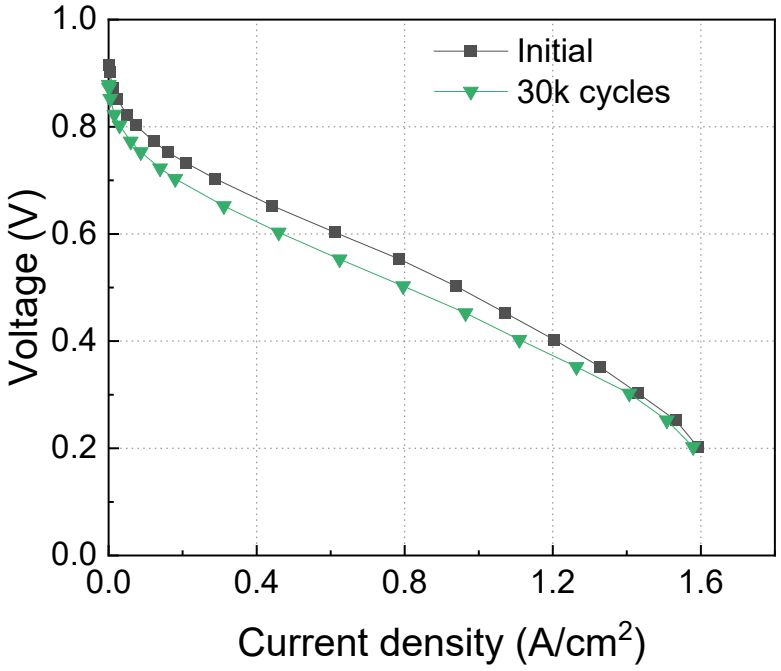

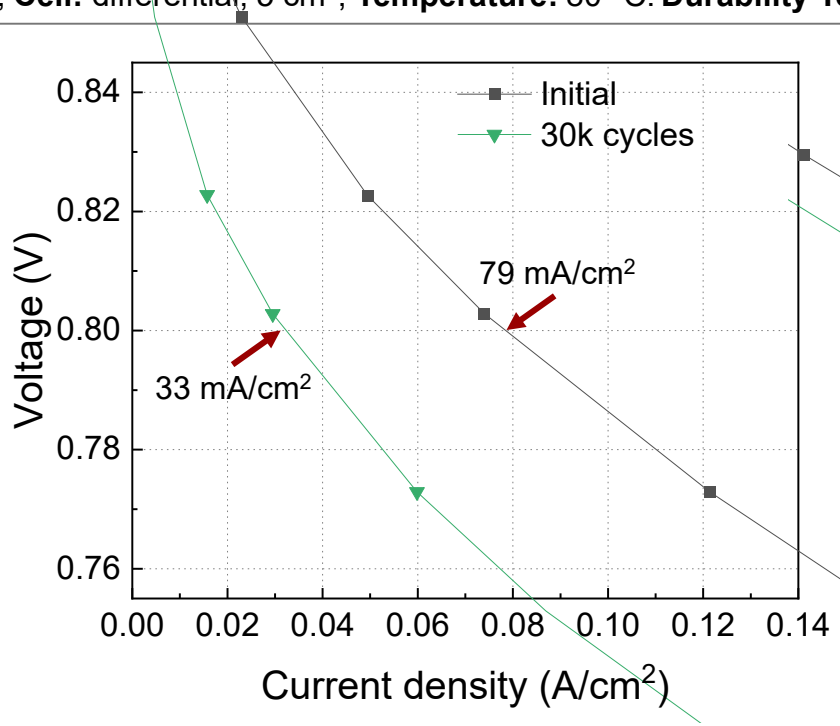

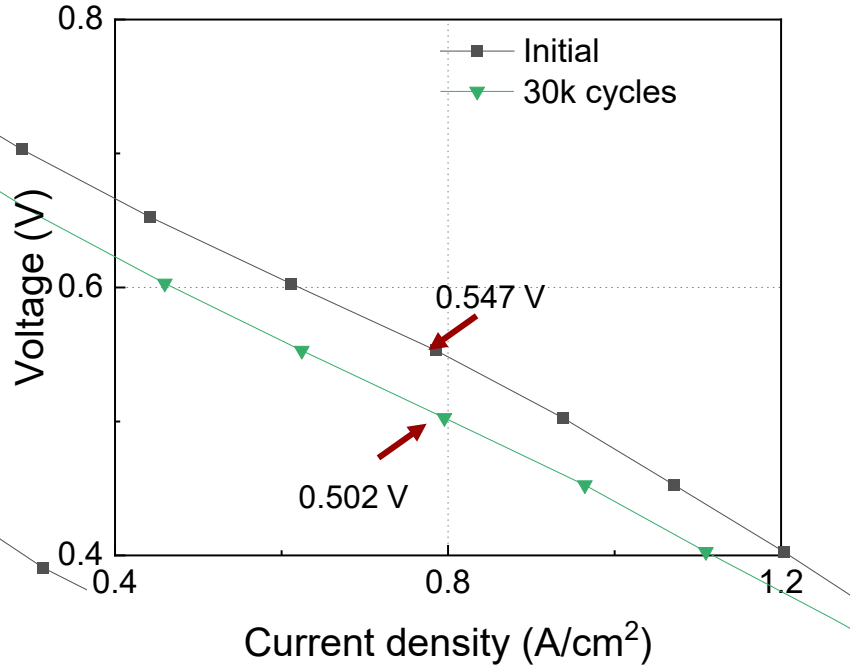

- **FY22 annual milestone:** Initial performance ≥ **75 mA/cm²** at **0.80 V** and ≤ **50 mV loss** at **0.80 A/cm²** after 30k AST cycles
- **Highlight:** Initial performance of 79 mA/cm² at 0.80 V and 45 mV loss at 0.80 A/cm² after 30k AST cycles exceeds the consortium **FY22 Q2 go/no-go** target (65 mA/cm² at 0.80 V, ≤ 50 mV loss at 0.80 A/cm² after 30k AST cycles) and **FY22 ORR annual milestone**, designed to combine ORR activity and performance durability of PGM-free ORR catalysts
- **Highlight:** Initial current densities achieved at 0.80 V and 0.675 V (377 mA/cm²) also meet the activity objective: *Improve PGM-free cathode H_2-air initial fuel cell performance by **25%** compared to FY21 baseline.*

FY22 ElectroCat ORR Milestone: High-throughput Fe-N-C

Cathode: 4 mg cm^{-2}, Fe-N-C, 1700 sccm, 1.0 bar air/O_2 partial pressure, 100% RH; **Anode:** 0.2 mg_{Pt} cm^{-2} Pt/C GDE, H_2, 700 sccm, 1.0 bar H_2 partial pressure, 100% RH; **Membrane:** Nafion®212; **Cell:** differential, 5 cm^2, **Temperature:** 80 °C; **Durability cycling:** (**OCV-0.01 V**) to **0.60 V**

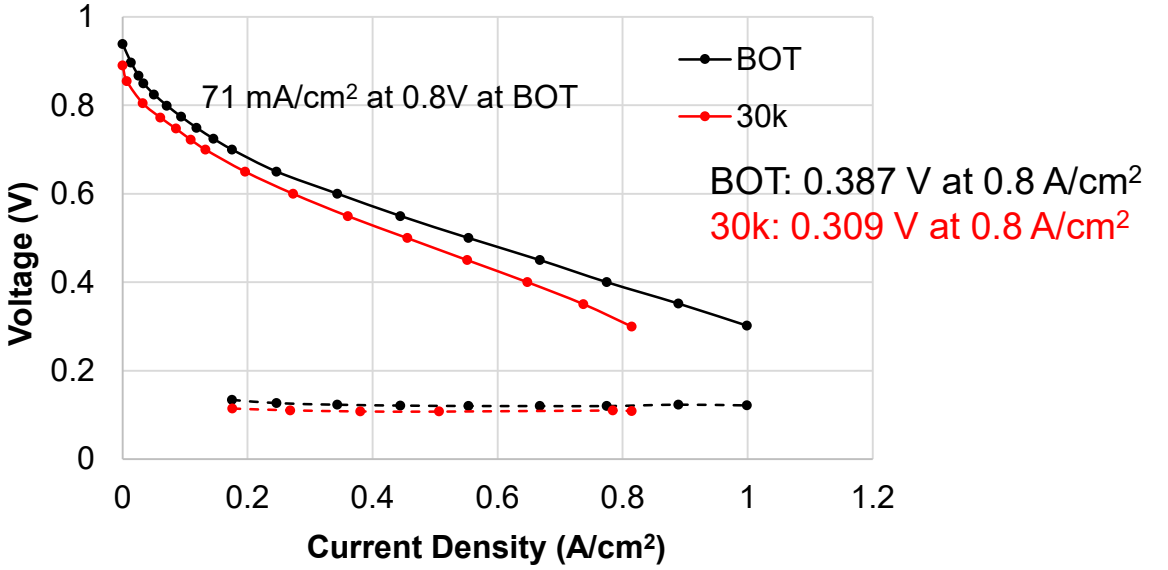

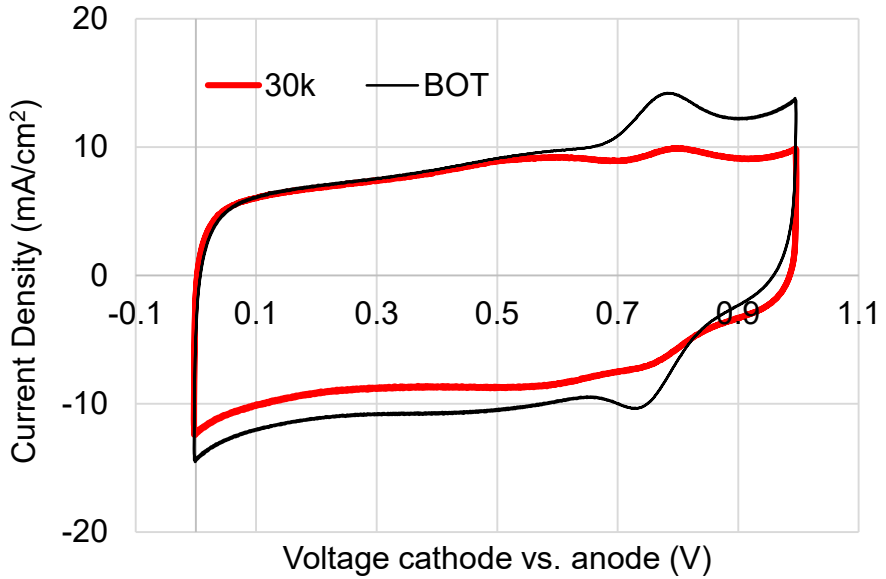

- H_2/Air beginning of life performance:
  - ✓ 71 mA/cm^2 at 0.8 V
  - ✓ 0.387 V at 0.8 A/cm^2
- Loss in H_2/Air current density after 30k AST cycles:
  - ✓ 33 mA/cm^2 at 0.8 V
  - ✓ ΔV at 0.8 A/cm^2: 78 mV

FY22 Q2 Go/No-Go: Current density of ≥ 65 mA/cm^2 at 0.8V at beginning of test and ≤ 50 mV voltage loss at 0.8 A/cm^2 after 30k catalyst AST cycles (LANL, ANL)

New ORR Catalyst Synthesis Approach: Template Synthesis of Fe-N-C Catalysts

Regular MOF-derived Fe-N-C Catalyst

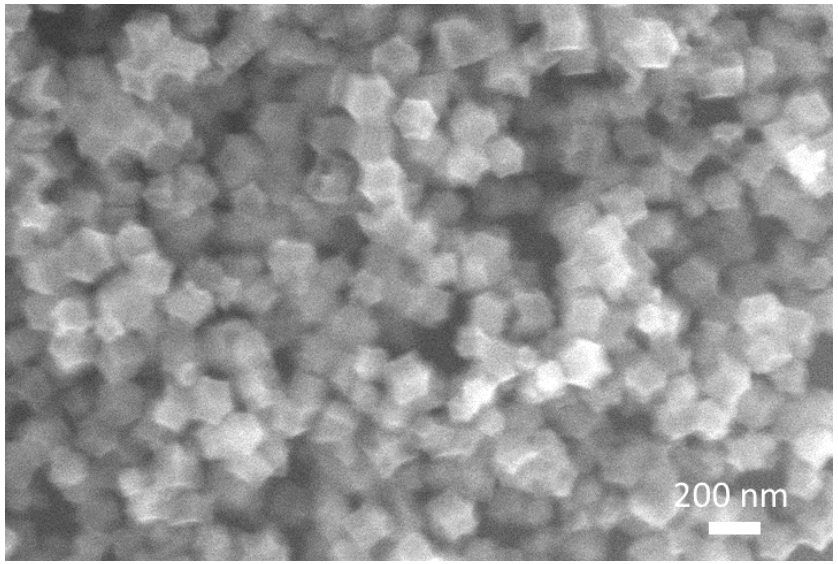

Templated Fe-N-C Catalyst

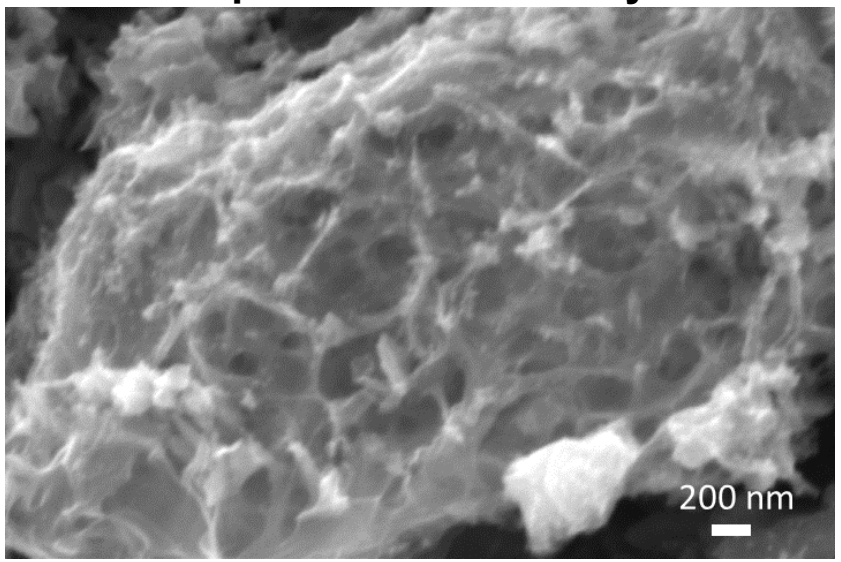

SiO_2-Template Synthesis of Fe-N-C Catalysts

MOF-coated SiO_2 nanoparticles → *high T* → Fe-N-C/SiO_2 nanoparticles → *leach* → templated Fe-N-C catalyst

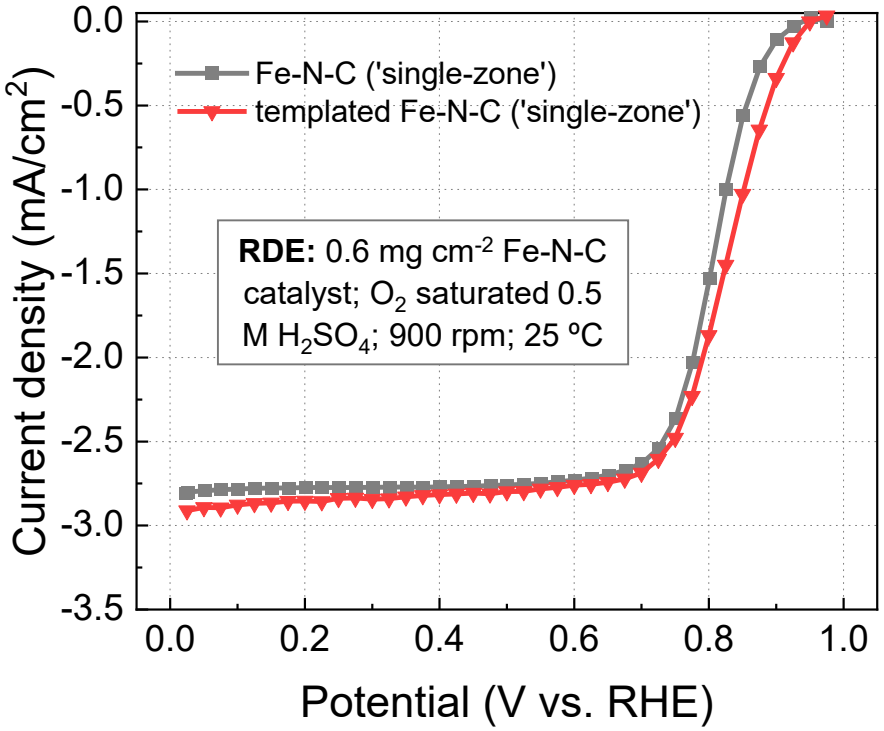

- **SiO_2-template synthesis of Fe-N-C catalysts**: ”Networked” morphology of Fe-N-C catalysts with substantial content of voids
- Slightly improved ORR performance of templated Fe-N-C catalyst in RDE testing compared to the catalyst obtained via standard method

New ORR Catalyst Synthesis Approach: 'Single-Zone' Catalyst Synthesized in H_2 Atmosphere

Rotating disk electrode (RDE) measurement: 0.6 mg cm^{-2} Fe-N-C catalyst; O_2 saturated 0.5 M H_2SO_4; 900 rpm; 25 ºC

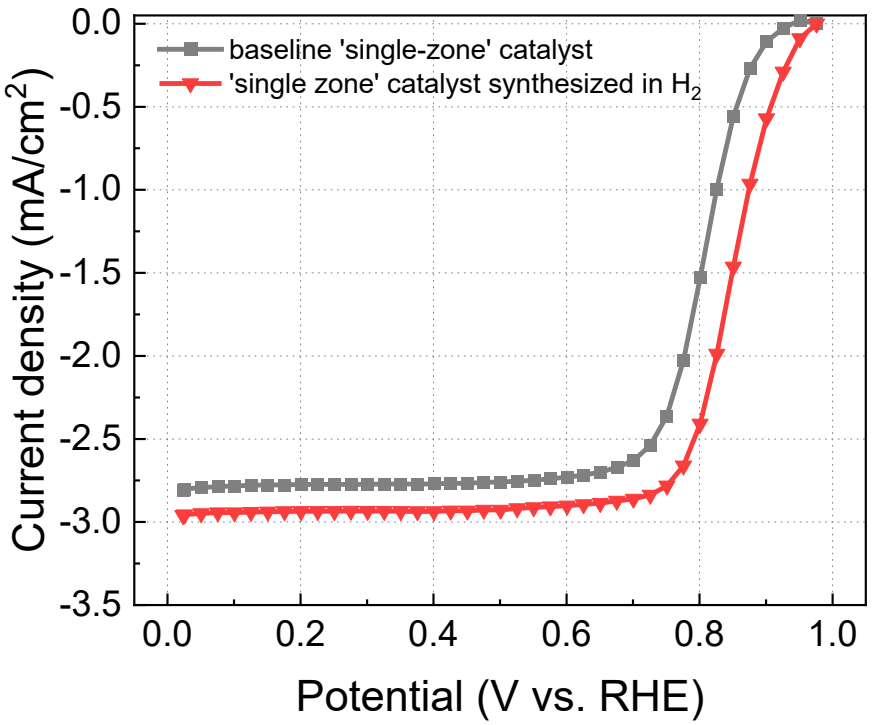

Cathode: *ca.* 4.0 mg cm^{-2}, Fe-N-C, 1700 sccm, 1.0 bar air partial pressure, 100 %RH; **Anode:** 0.3 mg_{Pt} cm^{-2} Pt/C, H_2, 700 sccm, 1.0 bar H_2 partial pressure, 100 %RH; **Membrane:** Nafion®211; **Cell:** differential, 5 cm^2, **Temperature:** 80 °C

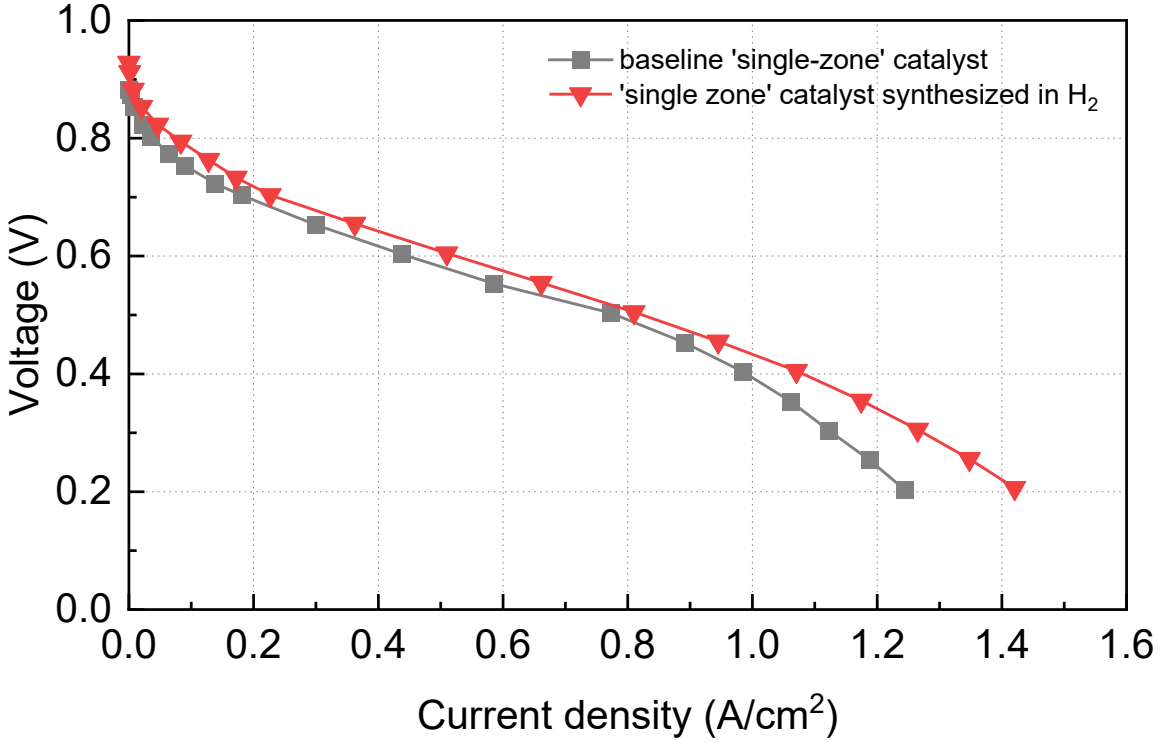

- **Highlight:** Improved performance of 'single zone' catalyst in both RDE and fuel cell testing by using H_2 during synthesis vs. inert gas
- $\Delta E_{½}$ = 40 mV improvement in RDE testing
- Fuel cell voltage increase by *ca.* 25 mV at a reference current density of 0.8 A/cm^2

High-Throughput Synthesis of ORR Catalysts

Catalyst System 2: Physical mixtures (ball milling) of Fe salt, carbon-nitrogen precursor, carbon support

(e.g., Zitolo *et al.*, *Nat. Mater.*, 14, 937, 2015)

- **Twenty-five** catalyst samples were prepared since the 2021 AMR for further performance optimization based on the ML findings from 36 catalyst samples with varied phenanthroline-to-ZIF ratios, varied content of Fe in the precursor, varied pyrolysis temperature and hold time, and varied heating/cooling rate/mode prepared for input into machine learning algorithms.

Catalyst System 3: Two step synthesis; formation of nitrogen-doped carbon followed by incorporation of Fe

(based on J. Li, D. Myers, Q. Jia *et al.*, *J. Am Chem. Soc.,* 142, 1417, 2020)

- Physical mixtures (ball milling) of carbon-nitrogen precursors pyrolyzed and heat-treated in NH_3 to form nitrogen-doped carbon (N-C)
- Physical mixtures (ball milling) of N-C and Fe salt pyrolyzed and heat treated in NH_3

Catalyst System 3b: Chemical vapor deposition of $FeCl_3$ into N-C; **72** unique samples

(based on L. Jiao, D. Myers, Q. Jia *et al.*, *Nature Materials*, 20 (2021) 1385.)

✓ Effect of ball-milling time of N-C, heat treatment temperature, Fe:N-C ratio, additive (Sn, Co…), carbon coating (Dopamine, propylene cracking, ZIF-8…)

Catalyst System 4: Physical mixtures (ball milling) of Fe_2O_3 nanoparticles and ZIF-8 pyrolyzed in fixed-bed reactor

(based on University of Buffalo ElectroCat project)

✓ Effect of Fe content (**8** samples thus far)
✓ Effect of pyrolysis conditions (on-going)

ORR Activity of High-Throughput System 2 Catalysts

RDE-determined ORR mass activity at 0.8 V for System 2 catalysts prepared in ANL high-throughput activity with synthesis parameters guided by machine learning approach. O_2-saturated 0.5 M H_2SO_4, 0.6 mg_{cat}/cm^2

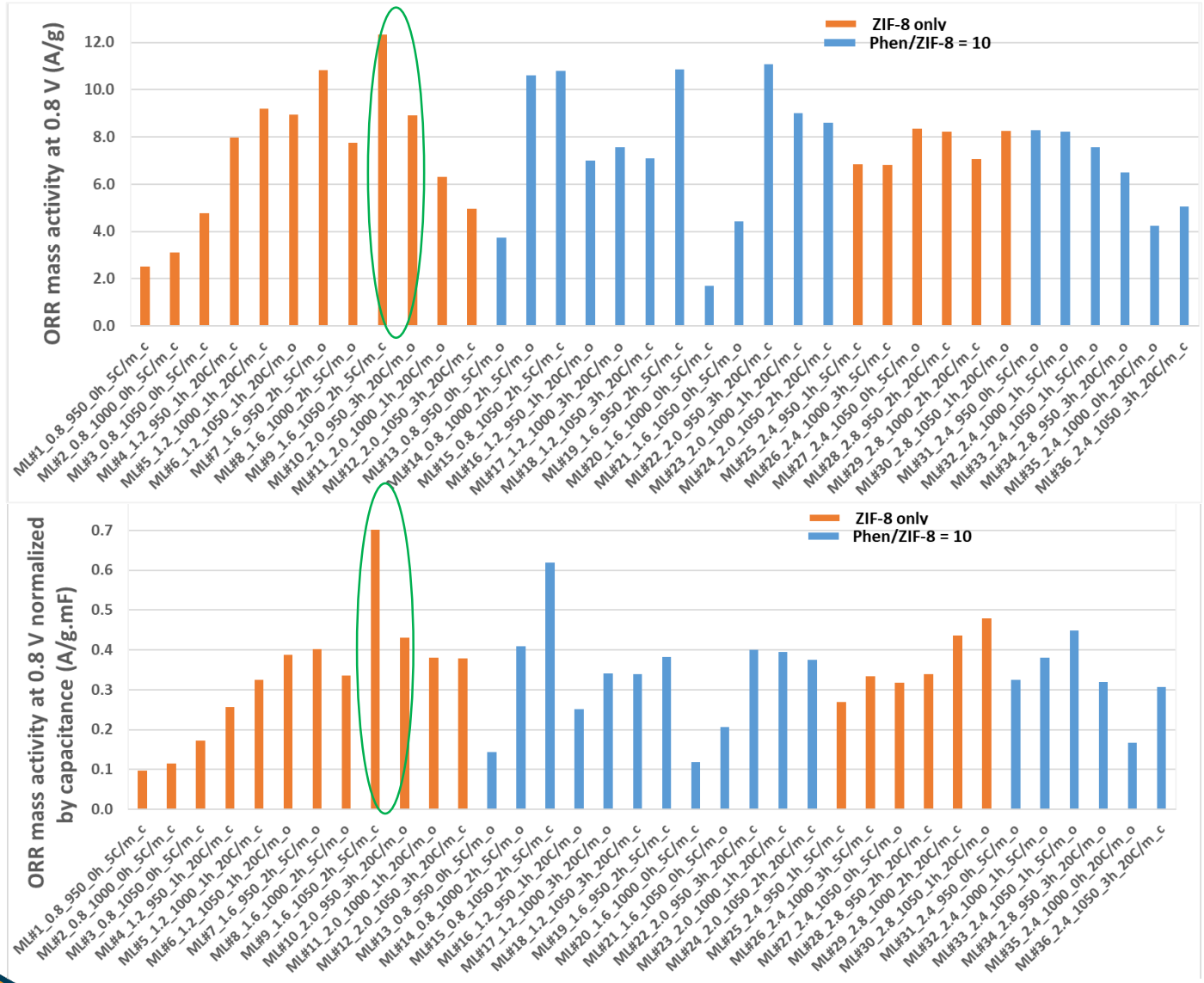

- Guided by ML findings, explored effect of Fe wt% in precursor (0.8 - 2.8 wt%), phenanthroline to ZIF-8 wt ratio (0, 10), and pyrolysis temperature (950 -1150 °C), hold time (0 - 3 h), heating rate (5 -10 °C/min) and cooling mode (furnace open or closed)
- Addition of phenanthroline did not improve the ORR performance
- Good correlation between ORR mass activity and capacitance
- ORR mass activity reported in literature for this class of catalysts: **2.8 A/g_{cat}** at 0.8 V*
- **Highlight:** Highest ORR mass activity observed for 1.6 wt% Fe content with no phenanthroline pyrolyzed at 1050 °C for 1 h, heating rate of 5 °C/min, and furnace closed during cooling (**ML#9**): **12.4 A/g_{cat}** @ 0.8 V

* Primbs et al., *Energy Environ. Sci.*, 2020, 13, 2480-2500.

ORR Activity of High-Throughput System 2 Catalysts

RDE-determined ORR mass activity at 0.8 V for System 2 catalysts prepared in high-throughput facility. Further optimization of ML samples. O_2-saturated 0.5 M H_2SO_4, 0.6 mg_{cat}/cm^2

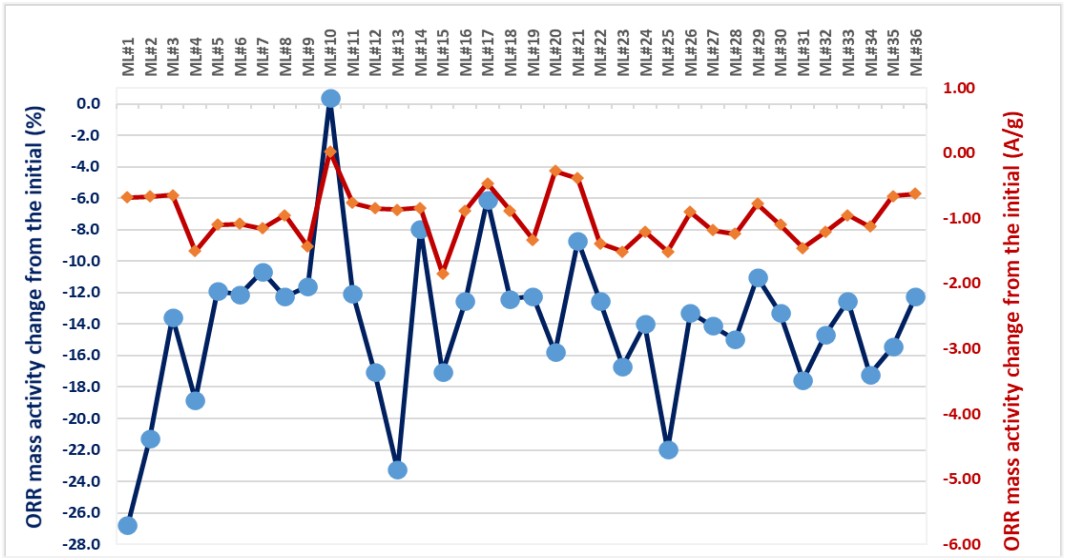

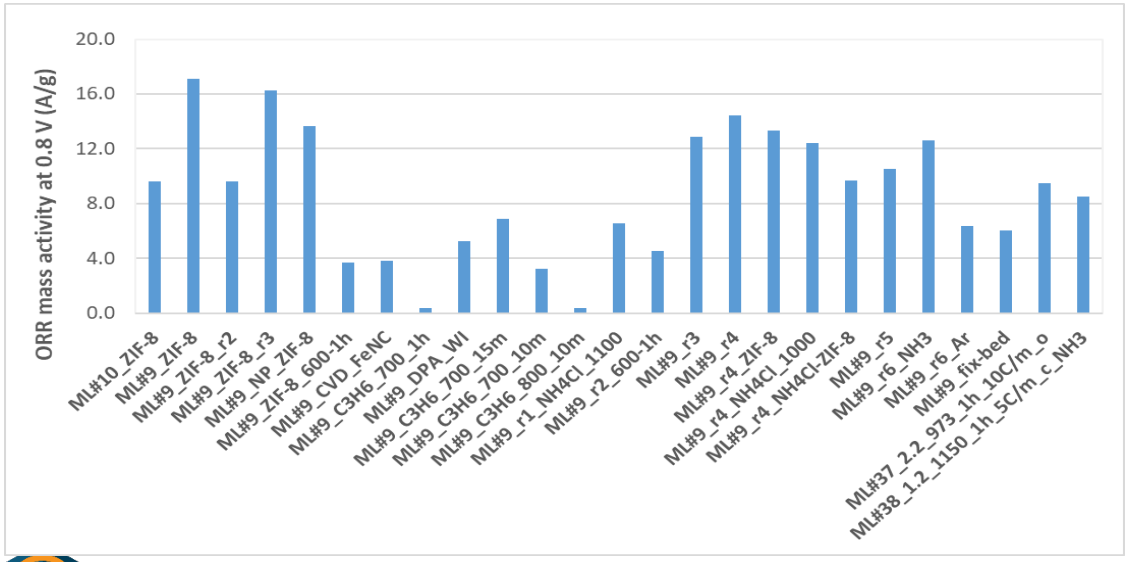

- ML#9 also showed reasonably good stability (activity deceased by 11%) in addition to its highest ORR mass activity (12.4 $A/g_{cat.}$)
- ML#10 showed the best stability (indicated by ORR mass activity increase by 0.4%) with good ORR mass activity (8.9 $A/g_{cat.}$)
- Optimized ML sample synthesis further to improve the catalyst stability while maintaining the high ORR mass activity by exploring formation of coatings using different precursors (ZIF-8, C_3H_6, dopamine, etc.)
- Significantly improved performance in both ORR activity (16.2 $A/g_{cat.}$) and stability (decrease by 3.1 %) observed for the ML#9 sample by coating catalyst with heat treatment in presence of ZIF-8 in upstream crucible.

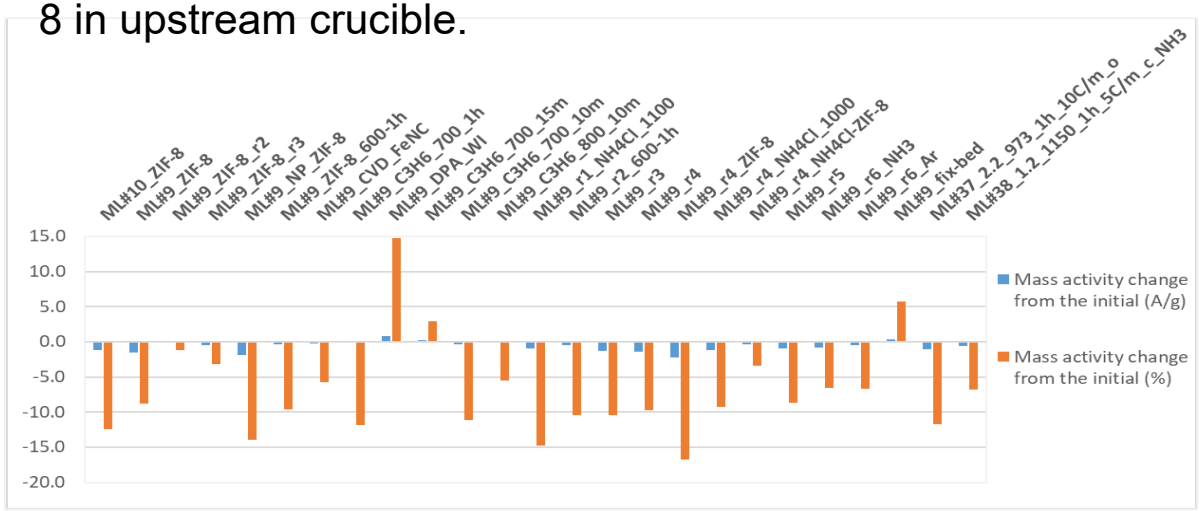

ORR Activity of High-Throughput System 3b and System 4 Catalysts

RDE-determined ORR mass activity at 0.8 V; O_2-sat. 0.5 M H_2SO_4, 0.6 mg_{cat}/cm^2

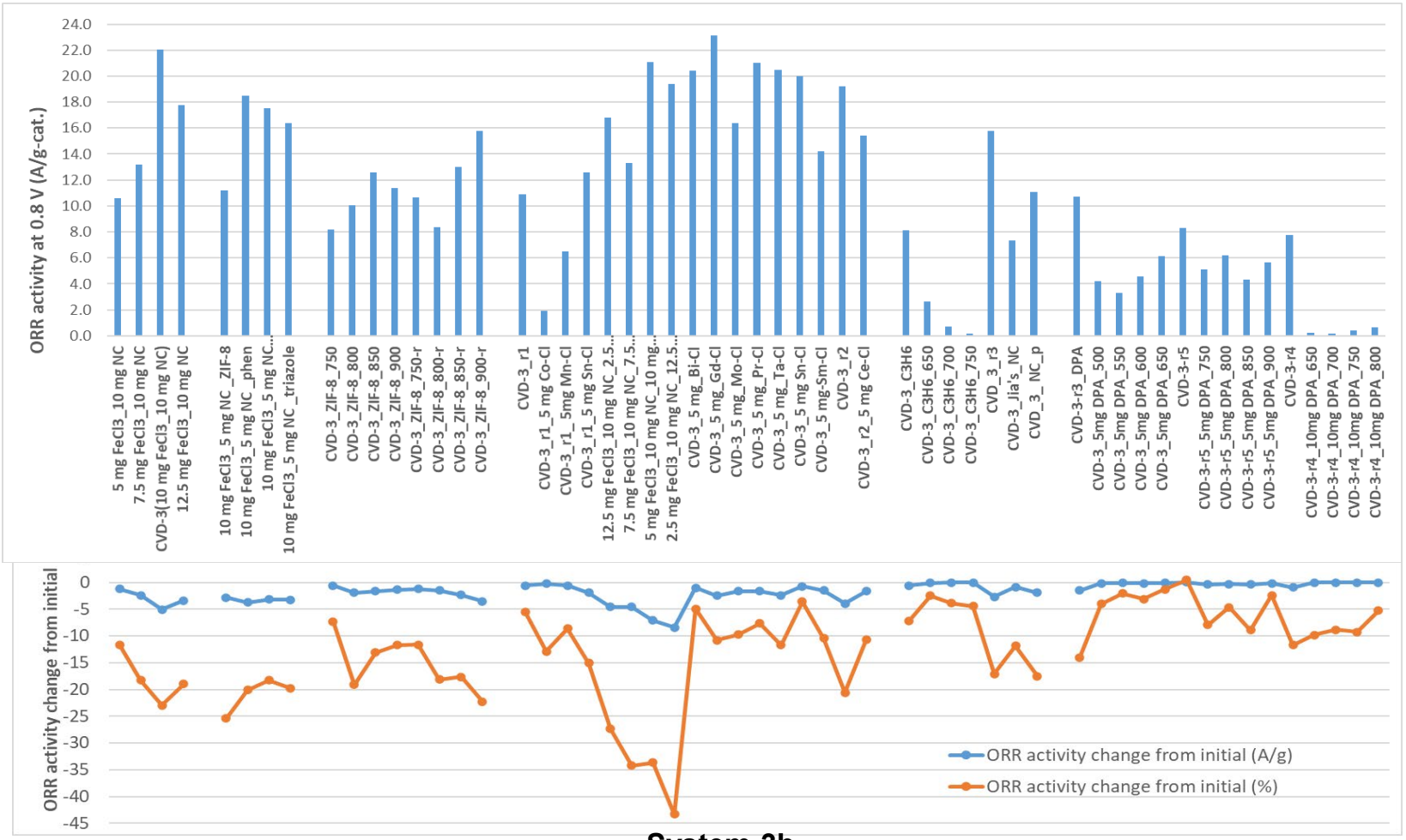

System 3b

- Highest ORR activity of **23 A/g_{cat}** achieved using CVD of Fe into N-C with deposition temperature of 800 °C and with ball-milled N-C; peroxide yield 0.9%
- Adding 2nd metal chloride (Bi, Sm) improved the stability with a small decrease in ORR activity
- Coating catalyst with various precursors showed reduced activity with improved stability

- System 3b: Multi-port parallel reactor system (Avantium T1224) for high-throughput exploration of parameters in chemical vapor deposition synthesis process

HT Parallel Reactor System (T1224, Avantium)

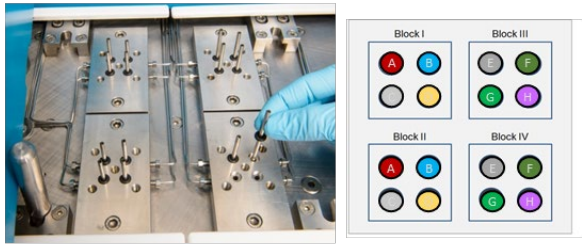

Each block can be temperature-controlled independently

System 4

- Excellent stability with nano-Fe_2O_3 as Fe source, in general, with 1.2% Fe exhibiting good balance between activity and stability
- Doubled heating rate further improved activity without reducing stability

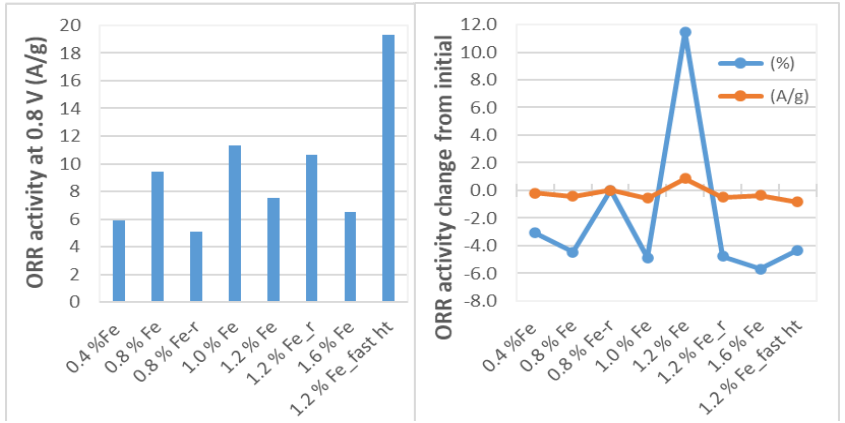

Developed Data Science-Guided High-Throughput Synthesis of PGM-free Electrocatalysts

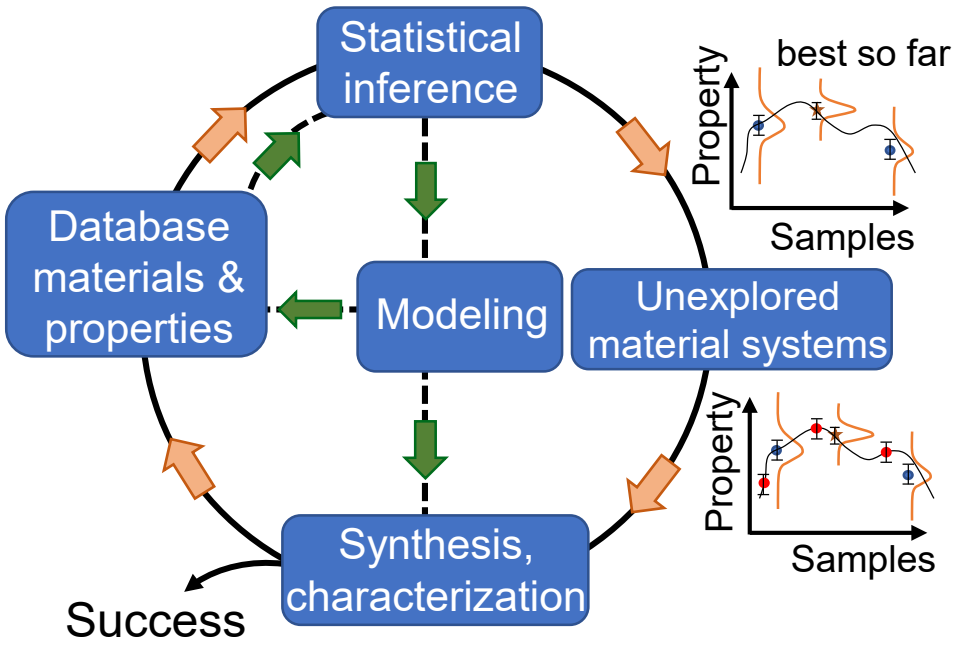

Fe	0.8-2.8 wt%
Phen/ZIF	0-10
Temperature	950-1050 ºC
Holding time	0-3 h
Heating rate	5-20 ºC/min
Furnace	open/closed

36 samples

Synthesis

<u>Dried chemicals</u>
Fe acetate
1,10-phenanthroline (N, C source)
ZIF-8 (N, C source)

↓

Ball milling
2h 400 rpm

↓

Pyrolysis in Ar

↓

Ammonia treatment
at 900 °C for 5 min

↓

Cooling

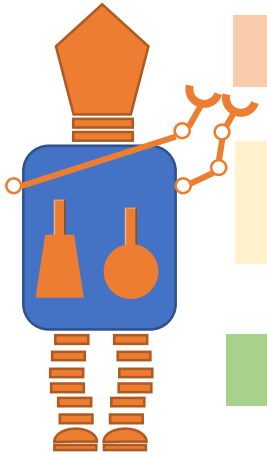

Machine learning descriptors

1. Weight % of Fe
2. Phen/ZIF-8 ratio

3. Heating rate
4. Pyrolysis temperature
5. Holding time

6. Cooling to room T (furnace open or closed)

Highlight: Developed and implemented **adaptive learning design loop** with uncertainty quantification to model and guide high-throughput synthesis of PGM-free ORR catalysts

Uncertainty Quantification, Machine Learning Model Regressors and Selectors

- Machine learning model regressors
  - ✓ Gaussian Process Regression (GPR)
  - ✓ Random Forest (RF)
  - ✓ Artificial Neural Network (ANN)
- Efficient Global Optimization Selectors Exploitation vs Exploration
  - ✓ Probability of Improvement (PI)
  - ✓ Expected Improvement (EI)
  - ✓ Knowledgeable gradient
- What is the best surrogated model/acquisition function pair?
  - ✓ No-free-lunch theorem: No universal optimizer!
  - ✓ Regressor/Selector guided search for best sample within existing dataset

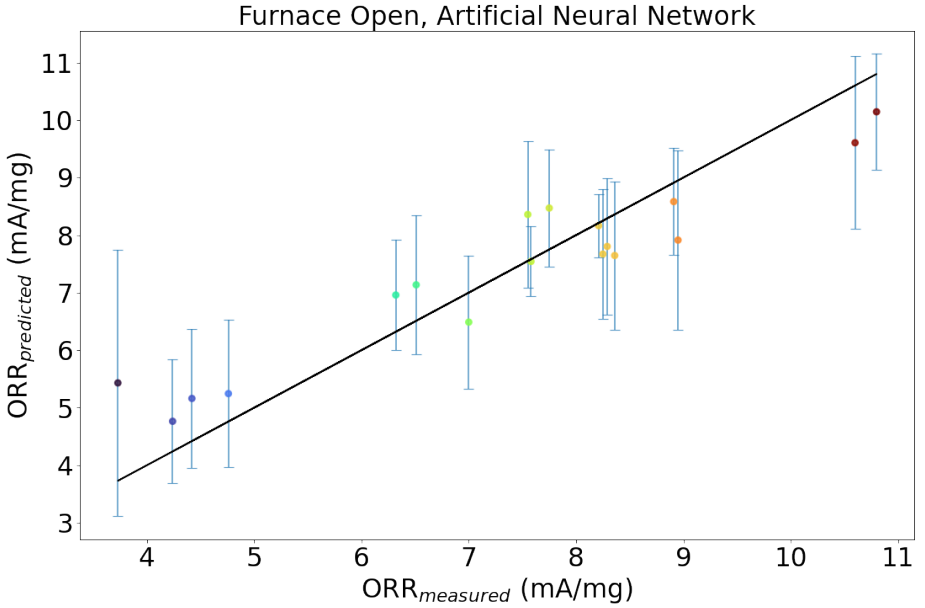

Count number of iterations

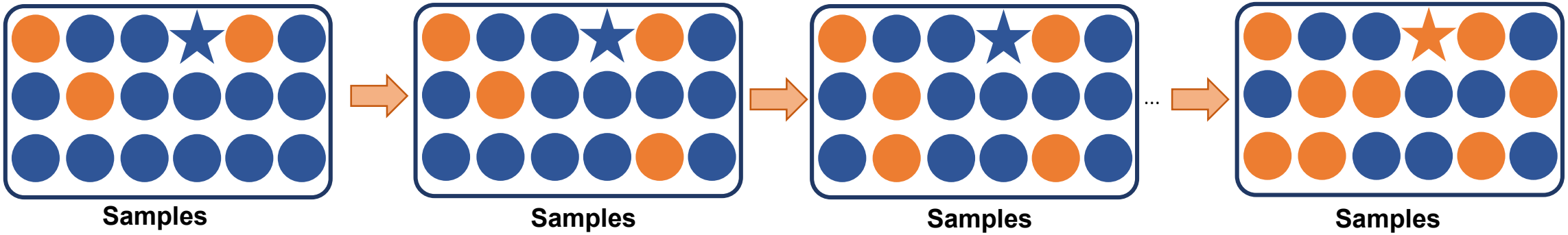

Highlight: Developed computational approach that leverages uncertainty quantification to unveil most promising regressor/selector pairs for optimum learning in adaptive learning loop

Uncertainty Quantification, Machine Learning Model Regressors and Selectors

- Key result: Best regressor/selector
  - ✓ Furnace closed: RF + EI
  - ✓ Furnace open: ANN + PI

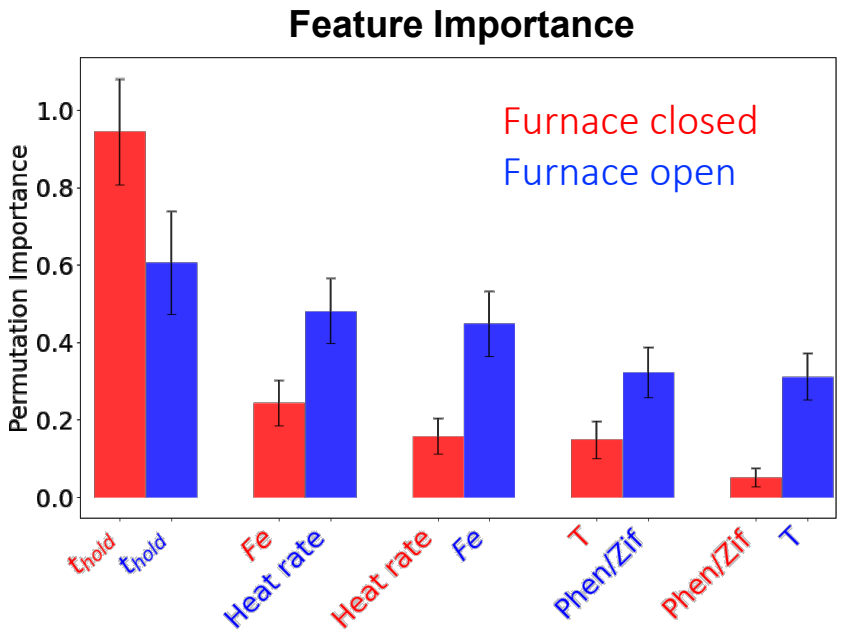

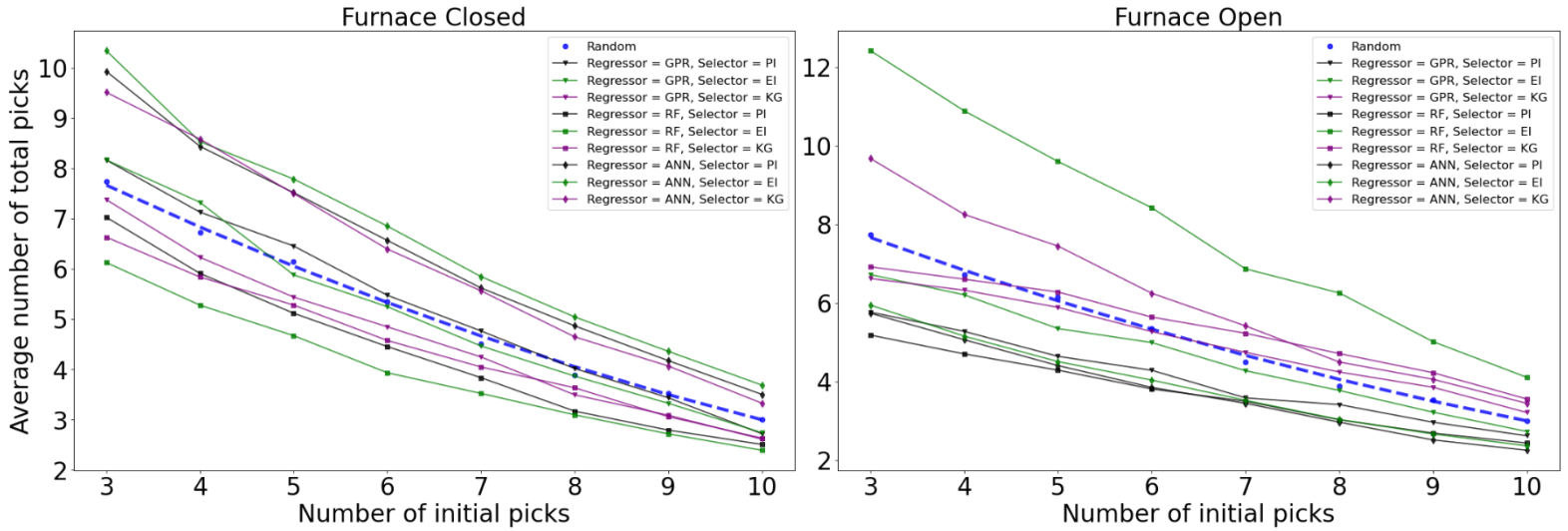

Highlight: Employed ML to uncover the relative importance of synthesis variables in the activity and predicted next samples to be synthesized and characterized, with potential increase of activity in > 5%

	Fe (%)	Phen/ZIF	T (ºC)	Hold time (h)	Heating rate (ºC/min)	ORR (mA/cm^2)	1.96*σ (mA/cm^2)
Best so far	1.6	0	950	2	5	10.8	-
Next 1	1.28	3.65	950	3	5	10.92	2.85
Next 2	0.8	0	1050	3	5	9.51	4.54
Next 3	0.8	7.75	950	3	5	11.36	2.59
Next 4	1.16	3.04	1002	1.3	9.3	7.70	1.28

Multi-Objective Optimization: Improving Activity and Stability in a Single Site

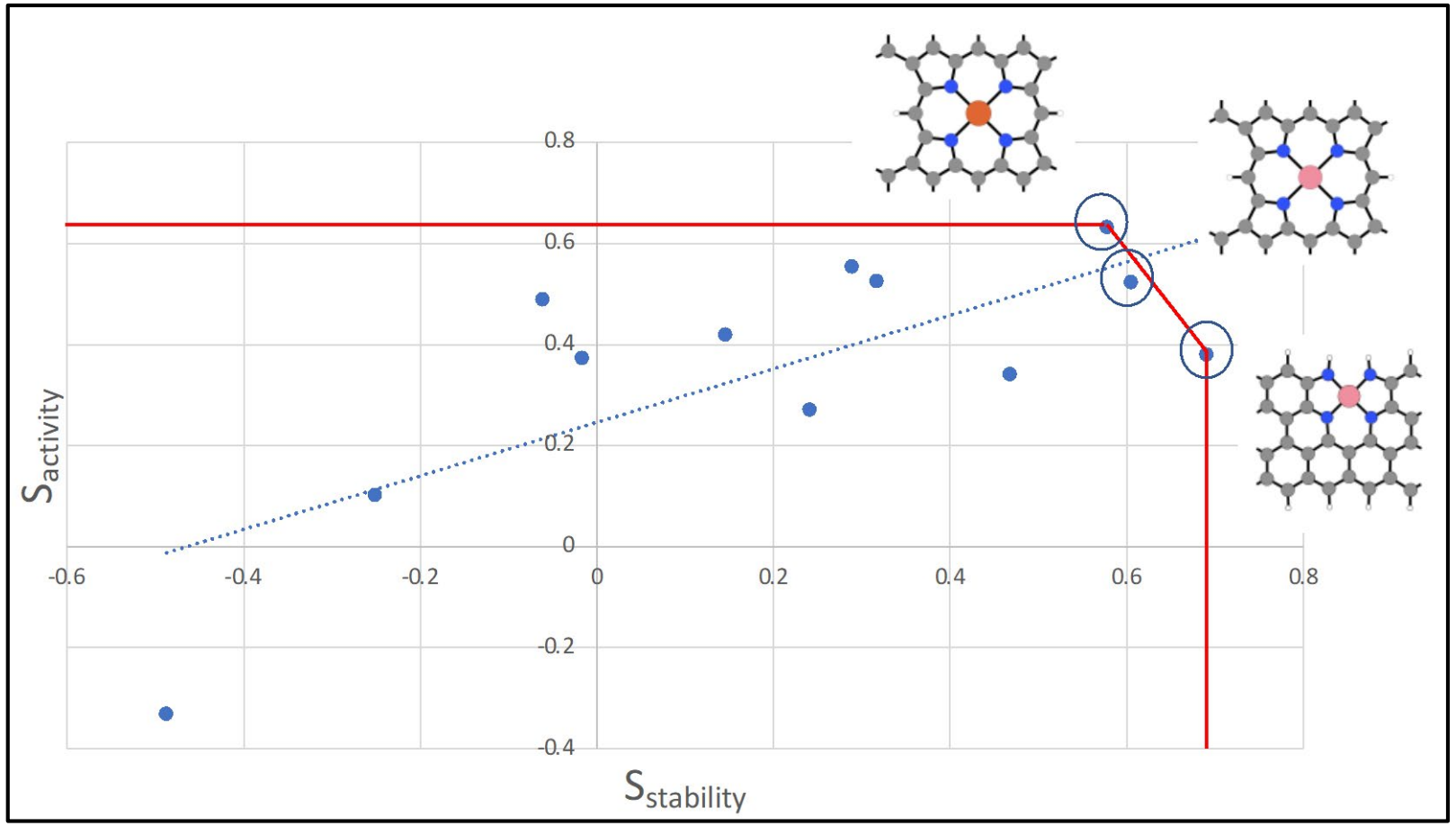

- $M\text{-}N_4\text{-}C_x$; M = Mn, Fe, Co; x = 8,10,12
  - ✓ Basal plane + $M\text{-}N_4\text{-}C_{10}$@ZZ-edge
- 3 weighted and scaled stability descriptors
  - ✓ M-dissolution potential
  - ✓ M-dissolution pH
  - ✓ 0K displacement threshold energy
- 1 scaled activity descriptor
  - ✓ Limiting potential (1^{st} or 4^{th} protonation step)
- Key findings:
  - ✓ Results sensitive to H_2 reference state
  - ✓ Close to linear correlation between activity and stability across structures
  - ✓ Inverse correlation at most active/stable sites
  - ✓ C_{12} – possible advantage due to strain relaxation/modification near defects
- *Need to confirm on larger cells*

Highlight: Combined 4 DFT-based descriptors of activity and stability to generate Pareto-front plot showing correlation between activity and stability

DFT/MD-based Stability Descriptor: KODTE at Finite Temperature

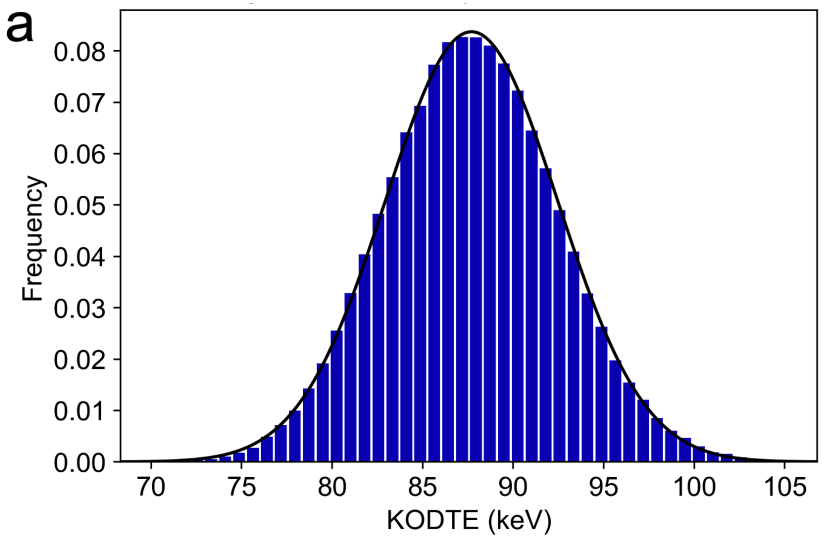

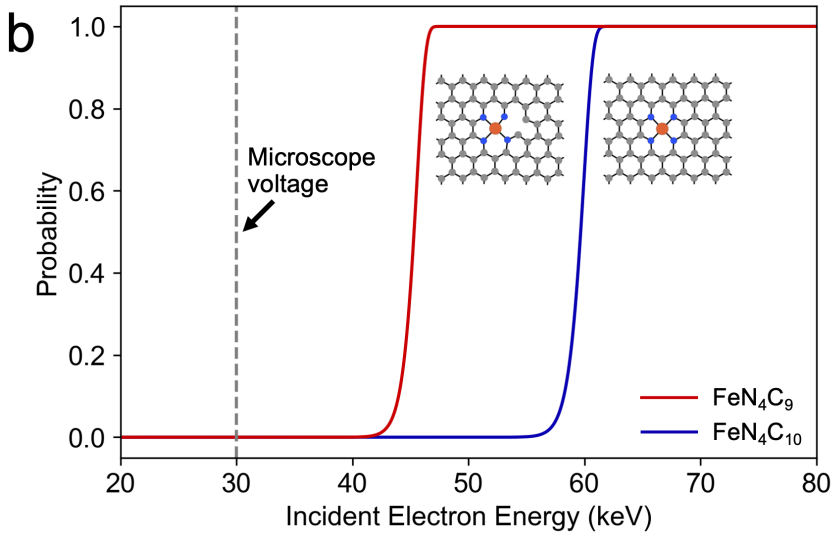

M. Zachman *et al.*, in final preparation

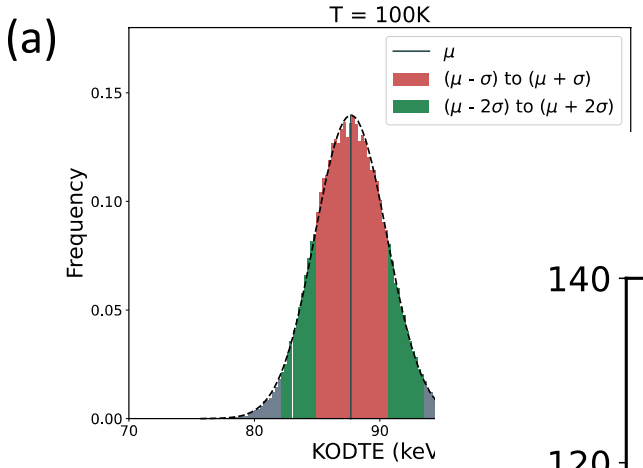

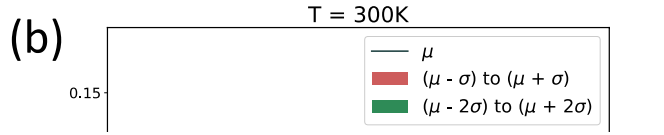

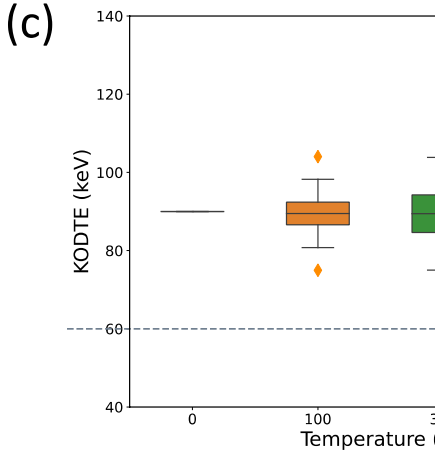

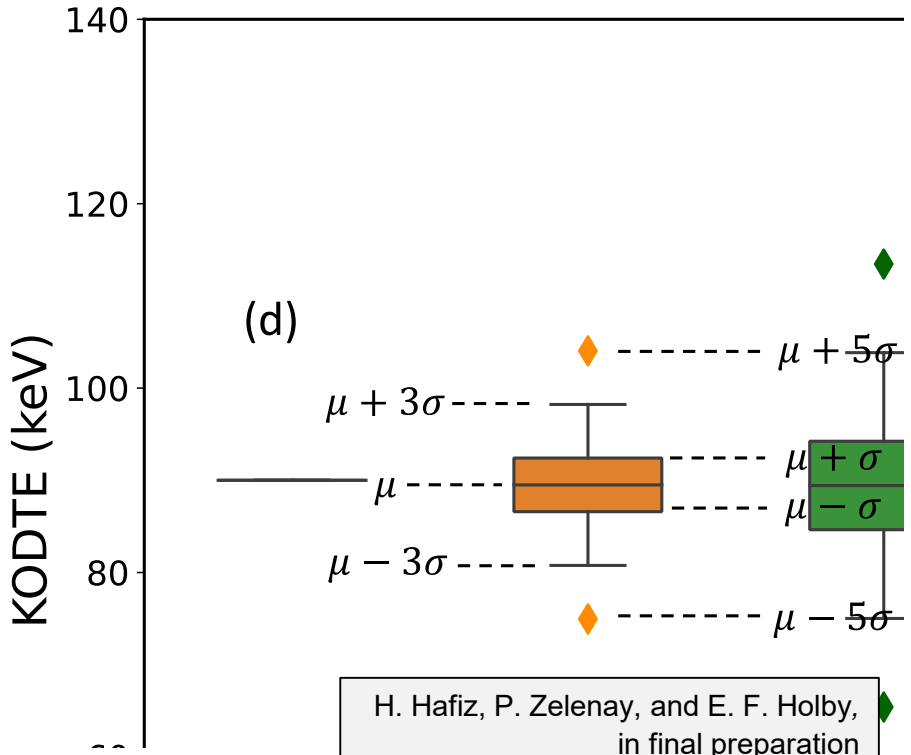

H. Hafiz, P. Zelenay, and E. F. Holby, in final preparation

- **Highlight:** Calculations motivate use of 30 keV beam in TEM
- Two publications on experiments/models in final preparation

DFT/MD-based Stability Descriptor: KODTE at Different Sites

(a)

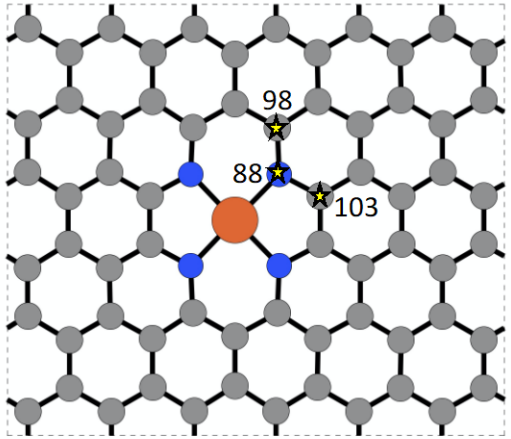

(b)

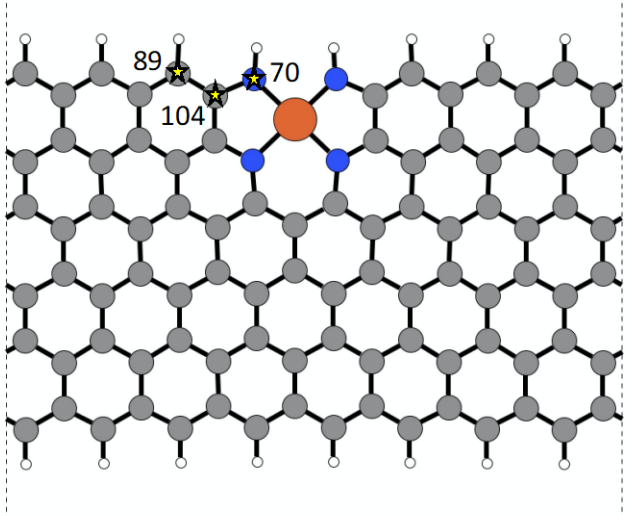

(c)

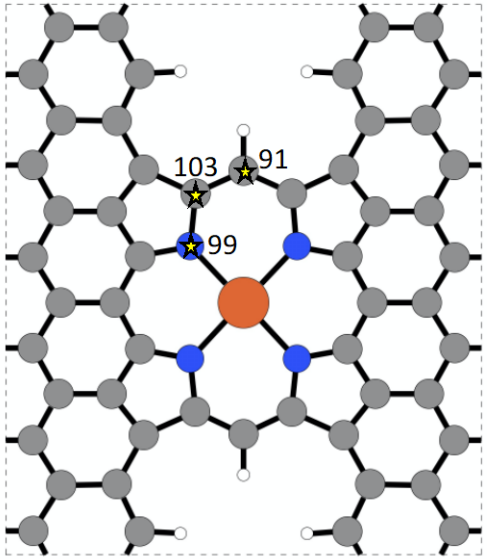

(d)

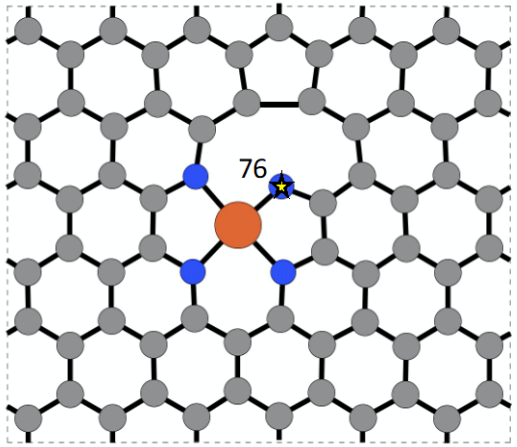

(e)

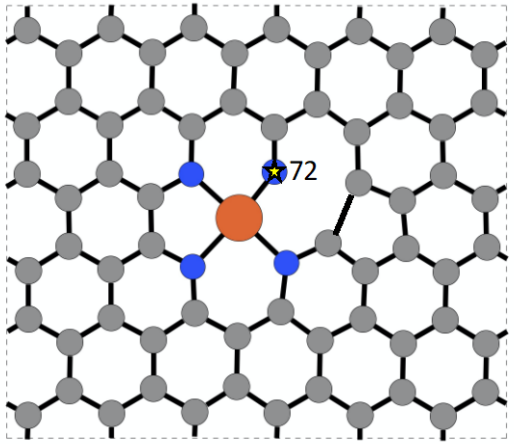

Highlight: Local C-structure can significantly impact "0 K" KODTE and even single C-vacancies can shift N-KODTE close to that of a full edge structure

H. Hafiz, P. Zelenay, and E. F. Holby, in final preparation

Automated Spectroscopy of Atomically Dispersed Transition Metal Sites

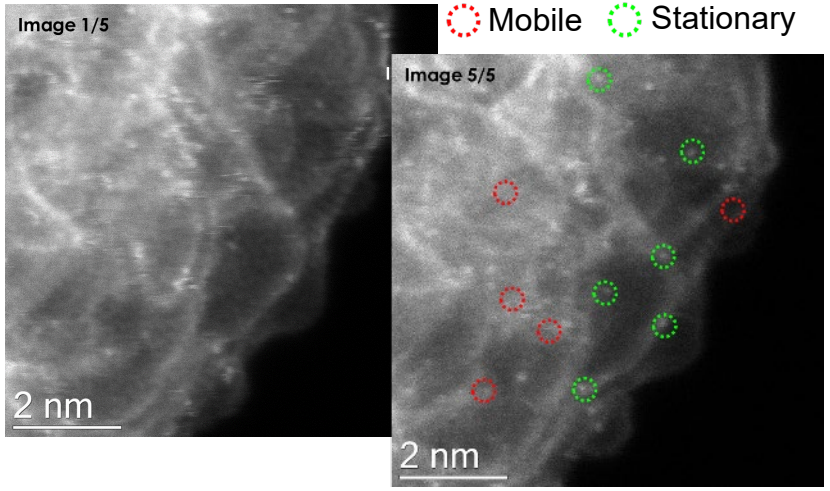

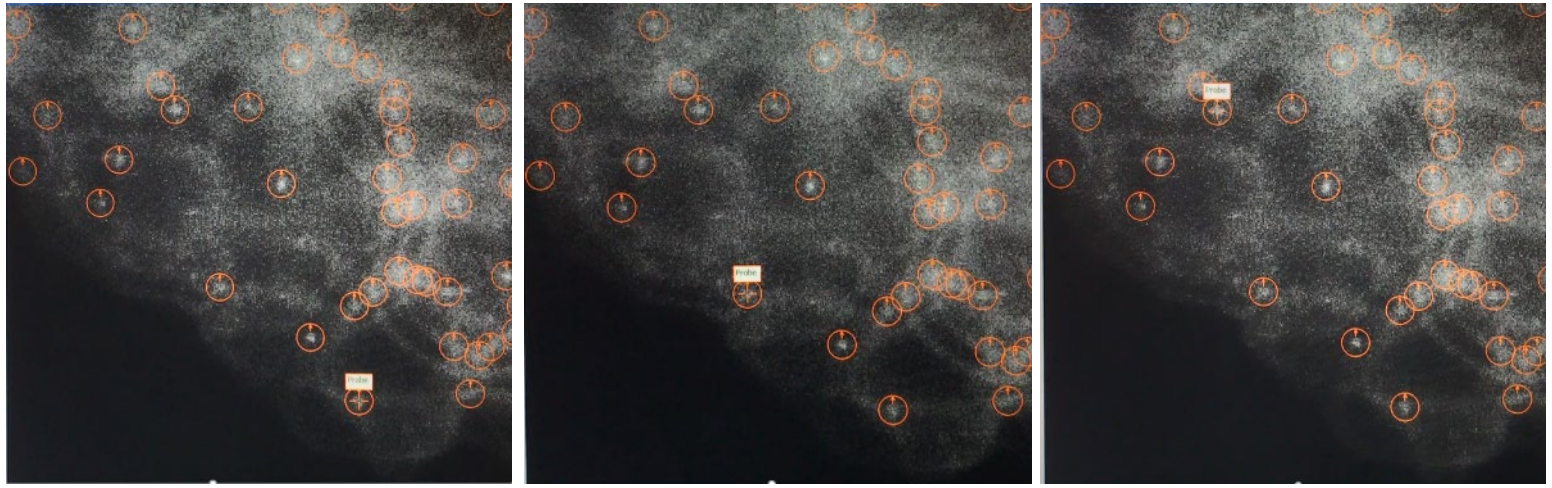

- Transition metal sites are perturbed by electron beam
- Leads to atom “hopping” during long EELS point spectra acquisition (3 sec)
- Online atom-finding technique rapidly scans dozens of atoms to generate a summed spectrum with improved S/N and reduced atom perturbation

Automated atom finding and probe positioning

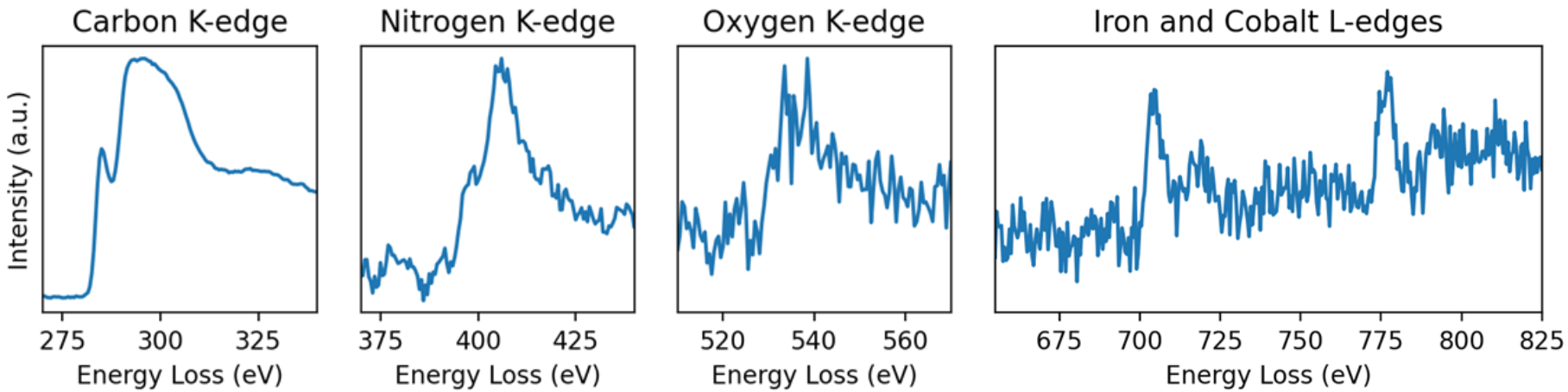

Simultaneous summed EELS point spectra yield improved signal-to-noise with quantifiable near-edge fine structure

FeCo-N-C ORR catalysts provided by Lior Elbaz, Bar Ilan University

Identical-location STEM Provides Insight into Impact of “CVD” Treatments

Before CVD Treatment

After CVD Treatment

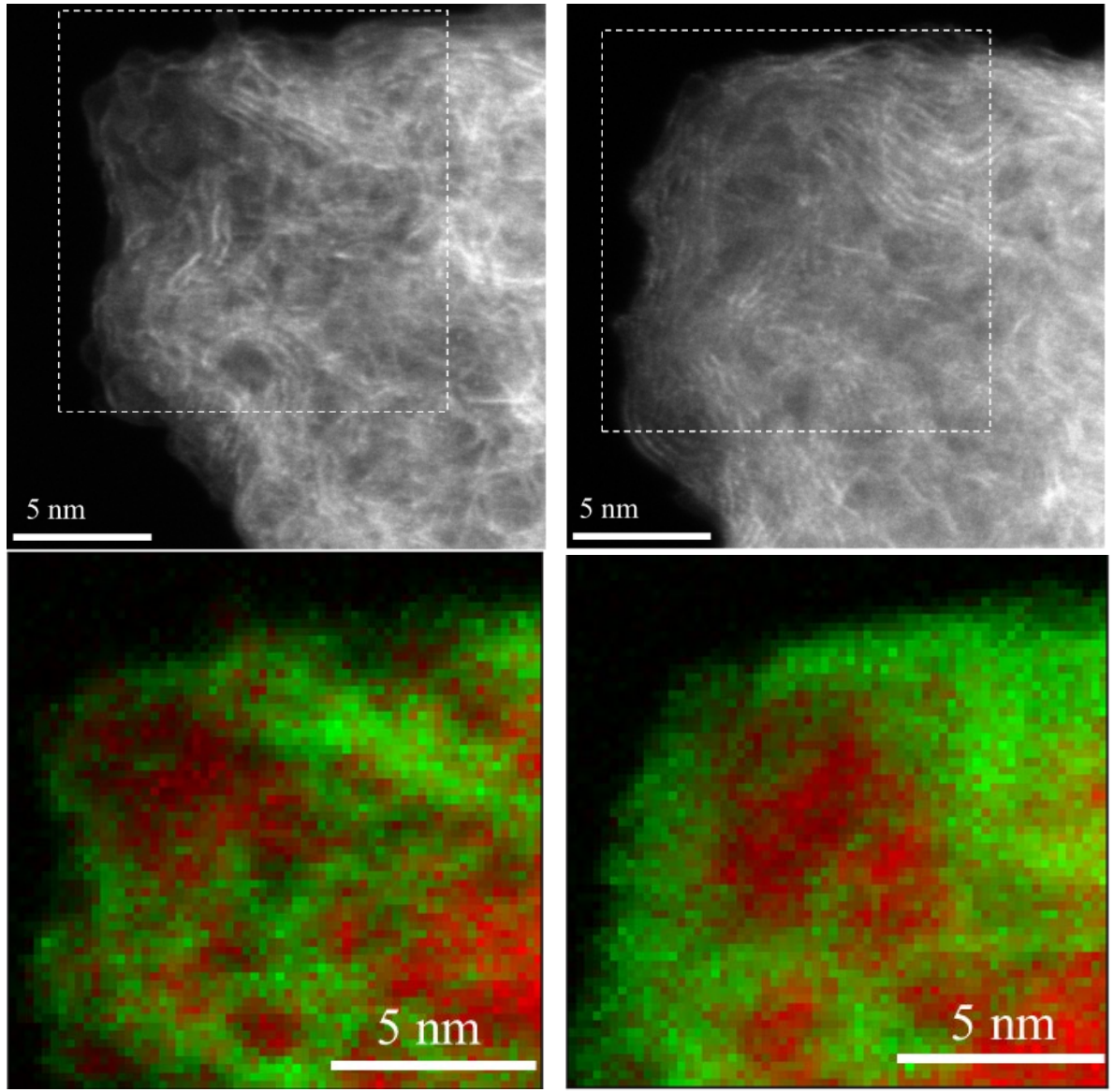

Graphitic Domain Orientation: Parallel vs Perpendicular

- Identical regions of a pyrolyzed FeNC catalysts were imaged before and after a CVD treatment
- C-N material from the upstream boat deposited as thin graphitic layers on the surfaces of the catalyst particles
- The N content in the deposited layers was slightly higher than the bulk

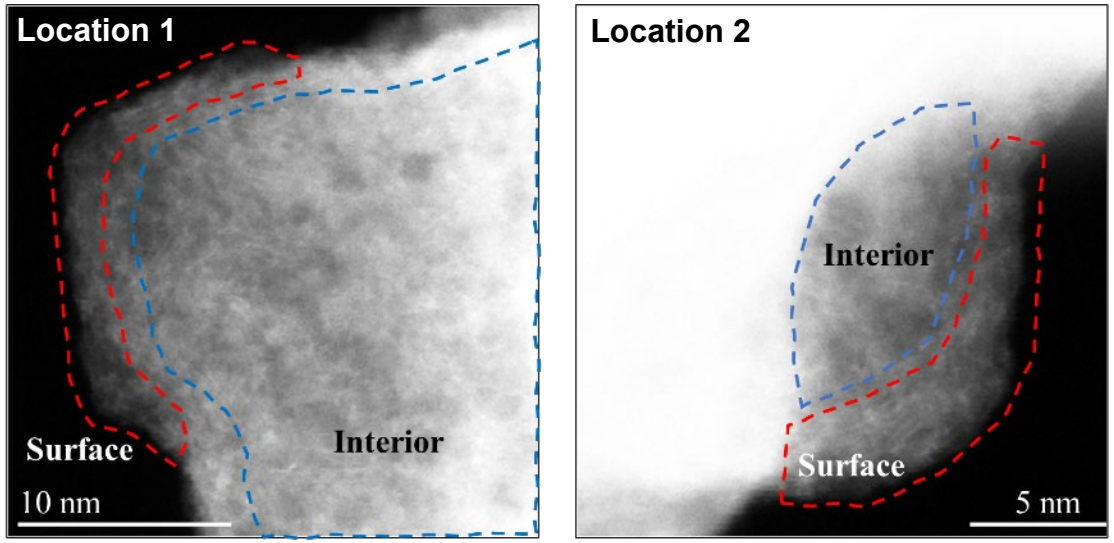

Atomic %	Location 1		Location 2	
	Interior	Surface	Interior	Surface
C	95.3	93.3	95.5	93.8
N	**2.1**	**3.1**	**2.3**	**3.8**
O	2.6	3.6	2.2	2.4

Exploring Subtle Changes in Catalyst Morphology by Combinatorial STEM/Raman/XPS

Identical-location STEM

- Decrease in graphitization and domain structure observed as result of AST cycling in aqueous environment
- No significant differences observed for single vs dual zone catalysts

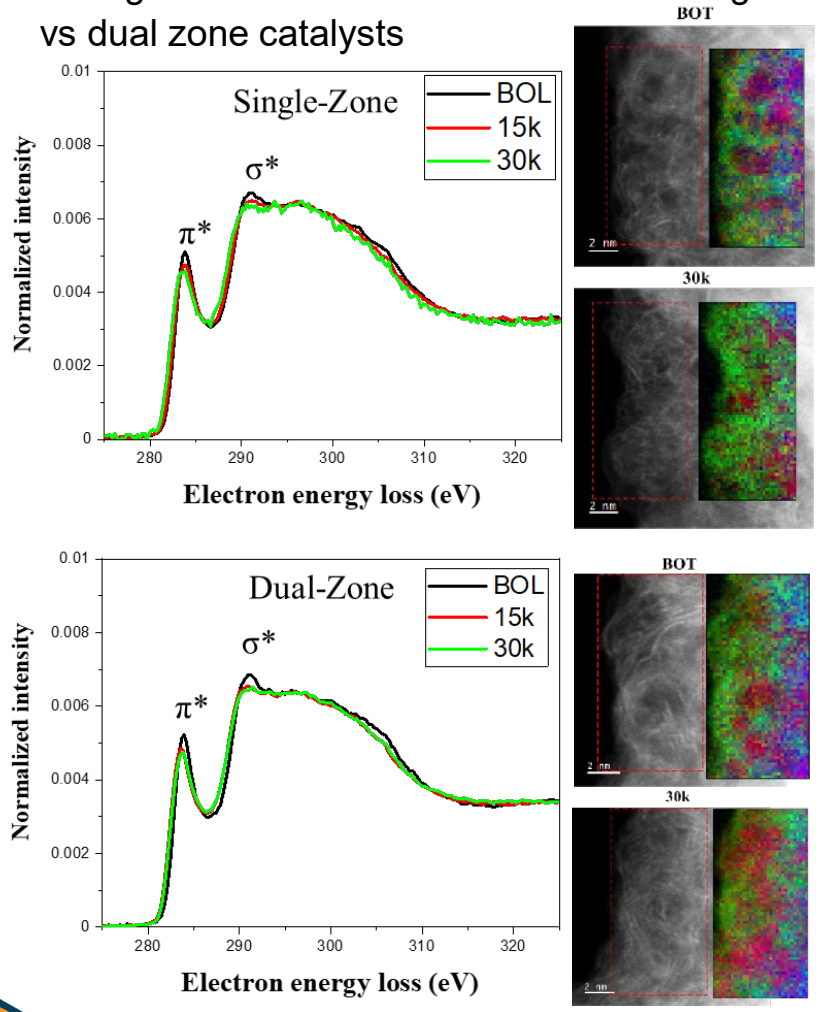

Raman Spectroscopy

D/G ratios before and after AST cycling indicate dual zone carbon structure is slightly more stable:

- Single zone: 0.86 → 0.91
- Dual zone: 0.87 → 0.89

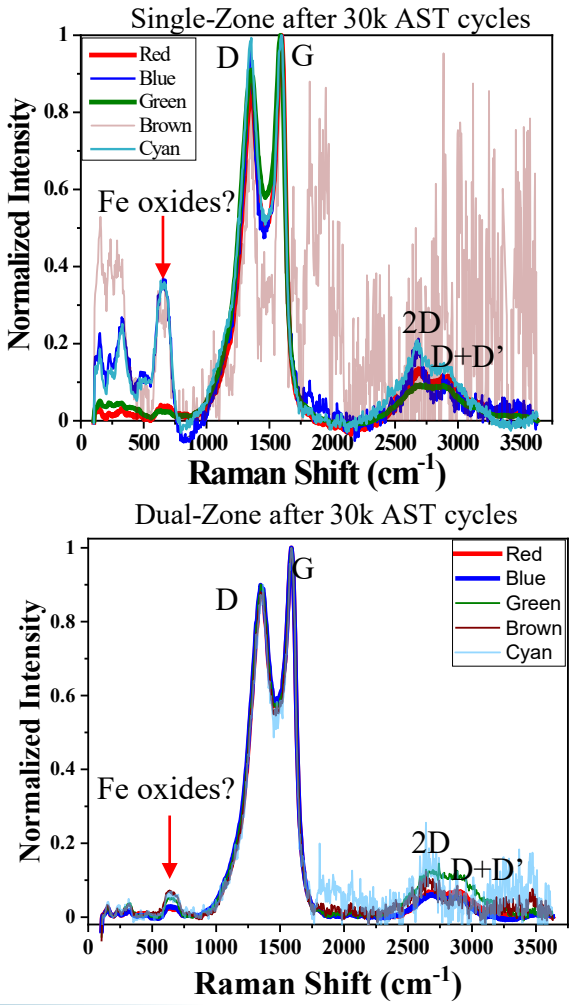

Identical-location XPS

Ongoing work aims to elucidate degradation differences between single and dual zone of IL-XPS

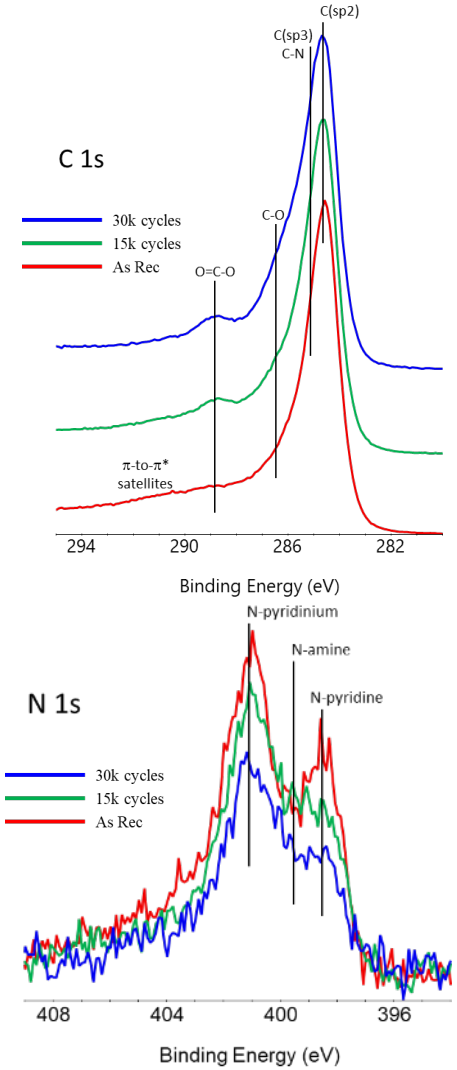

Multimodal Spectroscopic Analysis of Fe-N-C

- Density functional theory (DFT) calculations used to identify Fe-N-C species observed in spectroscopic experiments (e.g., in situ potential dependence; NO probe molecule)

FeN_4-C_{10}-basal	FeN_4-C_{10}-edge	FeN_4-C_{12}-basal

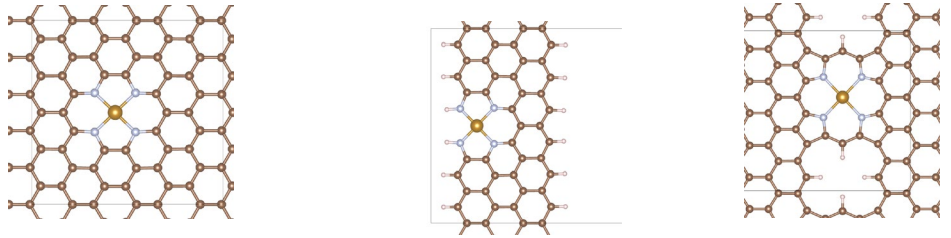

Mössbauer Spectroscopy

Experimental

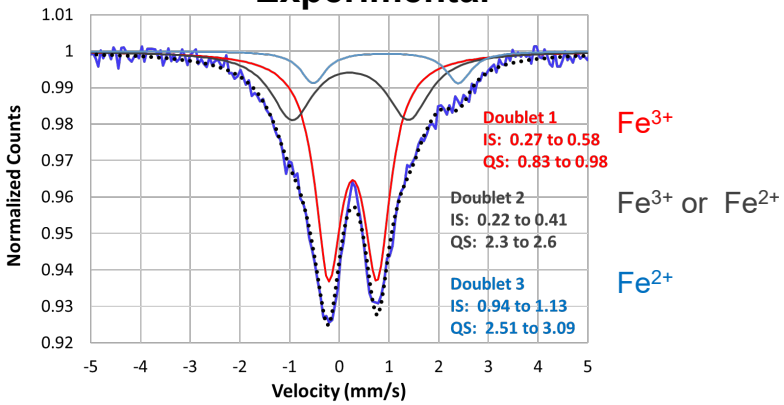

Fe^{3+}

Fe^{3+} or Fe^{2+}

Fe^{2+}

DFT Modeling

D1: H_2O-SO_4, SO_4, OH
D2: H_2O, bulk

D1: Fe^{3+} and S=2.5
D2: Fe^{2+} and S=0,1
D3: Fe^{2+} and S=2

Nuclear Resonance Vibrational Spectroscopy (NRVS)

Experimental

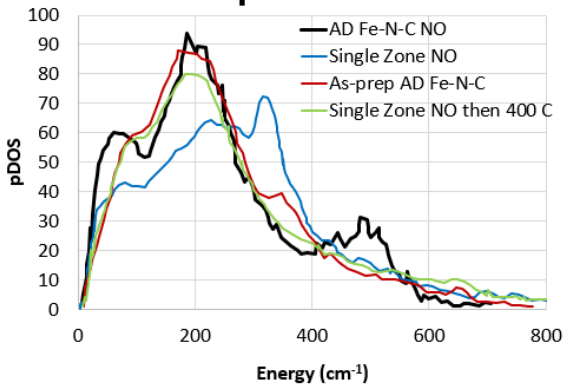

DFT Modeling

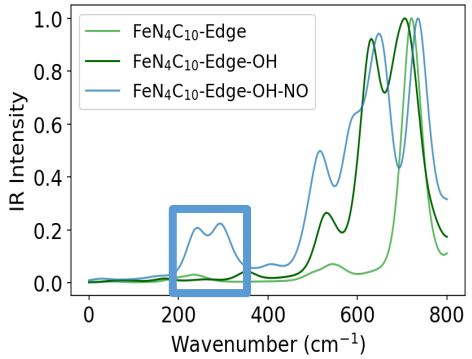

X-ray Absorption Spectroscopy

Experimental

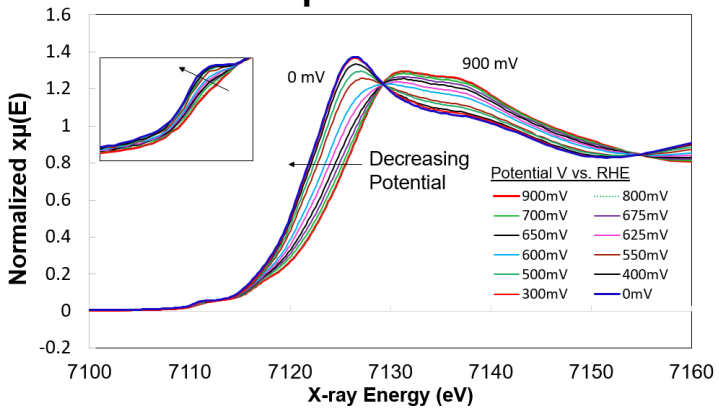

DFT Modeling

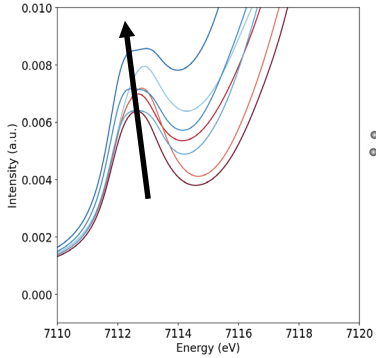

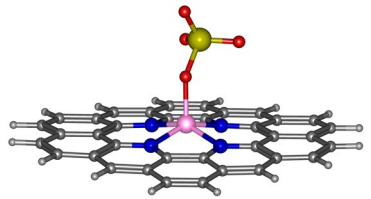

Nuclear Resonance Spectroscopy of Fe-N-C Catalyst with NO Probe

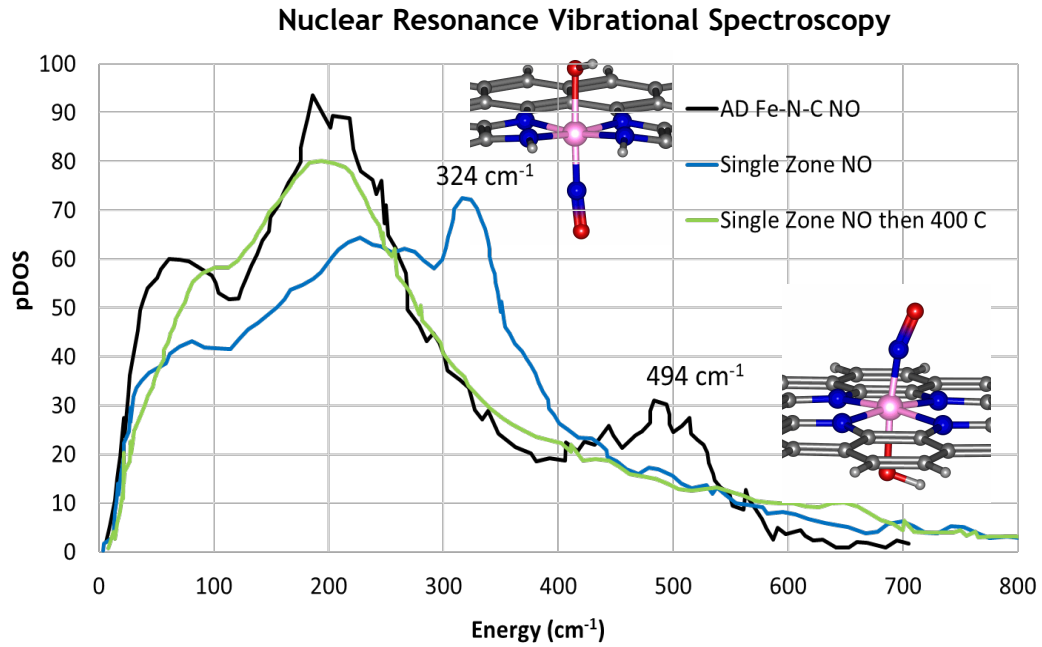

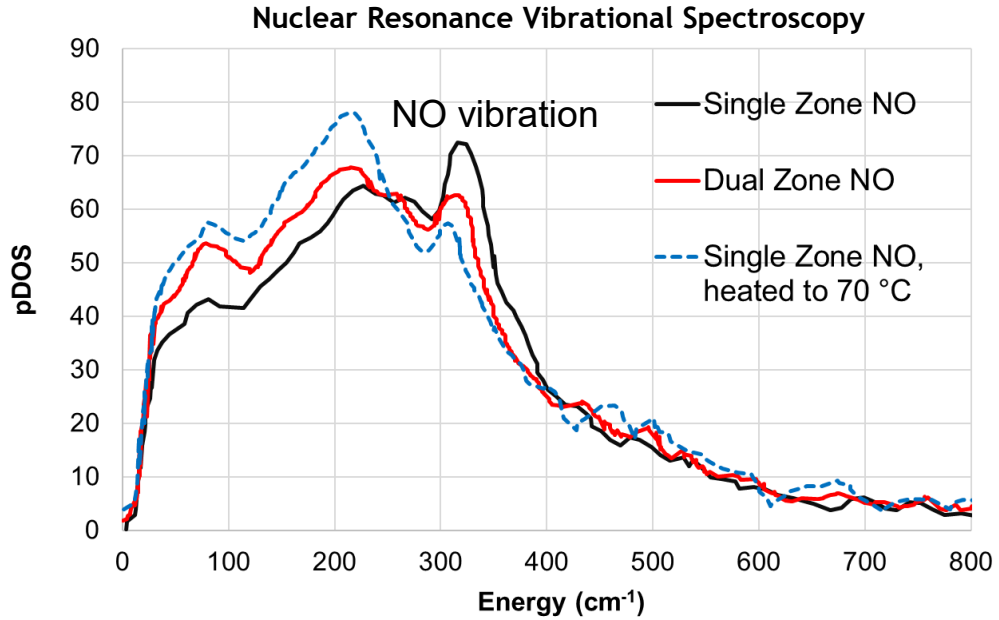

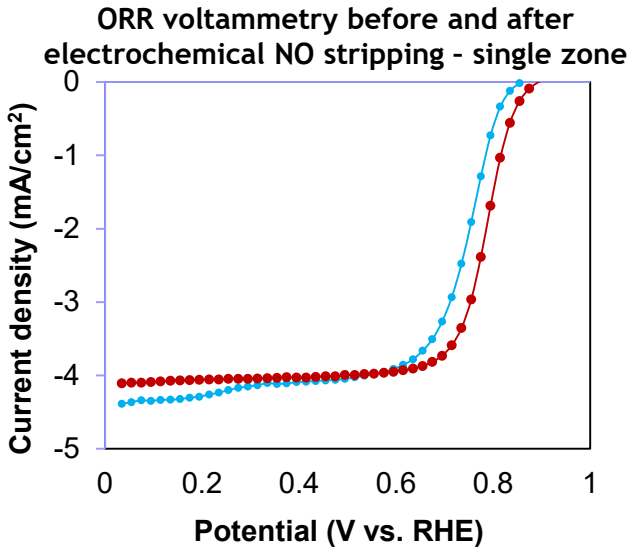

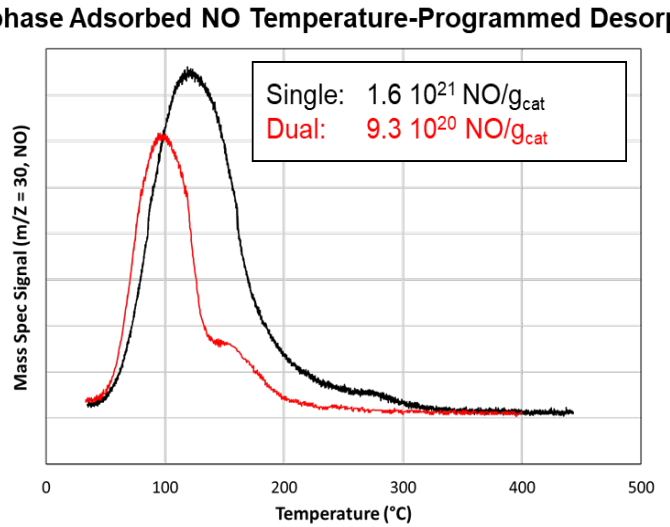

- "Dual zone" and "single zone" Fe-N-C catalysts reversibly adsorb NO from gas phase; 'single zone' adsorbs more NO; NO reversibly poisons ORR
- DFT calculations of Fe vibrational energies (i.e., NRVS bands):
  - ✓ Band at 494 cm^{-1} FeN_4-OH-NO in basal plane for (AD)Fe-N-C
  - ✓ Band at 324 cm^{-1} FeN_4-OH-NO at edge site for single and dual zone catalysts

NO Probe Molecule Studies of Fe-N-C

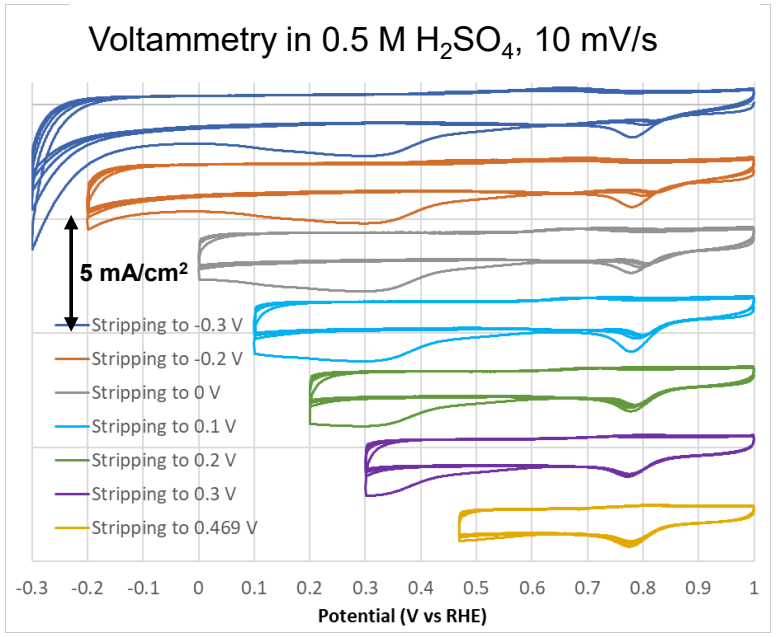

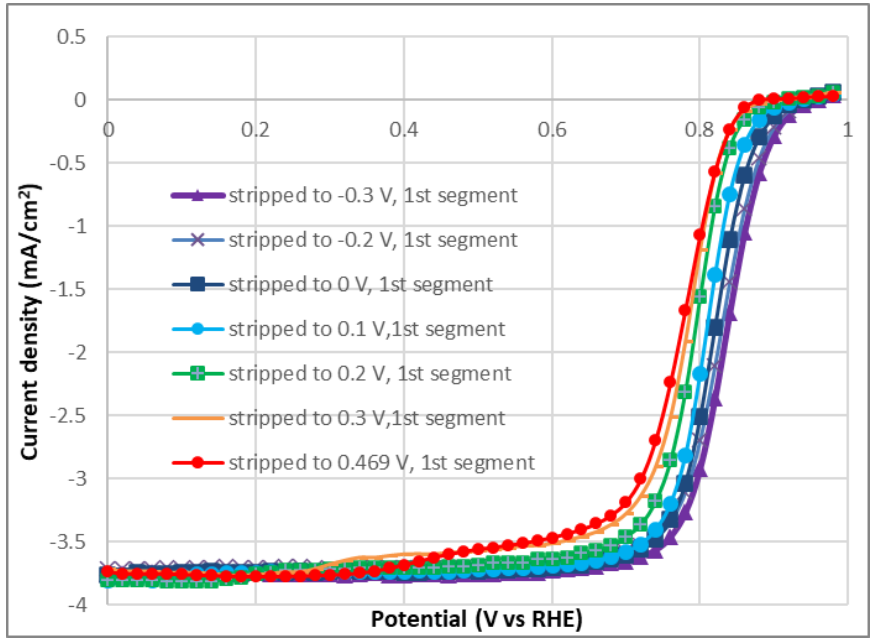

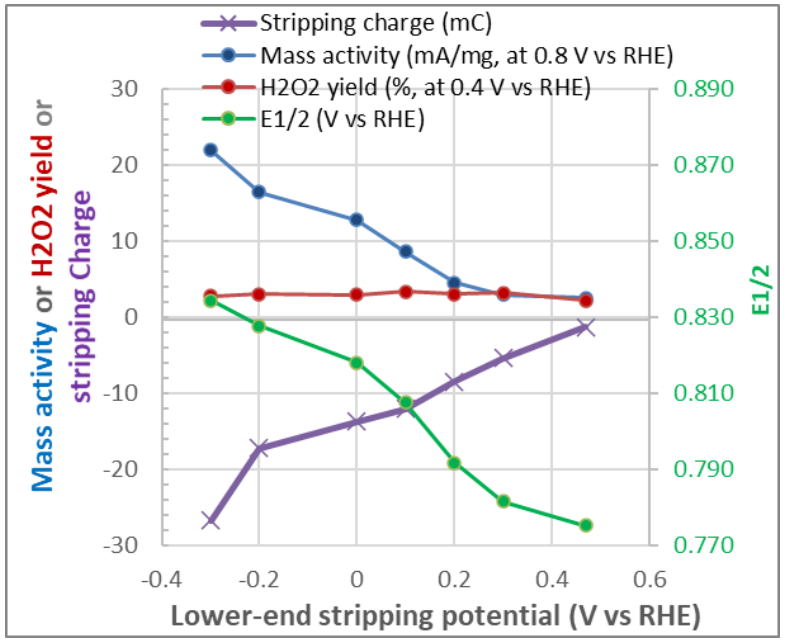

- Exposure of catalyst to gas-phase NO reversibly poisons ORR activity
- ORR activity can be restored in voltametric sweeps to <0.6 V vs RHE
- *In situ* X-ray absorption spectroscopy at Fe K-edge of NO-poisoned Fe-N-C as a function of potential shows that NO adsorbs on Fe (in agreement with NRVS data)
- Potential range over which XAS recovers to that observed for Fe-N-C not exposed to NO correlates with recovery of ORR activity
  - ✓ Fe is part of active site or NO stripping from active site is coincident with NO stripping from Fe
  - ✓ Substantial recovery of ORR between 0 V and -0.3 V with minimal change in Fe XAS indicates that sites other than the Fe sites that adsorb NO are also active for ORR

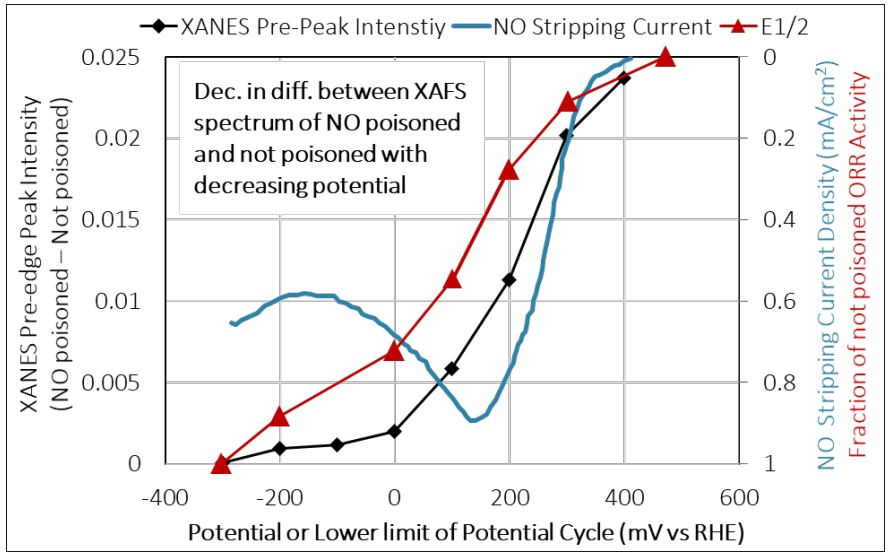

Electrolyte Dependence of Fe Redox in Fe-N-C by In Situ X-ray Absorption Spectroscopy

In situ Fe K-edge X-ray Absorption Spectroscopy

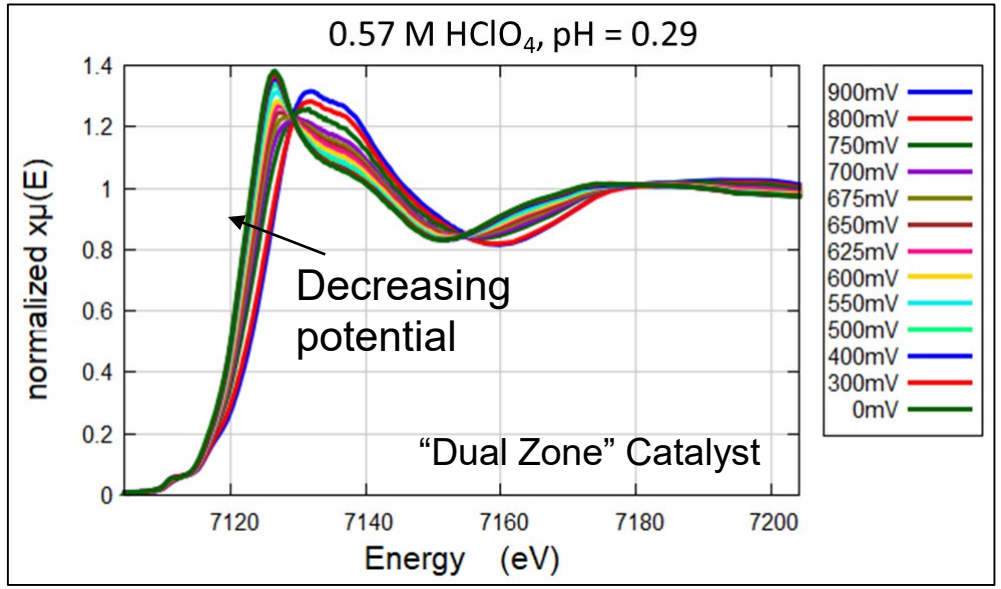

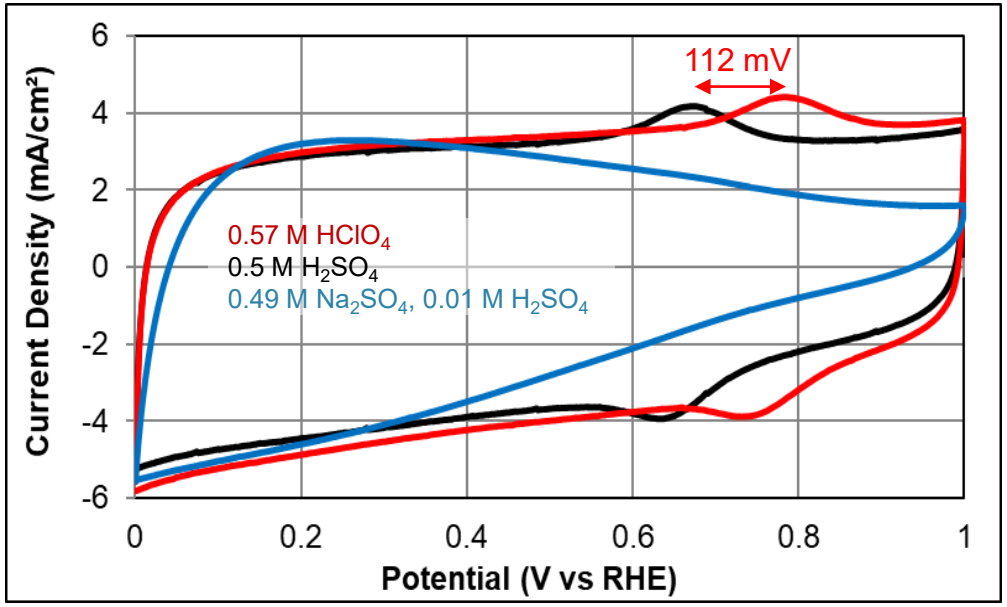

pH 0.29 and 1.9 (acid and sodium sulfate/acid respectively)

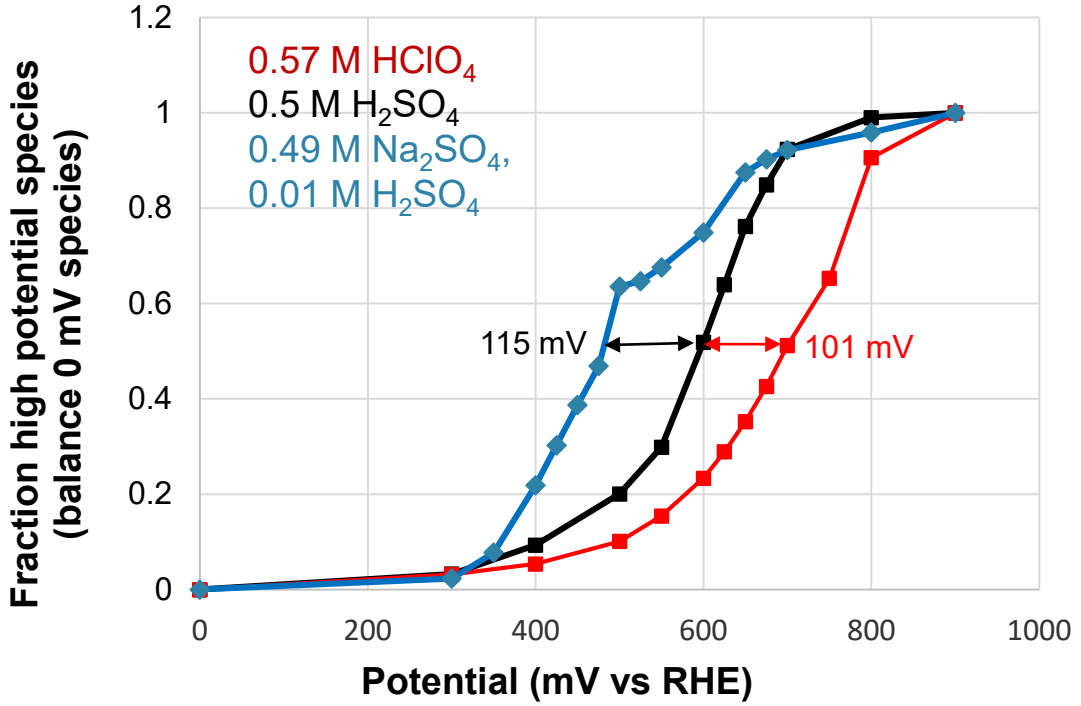

- Observed electrolyte pH dependence of Fe redox potential greater than the 59 mV/pH dependence of RHE
- Observations consistent with electrolyte anion affecting relative stability of Fe in 3+ and 2+ state. Fe^{3+} stability order: SO_4^{2-} > HSO_4^- >> ClO_4^-
- RDE-determined $E_{1/2}$ for ORR are 0.80, 0.79, and 0.63 V for 0.5 M H_2SO_4, 0.57 M $HClO_4$, and 0.49 M Na_2SO_4+0.01 M H_2SO_4, respectively. (single zone catalyst)

Binding Energies of Electrolyte Species to Three Proposed FeN_4 Sites

- Density functional theory calculations using PBE functionals
- C_{10} basal and edge sites more stable in adding OH· to Fe-N-C
- C_{12} basal sites have high binding stability with ionomer analog (CF_3SO_3H)

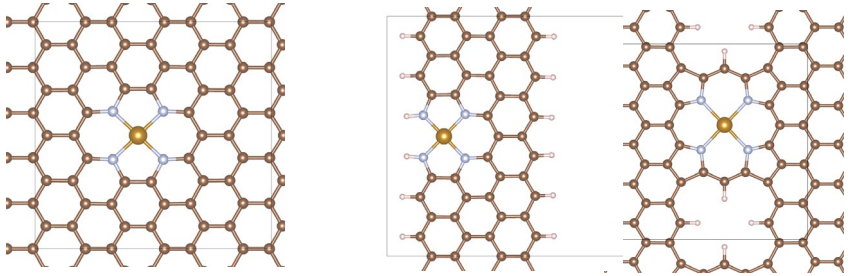

- Calculations show stability order of FeN_4 species is SO_4^{-2} > HSO_4^- > CF_3SO_3H
- Order agrees with order of Fe^{3+}/Fe^{2+} redox couple potential in different electrolytes (as determined via XANES)
- Aqueous electrolyte anions, SO_4^{2-} and HSO_4^- bind stronger than the ionomer analog; ClO_4^- binding strength lower than that of ionomer

Reaction	FeN_4-C_{10}-basal $\Delta G°$ (kcal mol^{-1})	FeN_4-C_{10}-edge $\Delta G°$ (kcal mol^{-1})	FeN_4-C_{12}-basal $\Delta G°$ (kcal mol^{-1})
FeN_4-CF_3HSO_3 + OH· → FeN_4-CF_3HSO_3-OH	-66.04	-66.69	-67.14
FeN_4-OH + CF_3HSO_3 → FeN_4-CF_3HSO_3-OH	-1.45	-1.28	-1.59
FeN_4 + CF_3HSO_3 → FeN_4-CF_3HSO_3	-2.56	-1.94	-4.28
$[FeN_4$-$HSO_4]^-$ + OH· → $[FeN_4$-HSO_4-$OH]^-$	-62.50	-52.98	-51.79
FeN_4-OH + $[HSO_4]^-$ → $[FeN_4$-HSO_4-$OH]^-$	10.99	-0.07	8.23
FeN_4 + $[HSO_4]^-$ → $[FeN_4$-$HSO_4]^-$	6.34	-13.91	-10.36
$[FeN_4$-$SO_4]^{-2}$ + OH· → $[FeN_4$-SO_4-$OH]^{-2}$	-63.96	-51.17	-56.23
FeN_4-OH + $[SO_4]^{-2}$ → $[FeN_4$-SO_4-$OH]^{-2}$	-8.95	-39.46	-26.37
FeN_4 + $[SO_4]^{-2}$ → $[FeN_4$-$SO_4]^{-2}$	-12.14	-55.10	-40.52

Reaction	FeN_4-C_{10}-basal $\Delta G°$ (kcal mol^{-1})	FeN_4-C_{10}-edge $\Delta G°$ (kcal mol^{-1})	FeN_4-C_{12}-defect $\Delta G°$ (kcal mol^{-1})
FeN_4-OH + H_2O → FeN_4-OH-H_2O	-1.01	-3.22	-4.01
FeN_4-H_2O + OH· → FeN_4-OH-H_2O	-62.97	-62.94	-62.49

Lowest energy

PGM-free OER Electrocatalysts

Water Electrolysis: PGM Performance Baseline in PEM and AEM Electrolyzers

CCM fabrication method; Anode: IrO_2, 0.4 mg_{Ir} cm^{-2}, spray coating on sintered Ti PTL; **Cathode:** 50% Pt on C, 0.1 mg_{Pt} cm^{-2}, MGL370 GDL; **Cell:** 5 cm^2 electrode area; **Membrane:** Nafion N115; **Temperature:** 80 °C

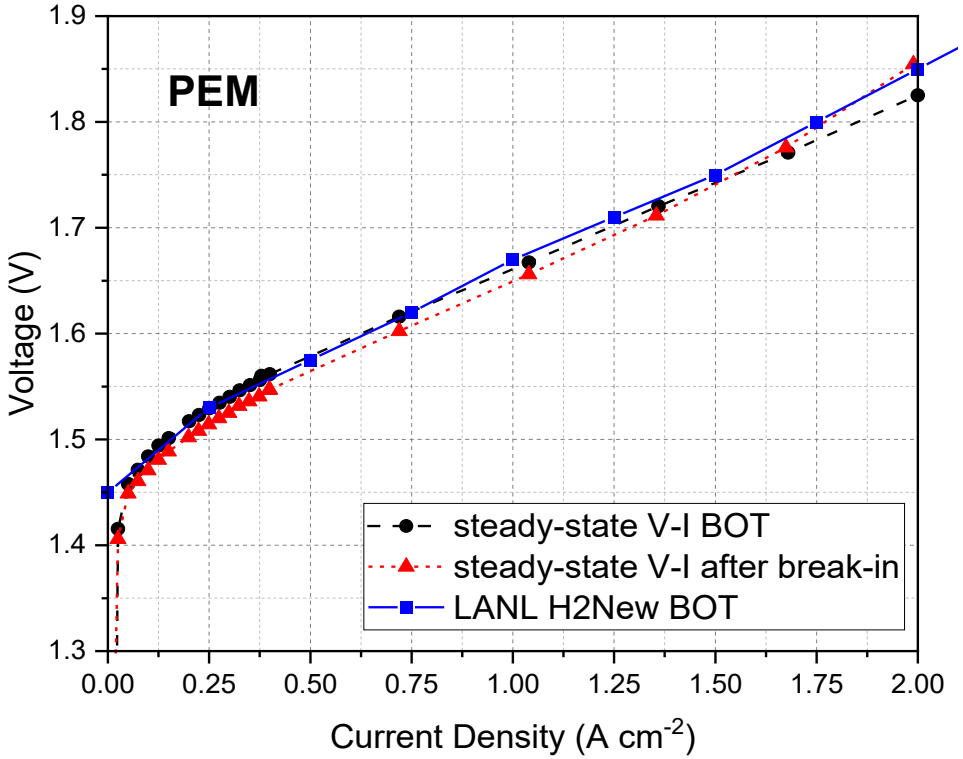

GDE fabrication method; Anode: IrO_2 (AlfaAesar) ~1.5 mg_{Ir}/cm^2, spray coating on sintered Ti PTL; **Cathode**: Pt 40% Ru 20% on C ~1 mg_{Pt}/cm^2, spray coating on MGL370 GDL; **Cell:** 5 cm^2 electrode area; **Membrane:** Versogen Piper-Ion (40 µm); **Temperature:** 70 °C

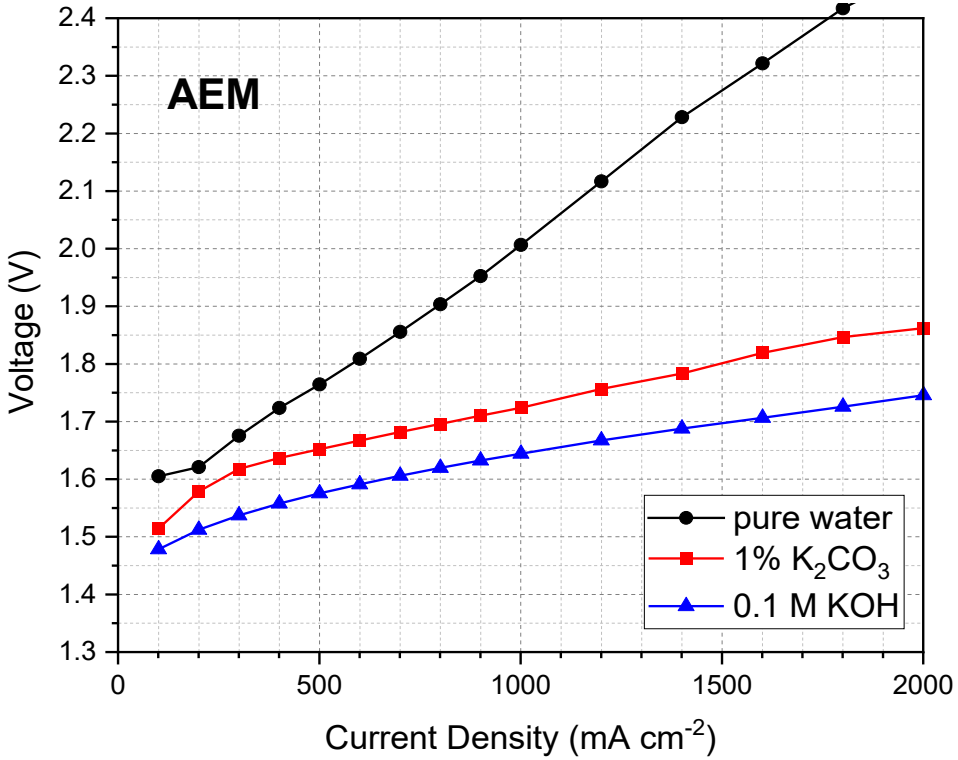

- **PEM:** H2NEW MEA fabrication and testing approach followed; electrolyzer performance matched
- **AEM:** Performance matching or exceeding recent literature results obtained with AEM LTE and PGM anode and cathode catalysts in both pure water and with supporting electrolyte*

* D. Li *et al.*, *Nat. Energy* **378**, 378–385 (2020); G. Lindquist *et al.*, *ACS Appl. Mater. Interfaces* **13**, 51917−51924 (2021)

LANL/Pajarito (OER49B) Perovskite Catalyst ($La_xSr_{1-x}CoO_{3-\delta}$): AEM Electrolyzer Testing

Unlike IrO_2, PGM-free catalysts detach from PTL when exposed to pure water if ink is prepared using only the AE ionomer → ***binder needed***

GDE fabrication method; Anode: ~3.5 mg cm^{-2} PGM-free catalyst, spray coating on sintered Ti PTL; **Cathode**: Pt 40% Ru 20% on C ~1 mg_{Pt}/cm^2, spray coating on MGL370 GDL; **Cell:** 5 cm^2 electrode area; **Membrane:** Versogen Piper-Ion (40 µm); **Temperature:** 80 °C

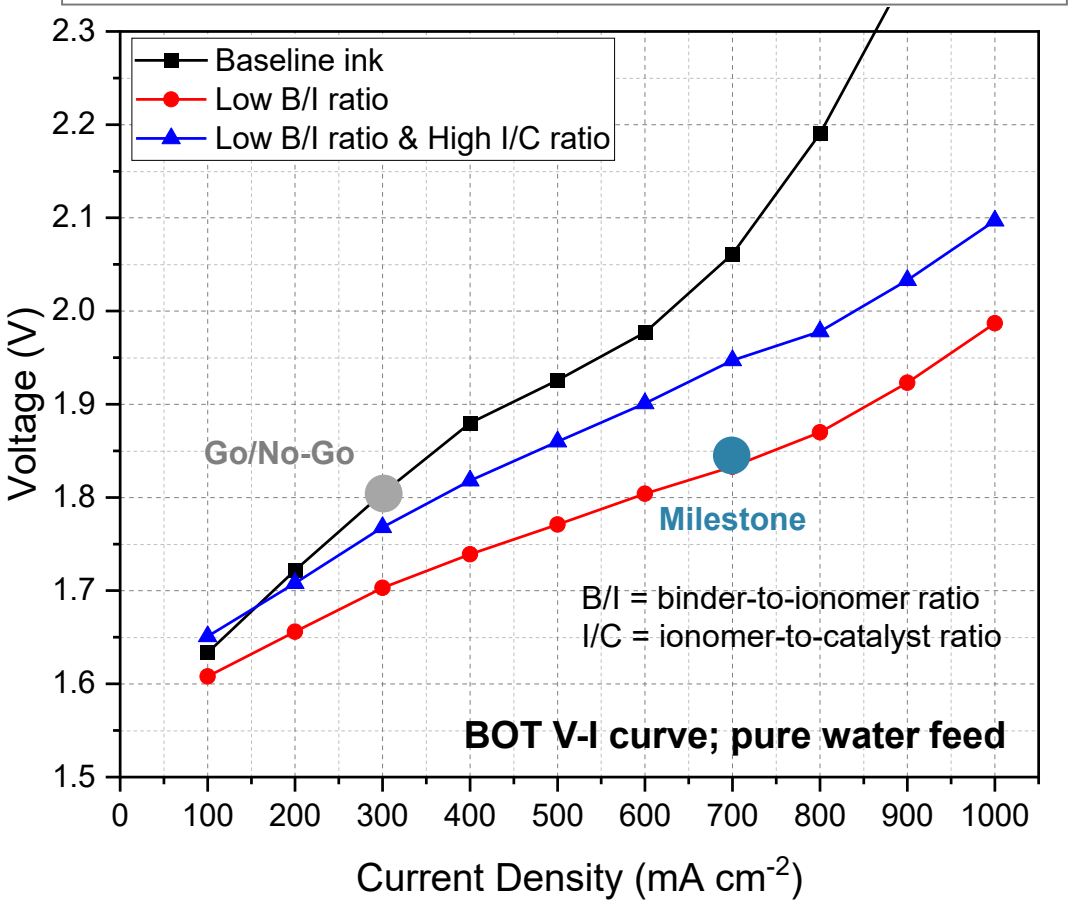

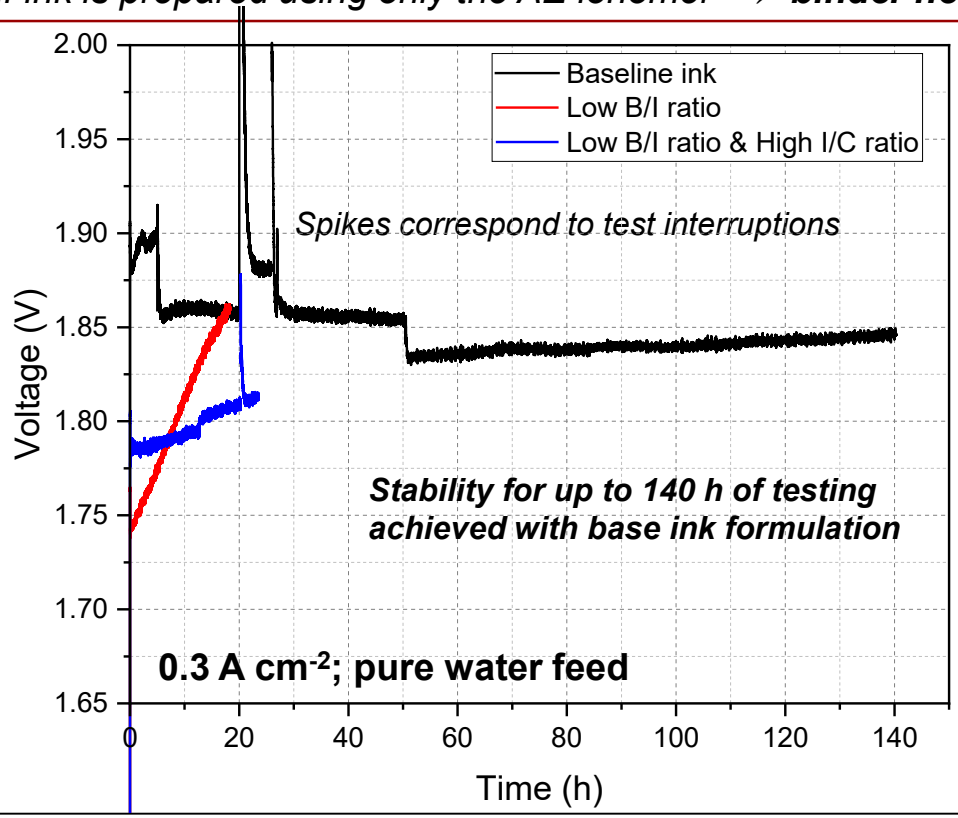

- **Highlight:** LSC OER49B catalyst meets **FY21 go/no-go target** with all ink formulations; baseline ink also satisfies both **FY21 go/no-go activity and durability targets**
- **Highlight:** LSC OER49B catalyst meets **FY21 activity milestone** with low B/I ratio ink
- Activity-durability tradeoffs observed with different inks

WSU NiFe Catalyst: AEM Electrolyzer Testing

GDE fabrication method; Anode: ~3.5 mg cm^{-2} PGM-free catalyst, spray coating on sintered Ti PTL; **Cathode**: Pt 40% Ru 20% on C ~1 mg_{Pt}/cm^2, spray coating on MGL370 GDL; **Cell:** 5 cm^2 electrode area; **Membrane:** Versogen Piper-Ion (40 µm); **Temperature:** 80 °C

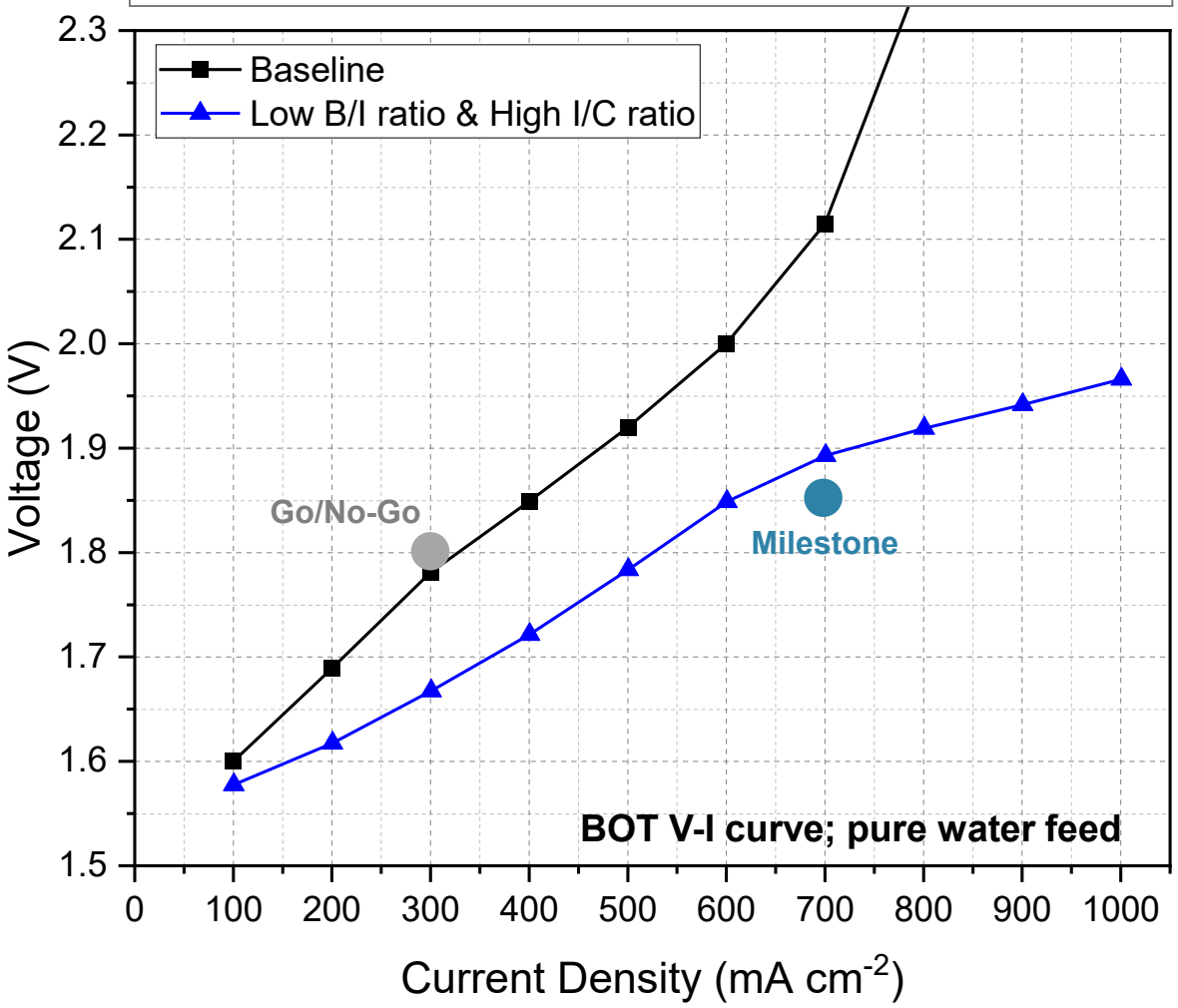

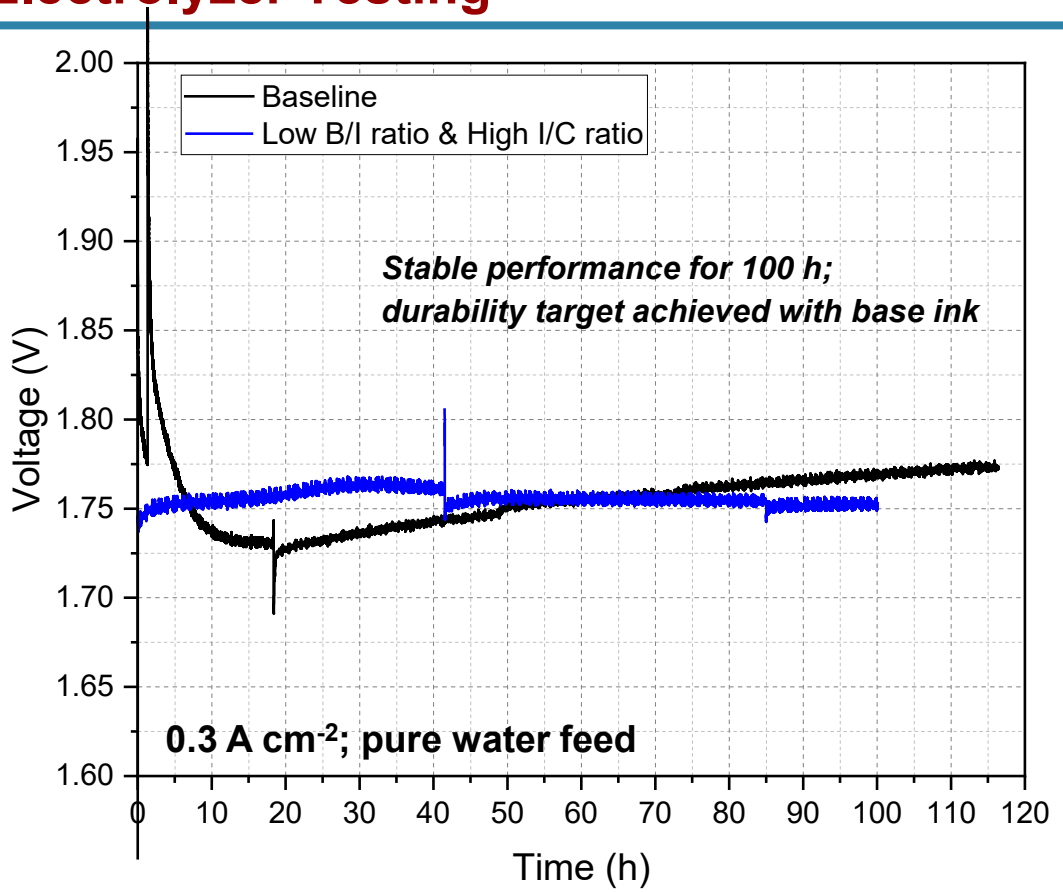

- **Highlight:** WSU NiFe catalyst meeting **FY21 go/no-go activity target** with both ink formulations
- Catalyst activity only *ca.* 40 mV away from **FY21 activity milestone** using optimized ink
- **Highlight:** NiFe catalyst **meeting go/no-go activity** and **durability milestone targets** in > 100 h test with both inks

Pure-Water Electrolyzer *vs.* "Pseudo" Pure Water Electrolyzer

GDE fabrication method; Anode: ~3.5 mg cm^{-2} NiFe WSU catalyst, spray coating on sintered Ti PTL; **Cathode**: Pt 40% Ru 20% on C ~1 mg$_{Pt}$/cm^2, spray coating on MGL370 GDL; **Cell:** 5 cm^2 electrode area; **Membrane:** Versogen Piper-Ion (40 μm); **Temperature:** 70 °C

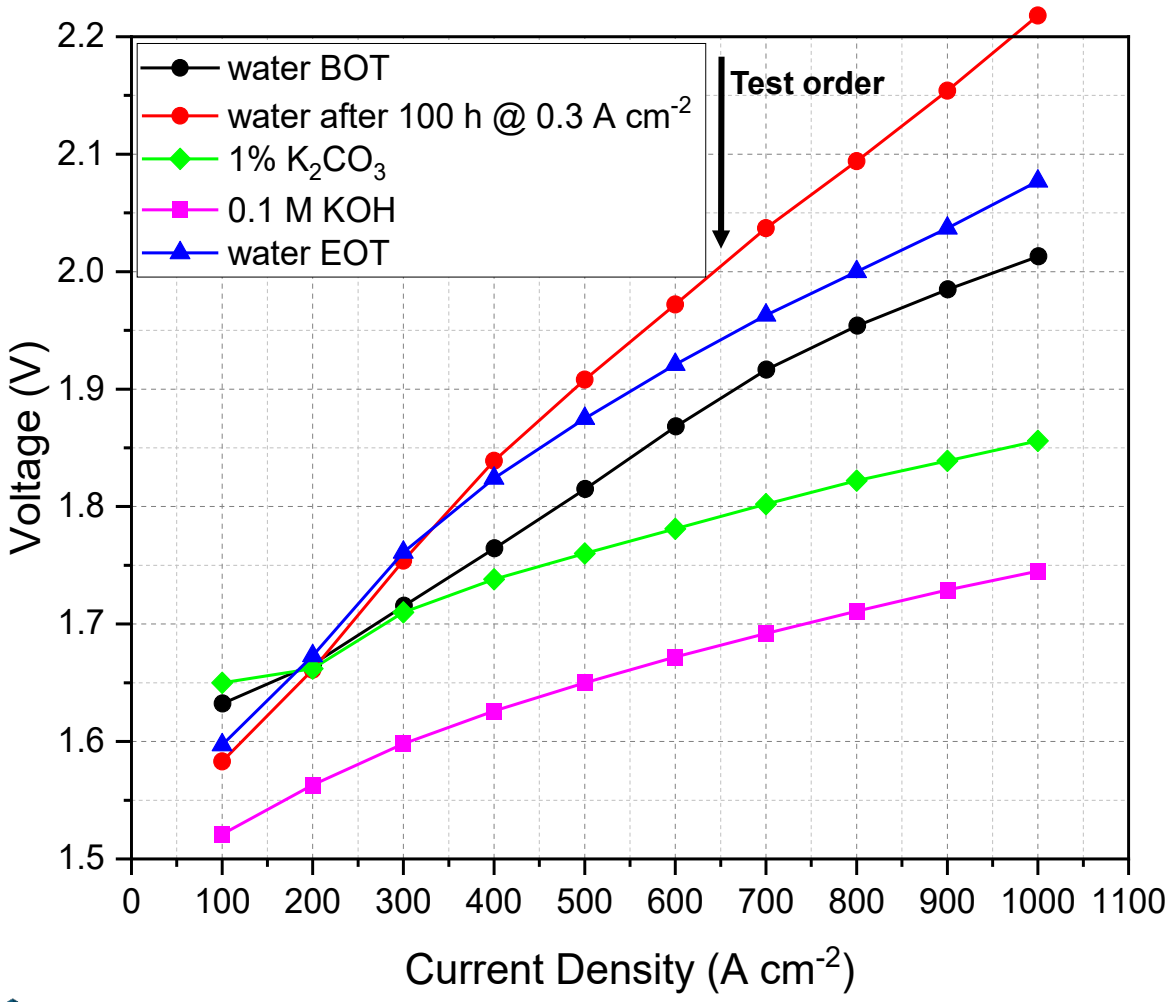

Ion Transport in Pure Water *vs.* KOH Electrolyte

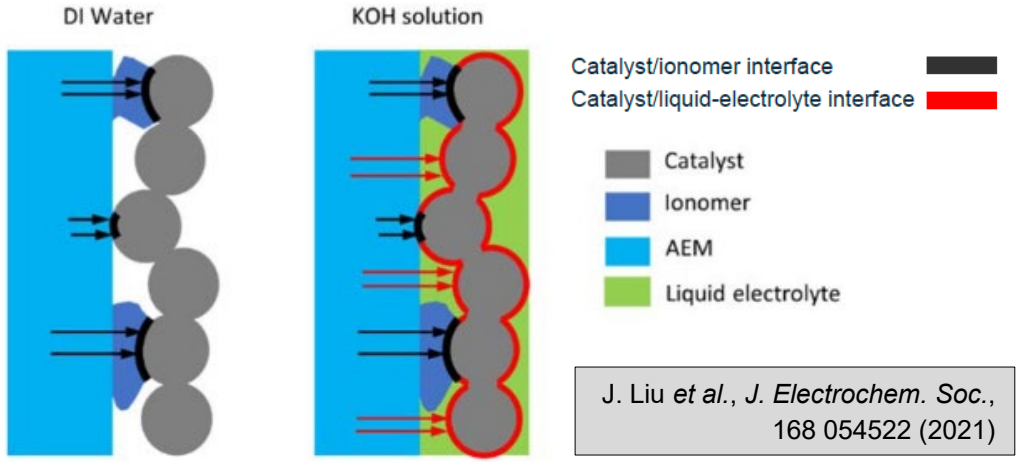

J. Liu *et al.*, *J. Electrochem. Soc.*, 168 054522 (2021)

- Electrolyzer performance in pure water after testing in a supporting electrolyte and flushing with > 2 L of water remains higher than on pure water before exposing to the supporting electrolyte
- **Highlight:** System **must not be exposed to electrolyte** before assessing electrolyzer performance on pure water
- The results agree with the findings by G. Lindquist *et al.*, *ACS Appl. Mater. Interfaces* **13**, 51917−51924 (2021)
- Modeling suggests benefits of the electrolyte use beyond mere lowering of the HFR, especially, to OER kinetics

Synthesis and Characterization of Aerogel-Derived NiFe Oxide Catalysts

Goal: *Increase the surface area of Ni-Fe oxide beyond typical 5-20 m^2/g*

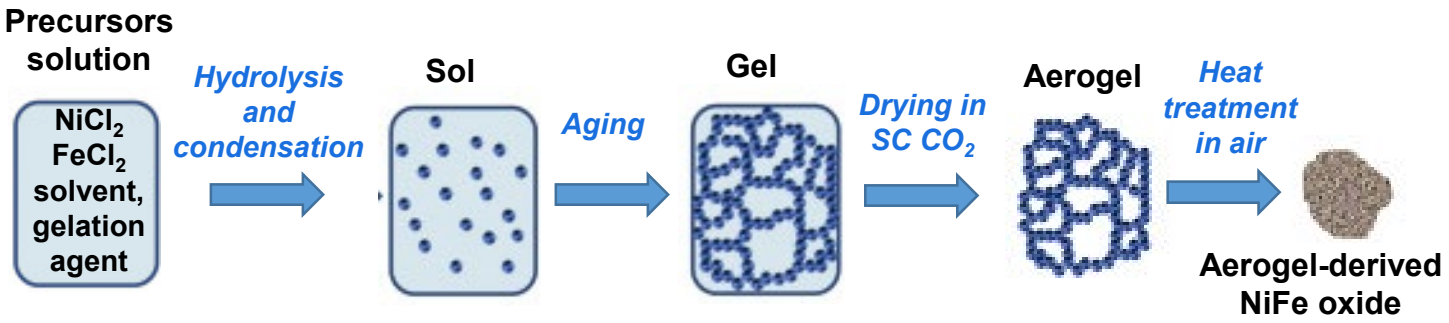

Solvent removed; "gel-like" morphology retained

Gels after aging for 2 days

NiFe 8:1 series aerogels

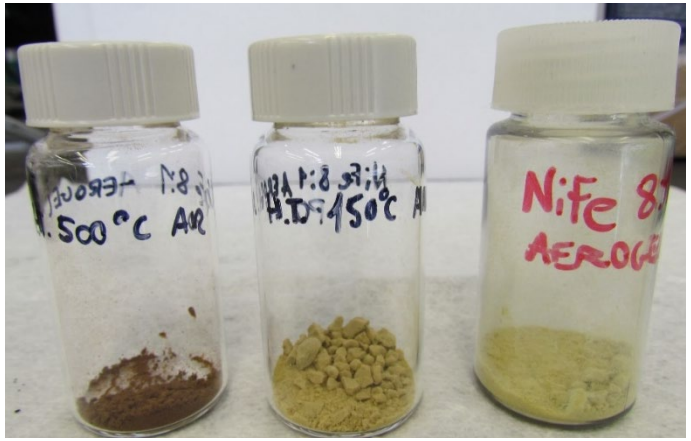

Aerogel after H.T. 500 °C | **Aerogel after H.T. 150 °C** | **Aerogel before H.T.**

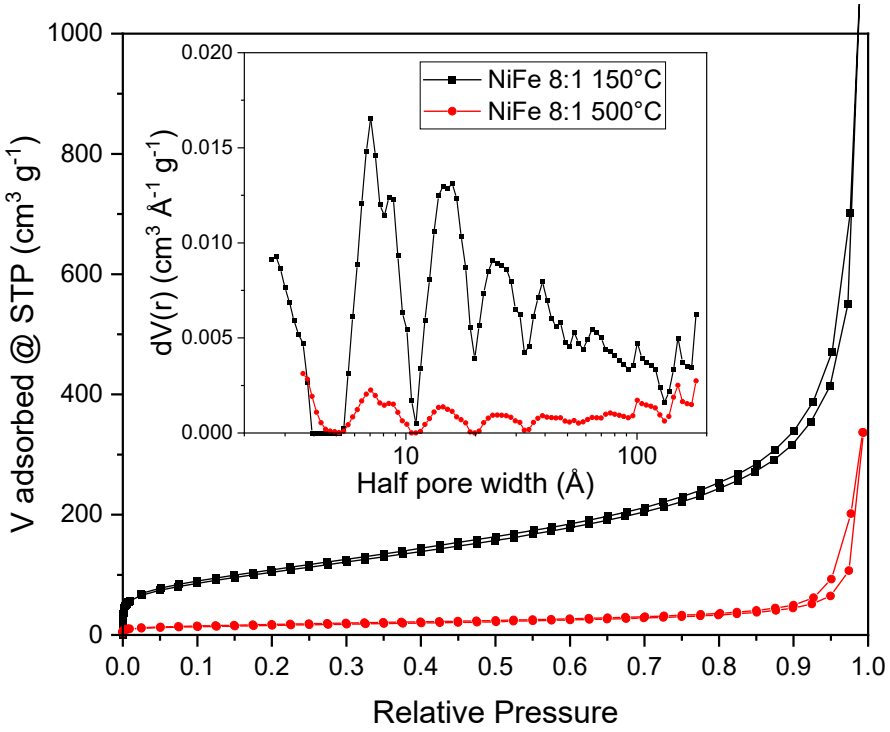

NiFe 8:1 H.T. 150 °C:

- BET surface area **382 m^2/g**
- Pore volume 0.85 cm^3/g
- Pore size 1-10 nm, with some 0.5 - 0.8 nm (micropores)

NiFe 8:1 H.T. 500 °C:

- BET surface area: 55 m^2/g
- Pore volume: 0.21 cm^3/g
- Pore size: like in H.T. 150 °C sample

OER Activity of Aerogel-Derived NiFe Oxide Catalysts

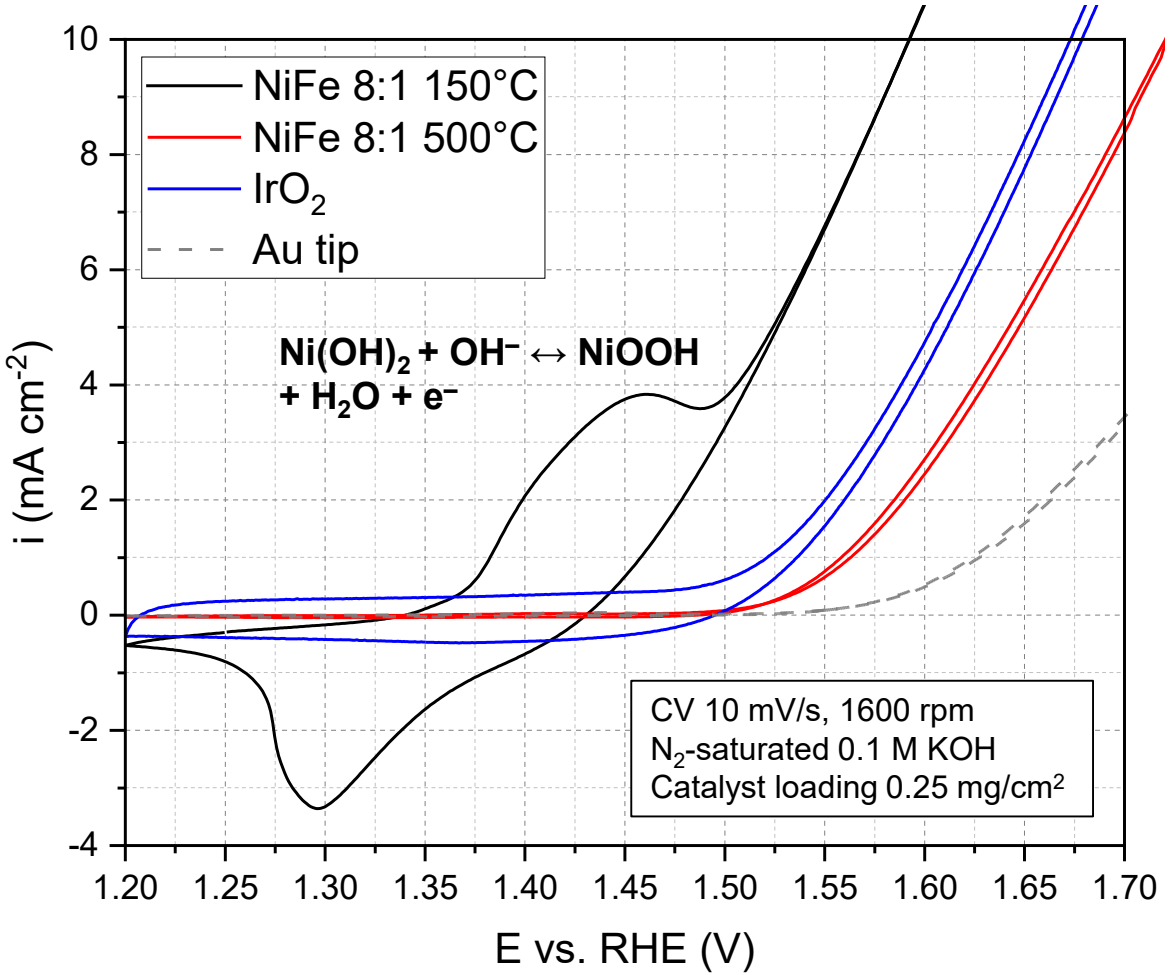

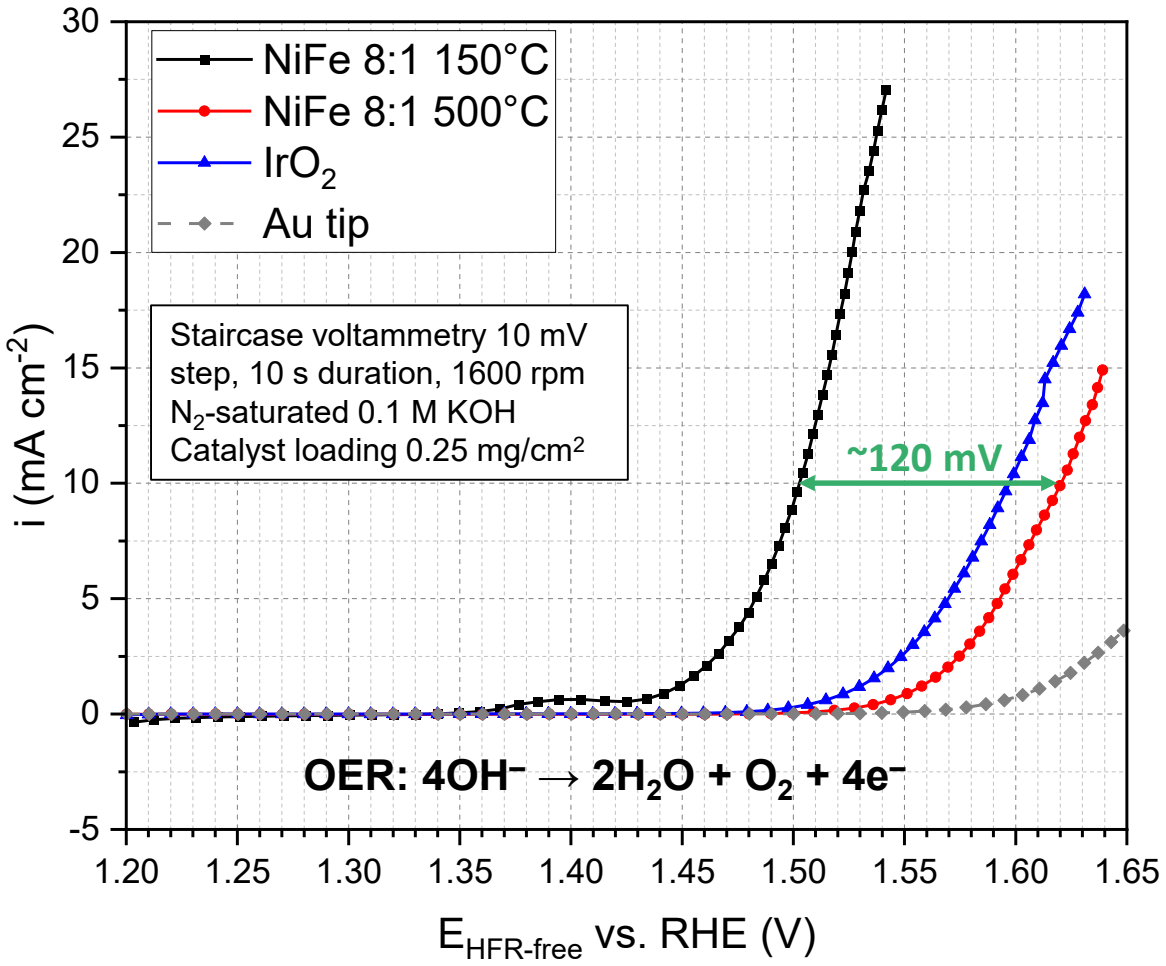

- **NiFe 8:1 H.T. 150 °C:** Large redox peaks at potentials below OER onset, attributed to Ni(II)/Ni(III) redox couple
- **NiFe 8:1 H.T. 500 °C:** No redox peak evident, low capacitance

- Loss of OER activity after heat treatment at 500 °C
- **NiFe 8:1 H.T. 150 °C:** $E_{HFR\text{-}free}$ (10 mA cm^{-2}) = 1.50 V *vs.* RHE
- **NiFe 8:1 H.T. 500 °C:** $E_{HFR\text{-}free}$ (10 mA cm^{-2}) = 1.62 V *vs.* RHE

Effect of Catalyst Heat Treatment Temperature: Electrolyzer Performance

GDE fabrication method; Anode: ~1.5 mg cm^{-2} catalyst, spray coating on sintered Ti PTL; **Cathode**: Pt 40% Ru 20% on C ~1 mg$_{Pt}$/cm^2, spray coating on MGL370 GDL; **Cell:** 5 cm^2 electrode area; **Membrane:** Versogen Piper-Ion (40 µm); **Temperature:** 70 °C

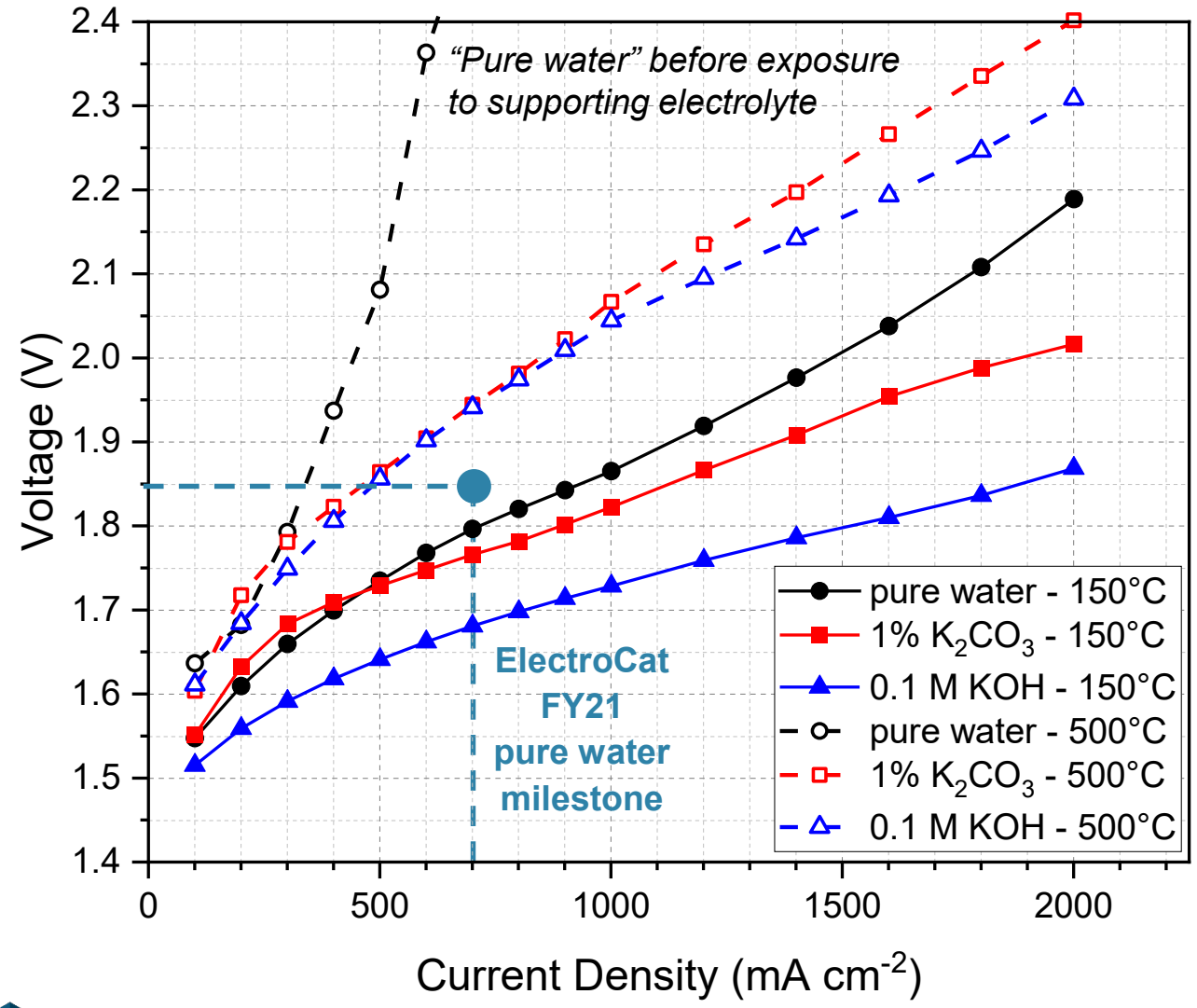

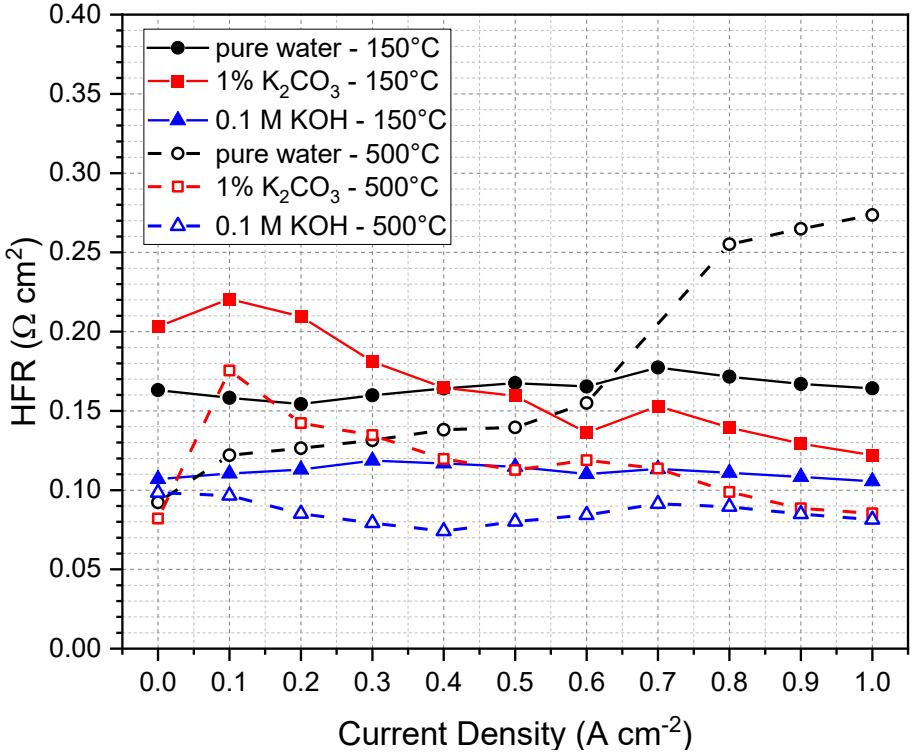

- Performance in AEM electrolyzer of catalyst heat-treated at 150 °C vs. 500 °C reflects OER activity trend determined in RDE testing
- HFR is not the reason for lower performance of MEA with catalyst heat-treated at 500 °C
- **Highlight:** Catalyst heat-treated at 150 °C **meets FY21 ElectroCat pure-water milestone**

NIFe Catalyst Characterization Before and After Testing

Elemental Composition by STEM-EDS

Sample	C	F	O	Fe	Ni
NiFe 8:1 aerogel	41.3 ± 4.0	-	44.2 ± 2.7	1.8 ± 0.15	12.7 ± 1.1
Catalyst H.T. 150 °C	38.0 ± 5.1	-	46.0 ± 3.3	1.9 ± 0.2	14.0 ± 1.6
Catalyst H.T. 500 °C	75.4 ± 10.4	3.9 ± 0.4	16.1 ± 8.1	0.6 ± 0.32	3.9 ± 2.1

Catalyst H.T. 150 °C	Ni/Fe (atomic ratio)	Fe at.% (of all metal)	Metal/O (atomic ratio)
Before testing	7.4 ± 0.1	11.9 ± 0.15	0.34 ± 0.015
After testing	6.9 ± 1.1	13.0 ± 2.0	0.27 ± 0.018

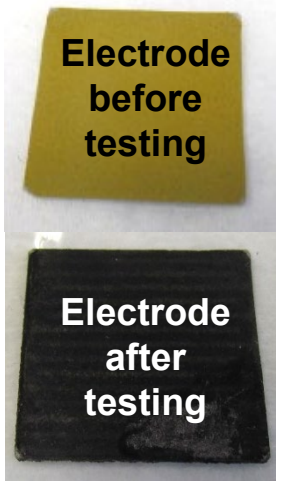

- No loss of Fe during testing
- Further oxidation during testing
- During testing, catalyst changed color from green-yellow to black (also observed in RDE)
- Aerogel and sample heat-treated at 150 °C are amorphous, also after testing
- Sample heat-treated at 500 °C is mostly NiO

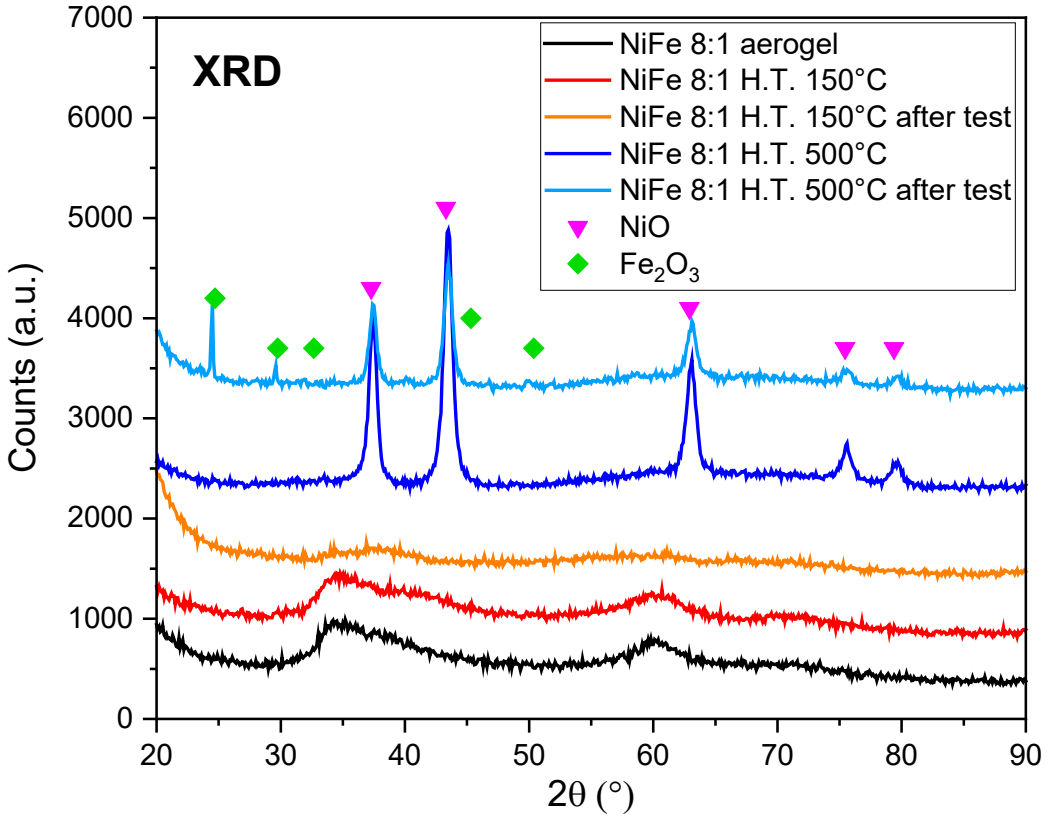

Characterization Before and After Testing: NiFe 8:1 Catalyst Heat-Treated at 150 °C

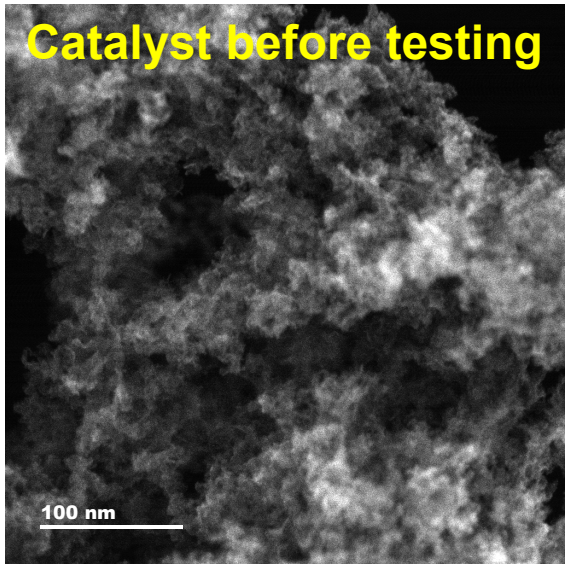

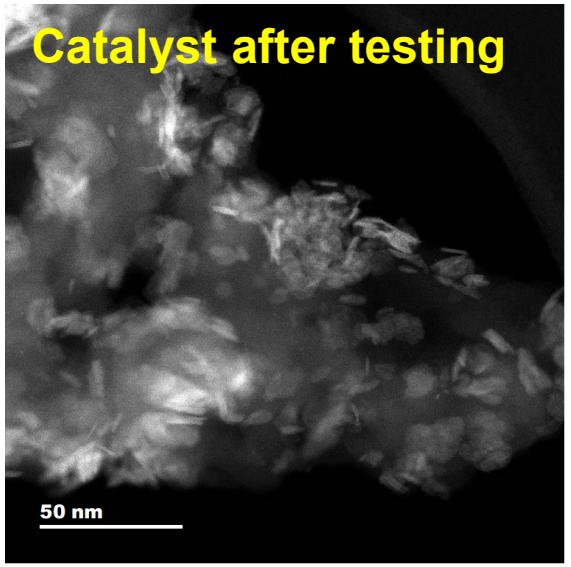

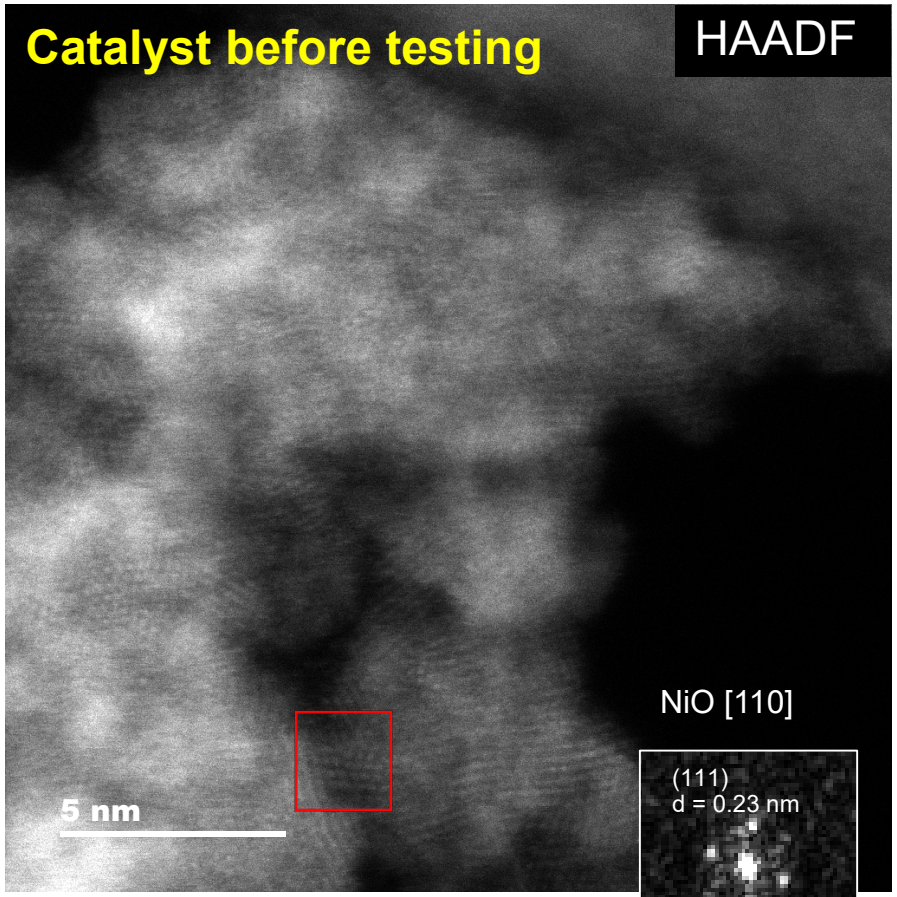

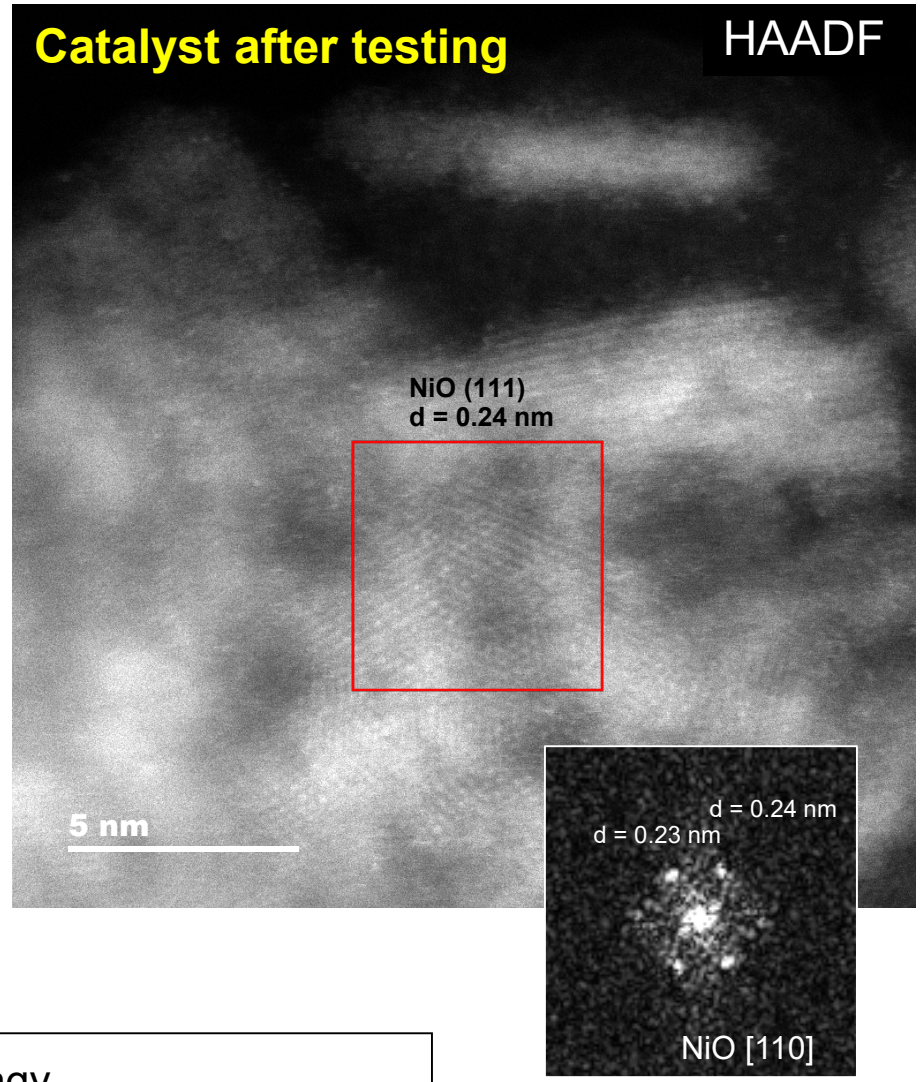

- Catalyst before testing is porous / spongy
- Crystal grains of the oxide become needle-like after testing

FY22 OER Go/No-Go & Milestone Status

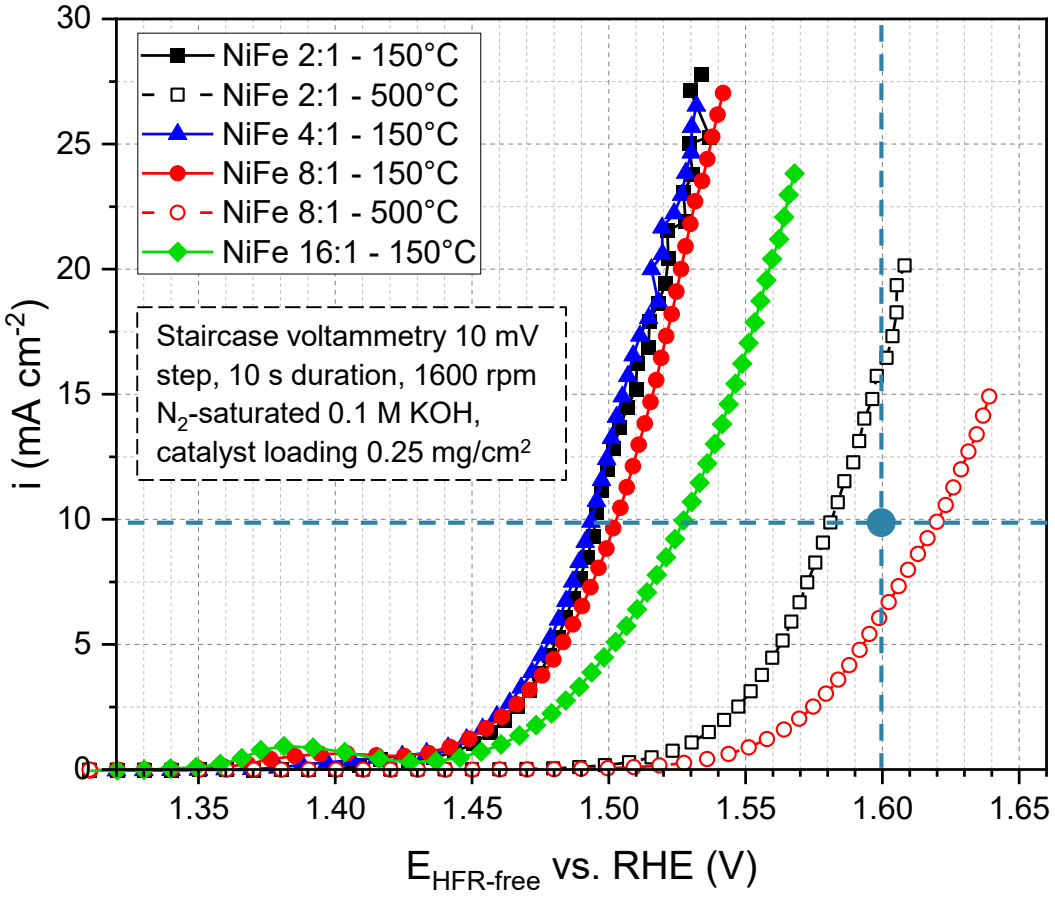

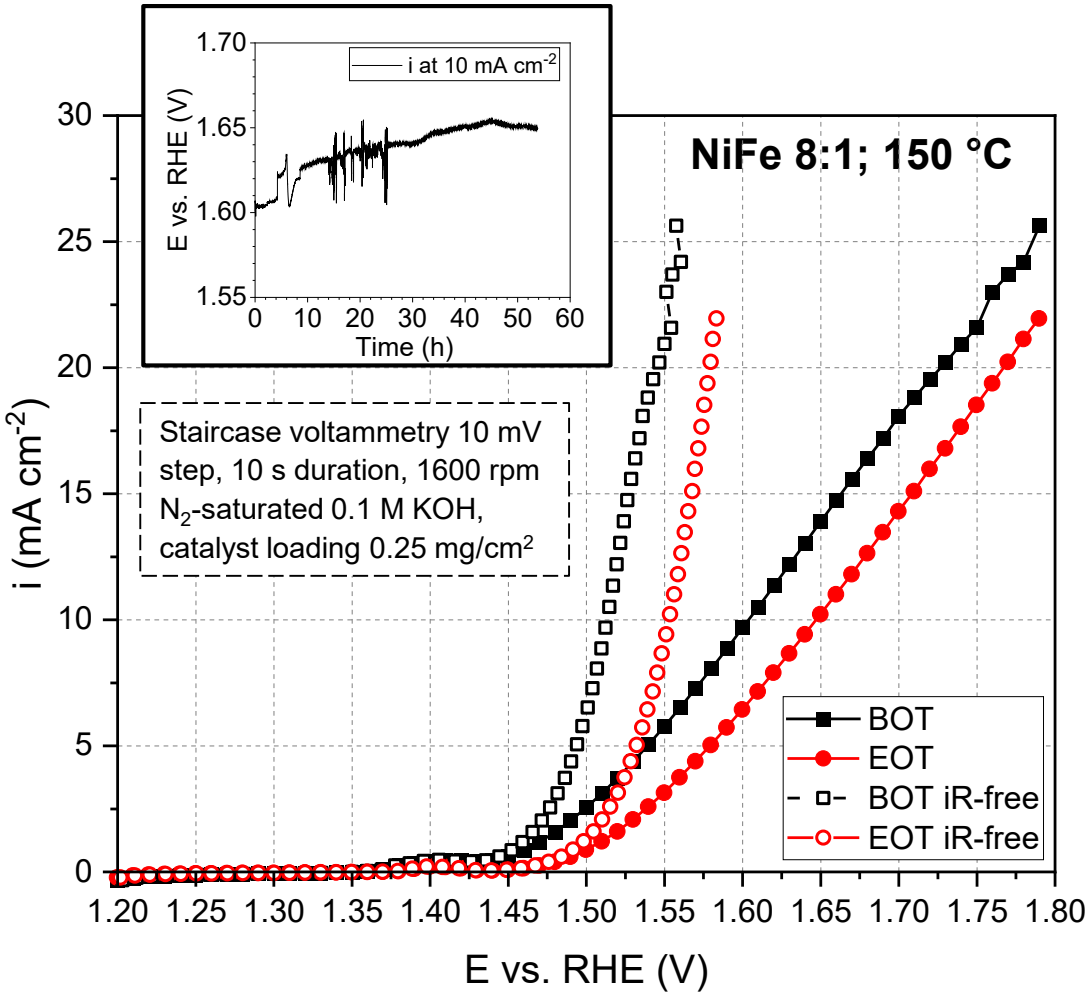

Highlight: **FY22 Go/No-Go** OER activity of ≤ 1.60 V *vs.* RHE (*iR*-free) at 10 mA cm^{-2} **exceeded** with several aerogel-derived mixed NiFe oxide catalysts

Highlight: **FY22 OER Annual Milestone** of 10 mA cm^{-2} at ≤ 1.55 V and ≤ 1.0 mV/h potential loss during 48 h durability test **exceeded** with 10 mA cm^{-2} at 1.51 V and 0.74 mV/h in 54 h test

Hierarchical Nanoporous OER Catalysts Derived from Multi-Cation MOFs

- A series of multi-cation MOF-derived OER catalysts were developed with varying ratios of the two active metals
- The catalysts displayed high OER activity and stability in aqueous electrolyte
- The effect of Ni/Fe ratio and Ni-Fe content in MOF on the structure and morphology of the catalyst and the resulting OER activity was studied
- Maintaining the precursor MOF structure is essential to achieve high OER activity. A critical Ni/Fe ratio to maintain this structure has been identified

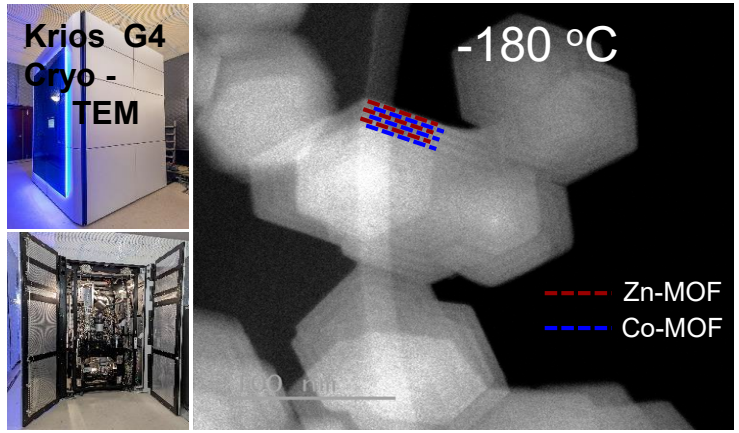

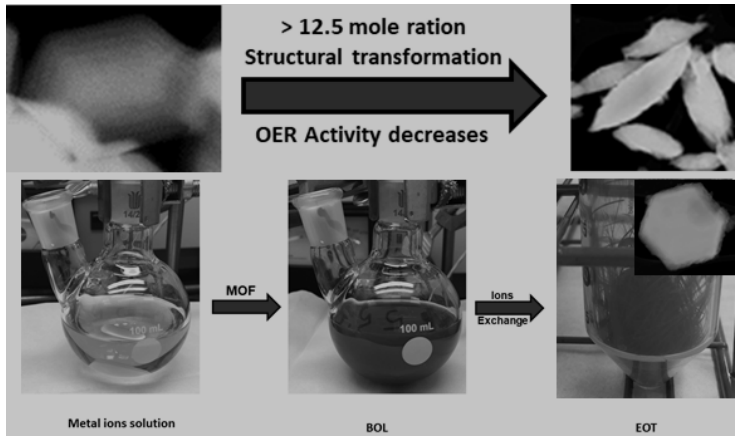

Catalyst loading: 50 μg/cm²; O_2-sat. 0.1 M KOH

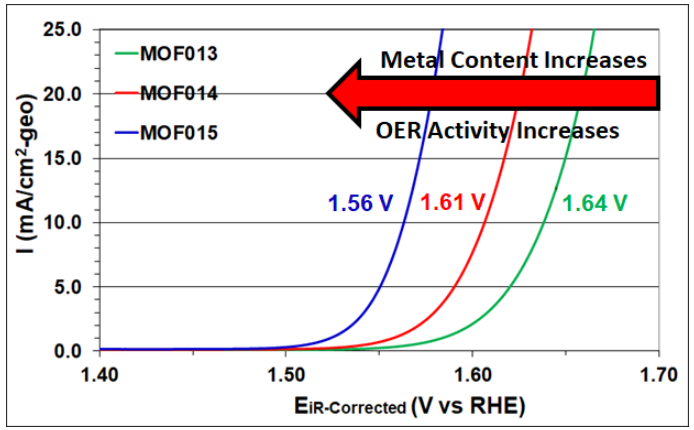

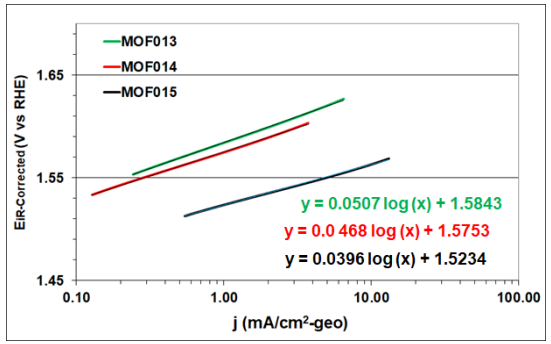

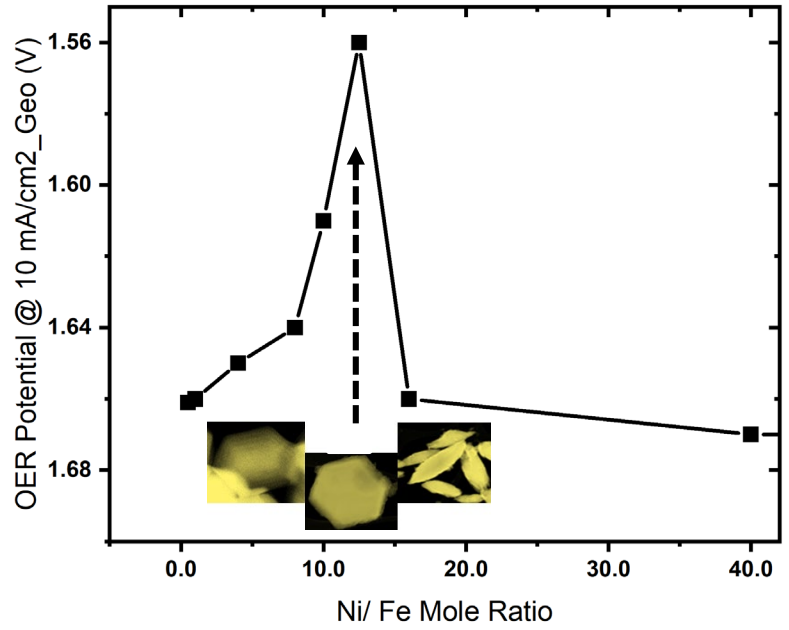

Hierarchical Nanoporous OER Catalysts Derived from Multi-Cation MOFs

- OER performance of MOF-derived catalyst with Ni/Fe ratio of 12.5 in MOF improved after the activation step (galvanostatic hold at 10 mA/cm^2)
- Catalyst passed go/no-go (48 h at 10 mA/cm^2) and was scaled up for MEA evaluation at LANL

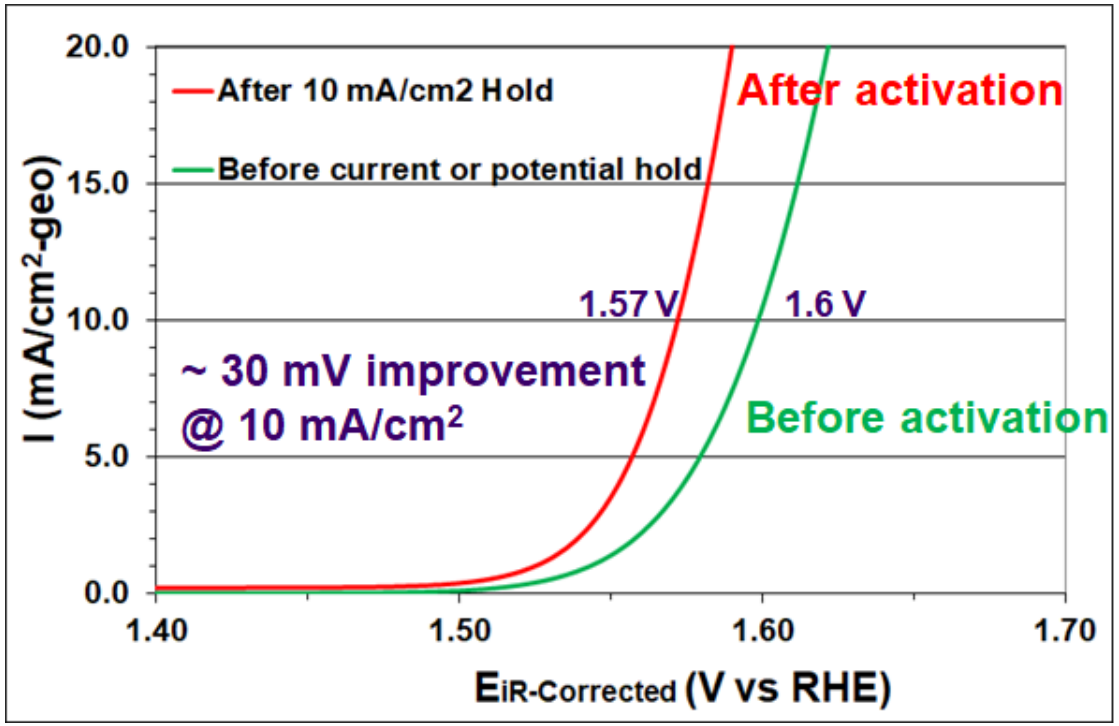

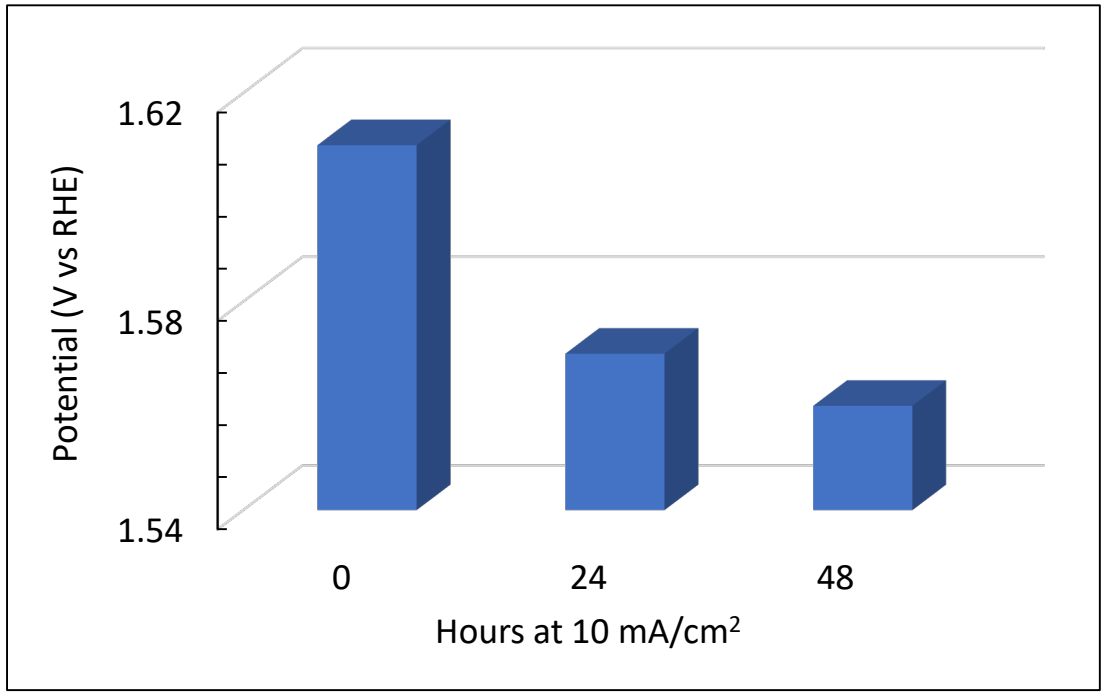

Highlight: **Exceeded FY22 Q1 Go/No-Go** of OER potential ≤1.6 V (iR-corrected) vs RHE at 10 mA cm^{-2} at beginning of test in aqueous alkaline electrolyte and ≤1 mV/hr potential loss during 48 h at 10 mA cm^{-2}.

Collaboration and Coordination: Summary

- **ElectroCat members:** Four national laboratories:

Los Alamos NATIONAL LABORATORY — Los Alamos National Laboratory – ElectroCat co-Lead

Argonne NATIONAL LABORATORY — Argonne National Laboratory – ElectroCat co-Lead

NREL — National Renewable Energy Laboratory

OAK RIDGE National Laboratory — Oak Ridge National Laboratory

- **Support of remaining FY2019 FOA and Lab Call project**
- **Collaborators not directly participating in ElectroCat** (no-cost)**:**

CRESCENDO — CRESCENDO, European fuel cell consortium focusing on PGM-free electrocatalysis – development and validation of PGM-free catalyst test protocols

PEGASUS PGM Free Catalyst — PEGASUS, European fuel cell consortium targeting PGM-free fuel cells – development and validation of PGM-free catalyst test protocols

IFC Israeli Fuel Cell Consortium — Israeli Fuel Cell Consortium (IFCC) – PGM-free activity indicators and durability

Bar-Ilan University — Bar-Ilan University, Israel – aerogels-based catalysts with high active-site density

University at Buffalo — University at Buffalo (SUNY), Buffalo, New York – novel PGM-free catalyst synthesis (independent of two ElectroCat projects involving UB)

PAJARITO POWDER — Pajarito Powder, Albuquerque, New Mexico – catalyst scale-up, PGM-free electrode design, catalyst commercialization (independent of ElectroCat project)

University of Warsaw — University of Warsaw, Poland – role of graphite in PGM-free catalyst design

Washington State University — Washington State University – electrocatalyst for low-temperature electrolyzer anode

Response to 2021 Reviewers Comments

- *"Validation of DFT predictions with experimental data is limited. The fact that there are some experimental motivations is understood, but the results need to come back to these to demonstrate causality."*

Models of idealized sites continue to produce testable hypothesis, but the heterogeneous and dynamic nature of real materials often makes testing these difficult experimentally. **These are not single-structure materials and they do evolve in time.** Qualitative trends from computational descriptors have been confirmed experimentally (dependence of metal stability on pH, metal stability in certain potential ranges at low pH, and identification of spectroscopic signatures, to name a few). In FY22, we have aimed to improve the predictive value of models to experimental efforts. LANL modeling and ORNL microscopy have collaborated to determine how TEM could aid in understanding C/N stability against corrosion for directly observed Fe-N sites. ANL/NREL models of active sites have aided in identifying likely structures for given sites/ligation state as a function of potential as measured with X-ray spectroscopy. These steps move us closer to understanding what structures are present in real materials and thus linking synthesis conditions to these structures, though this connection needs to be further strengthened. Our machine learning efforts have focused on optimizing performance, but we hope to extend to causational relationships based on active site structures. This is a significant effort, however, and will not be possible in the near term without a significant increase in funding for combined modeling and experimental efforts to this end. Furthermore, we would highlight that modeling efforts have directly aided experimental work through "asking better questions" and targeting particular, specific questions that can be motivated by DFT findings. In particular, the existence and suggestion of possible chemistry of axial 5th ligands and their effect on activity, stability, and spectroscopy originally came from fundamentally motivated DFT calculations.

Reviewers' Comments from 2021 Annual Merit Review

- *Significant progress has been made in PEMFC development, but there are weaknesses that need to be addressed—particularly, performance of the catalyst in the electrolyzer setting. The cell voltage of 2.0 V at 600 mA/cm2 is too high. Much more focus should be put on the study conditions for the electrolyzer performance if the project is ever going to achieve a goal of an 80,000-hour lifetime. An early understanding of the fundamental mechanisms associated with the IrO2 anode's operation in the electrolyzer should be used to guide the catalyst development.*

ElectroCat 2.0 is solely focused on electrocatalyst development and implementation. The study of conditions and the understanding of IrO_2 anode operation in acidic electrolyte is one of the focuses of H2NEW. The study and understanding of IrO_2 and other catalysts in the alkaline environment is part of the HydroGEN effort. We are collaborating with H2NEW and HydroGEN and building on the learnings in these two consortia to guide the development of PGM-free OER catalysts for anion-exchange membrane water electrolyzers.

Remaining Challenges and Barriers

- **Fuel Cell**
  - ✓ Further identifying the source of the durability of the active sites in stable catalysts, such as the ‘dual zone’ catalyst.
  - ✓ Increasing the density of stable active sites and oxygen reduction reaction turnover frequency (TOF) to meet DOE H_2-air performance targets
  - ✓ Reducing cathode proton resistance while maintaining high oxygen permeability
- **Low Temperature Electrolysis**
  - ✓ Increasing performance of electrolyzer operating with PGM-free anode and cathode catalysts performance, to the level demonstrated with PGM electrodes
  - ✓ Improving durability of alkaline membrane electrolyzer operating on pure water and at temperatures of ≥ 60 °C
  - ✓ Minimizing degradation of anion-exchange ionomers
  - ✓ Understanding key factors determining performance and durability of PGM-free catalysts in AEM electrolyzers

Proposed Future Work

- **ElectroCat Development**
  - ✓ Expand capabilities of to include methods developed specifically for OER catalyst development, evaluation, and implementation
- **Improvement in Performance and Durability of Fuel Cell Catalysts and Electrodes**
  - ✓ Further identify primary factors governing the durability of PGM-free catalysts and electrodes and continue to develop means to prevent performance degradation
  - ✓ Advance performance of catalysts by maximizing volumetric density and accessibility of active sites, through alternative synthetic methods, in particular:
    - Synthesize catalysts with high density of active sites using novel Fe precursors and “protect” these active sites with various coating methods
  - ✓ Optimize the fuel cell performance of the Fe_2O_3 (N-C) catalyst (from high-throughput System 4) by subjecting it to high-throughput ink optimization, cell testing, and associated ink characterization and cell diagnostics
  - ✓ Complete characterization of ‘dual-zone’ catalyst to determine source of promising durability and develop method to increase activity
- **Electrolyzer Catalysts and Electrodes**
  - ✓ Evaluate performance of multi-metallic MOF-derived OER catalyst in MEAs
  - ✓ Synthesize perovskite-based nanoparticle catalysts and Ni-based catalysts with hierarchical porosity
  - ✓ Explore high surface-area OER catalyst supports derived from aerogels
  - ✓ Introduce atomic-scale modeling into catalyst development and kinetic/transport modeling into electrode development
  - ✓ Identify and quantify products of anode degradation

Accomplishments and Progress

- **ElectroCat Development and Communication**
  - ✓ Consortium-wide in-person meeting held on April 5 - 6, 2022
  - ✓ 9 papers published, including one in *Nature Catalysis* on PGM-free PEFC cathode catalyst test protocols
  - ✓ Developed automated spectroscopy to rapidly scan dozens of atomically-dispersed transition metal sites
  - ✓ Developed density functional theory calculations to identify Fe-N-C species in spectroscopic experiments
  - ✓ Developed and implemented adaptive learning design loop with uncertainty quantification to model and guide high-throughput synthesis
- **Progress in Performance and Performance Durability of PGM-free ORR Catalysts**
  - ✓ ElectroCat FY22 Annual Milestone of PGM-free cathode MEA performance and durability of 75 mA cm^{-2} at 0.80 V and ≤ 50 mV voltage loss at 0.80 A cm^{-2} after 30,000 catalyst AST cycles exceeded: 79 mA cm^{-2} and 45 mV loss at 0.8 A cm^{-2}
  - ✓ MEA H_2-air current density at 0.675 V increased by 12% (340 mA cm^{-2} to 381 mA cm^{-2})
  - ✓ Synthesized 106 unique catalysts using high-throughput approach, with 70% enhancement in ORR activity versus highest ORR activity reported in 2021 AMR
- **Progress in PGM-free OER Catalysts**
  - ✓ FY22 Go/No-Go OER activity of ≤ 1.6 V *vs.* RHE (*iR*-free) at 10 mA cm^{-2} exceeded with several aerogel-derived mixed NiFe oxide catalysts
  - ✓ FY22 OER Annual Milestone of 10 mA cm^{-2} at ≤ 1.55 V and ≤ 1 mV/h potential loss during 48 h durability test exceeded with 10 mA cm^{-2} at 1.51 V and 0.74 mV/h in 54 h test with aerogel-derived NiFe oxide catalysts
  - ✓ FY22 Q1 Go/No-Go of OER potential ≤ 1.6 V *vs.* RHE (*iR*-free) at 10 mA cm^{-2} at beginning of test in aqueous alkaline electrolyte and ≤1 mV/h potential loss during 48 h at 10 mA cm^{-2} exceeded with 1.57 V and decrease in OER potential over 48 h test with multi-metallic MOF-derived oxide catalyst

Co-Authors

PGM-free catalyst development, electrochemical and fuel cell testing, atomic-scale modeling, machine learning

Piotr Zelenay (PI), Towfiq Ahmad, Bianca Ceballos, Hasnain Hafiz, Yanghua He, Edward (Ted) Holby, Wilton Kort-Kamp, Luigi Osmieri, John Weiss, Hanguang Zhang

High-throughput techniques, mesoscale models, X-ray studies, aqueous stability studies

Debbie Myers (PI), Magali Ferrandon, Jaehyung Park, Xiaoping Wang, Nancy Kariuki, A. Jeremy Kropf, Cong Liu, Prajay Patel

High fidelity modeling, electrode design and performance evaluation

Derek Vigil-Fowler (PI), Jacob Clary, K. C. Neyerlin

Advanced electron microscopy, atomic-level characterization, XPS studies

Dave Cullen (PI), Shawn Reeves, Alexey Serov, Haoran Yu, Michael Zachman

Technical Back-Up Slides and Additional Information

ElectroCat Status: PGM-free Catalysts in H_2-Air Fuel Cells

Catalyst	H_2-air fuel cell					
	Initial			After 30k cycles[1]		
	i (mA/cm^2)		V (V)	i (mA/cm^2)		V (V)
	0.8 V	0.675 V	0.8 A cm^{-2}	0.8 V	0.675 V	0.8 A cm^{-2}
ANL Fe (N-C) 2021 AMR	55	340	0.56	9	122	0.44
ANL Fe (N-C) 2022 AMR (ML #9)	85	379	0.53	13	122	-
LANL 'Dual-Zone' Fe-N-C 2021 AMR[3]	31	181	0.32	24	170	0.32
LANL H_2-synthesized "Dual-Zone" Fe-N-C	79	381	0.55	33	185	0.50
LANL (AD)$Fe_{1.5}$-N-C	37	211	0.44	3	47	0.28
LANL CM-PANI-Fe-C(Zn)[2,4]	105	440	~ 0.47	*not cycled*		

[1] AST cycles in air (0.2 bar partial pressure of O_2), voltage range from 0.6 V to OCV-0.01 V; [2] Non-differential conditions; [3] After 80k AST cycles; [4] No AST cycling performed.

H_2-treated 'Dual-Zone' Catalyst

Cathode: *ca.* 4.0 mg cm^{-2}, H_2-treated 'dual-zone' Fe-N-C catalyst, 1700 sccm, 1.0 bar air partial pressure, 100% RH; **Anode:** 0.3 mg_{Pt} cm^{-2} Pt/C, H_2, 700 sccm, 1.0 bar H_2 partial pressure, 100% RH; **Membrane:** Nafion® 211; **Cell:** differential, 5 cm^2, **Temperature:** 80 °C. **Durability Testing:** square-wave cycle from (OCV-0.01) V to 0.60 V

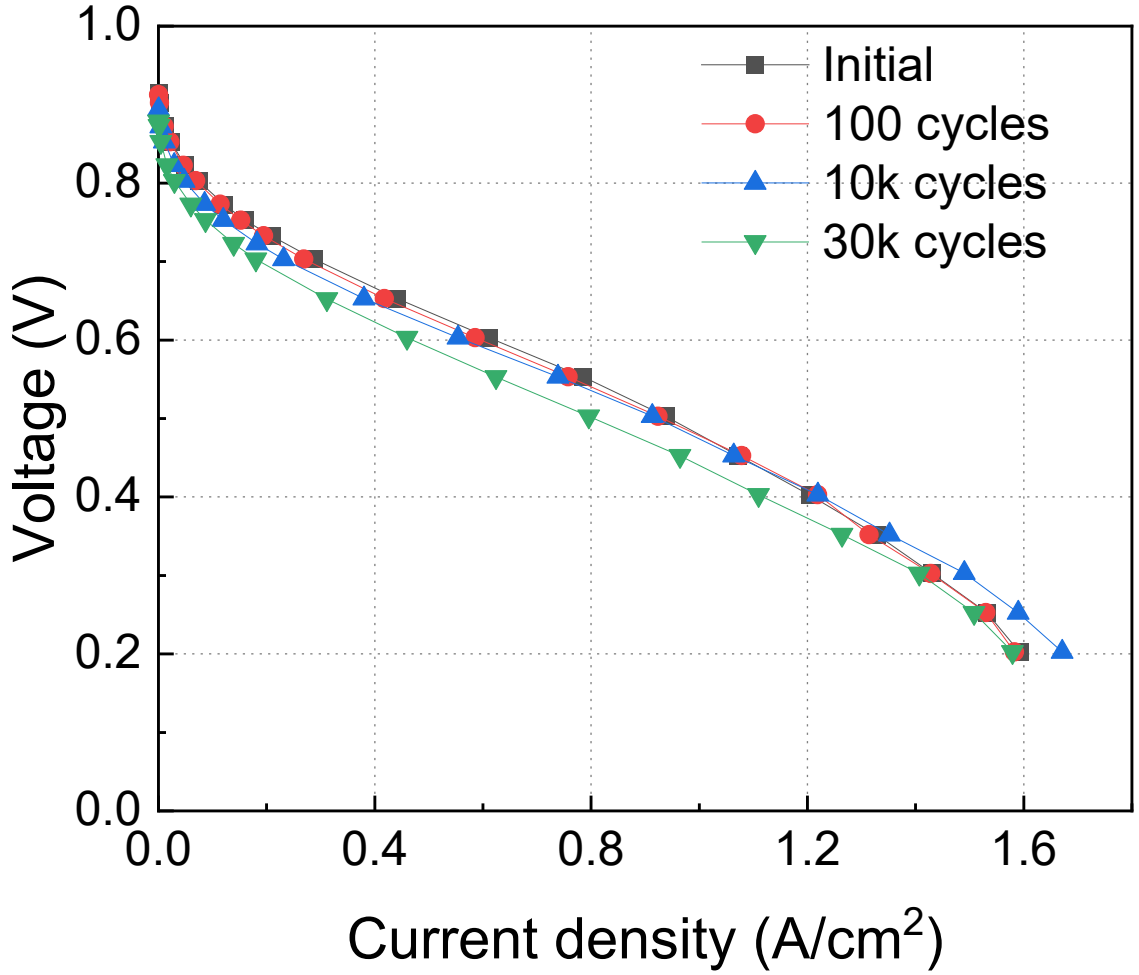

Number of cycles	Current density at 0.80 V (mA/cm^2)	Voltage at 0.80 A/cm^2 (V)
Initial	**79**	**0.547**
100 cycles	73	0.540
10k cycles	51	0.535
30k cycles	**33**	**0.502**

- 35% loss of initial performance at 0.80 V and 12 mV loss at 0.80 A/cm^2 after 10k cycles
- 58% loss of initial performance at 0.80 V and 45 mV loss at 0.80 A/cm^2 after 30k cycles

Novel Synthesis Approaches: Electrospinning Synthesis of Fe-N-C Catalysts

MOF-derived Fe-N-C catalysts

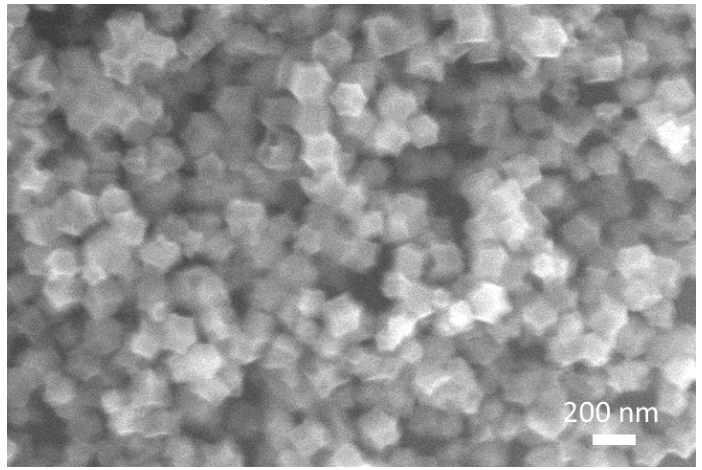

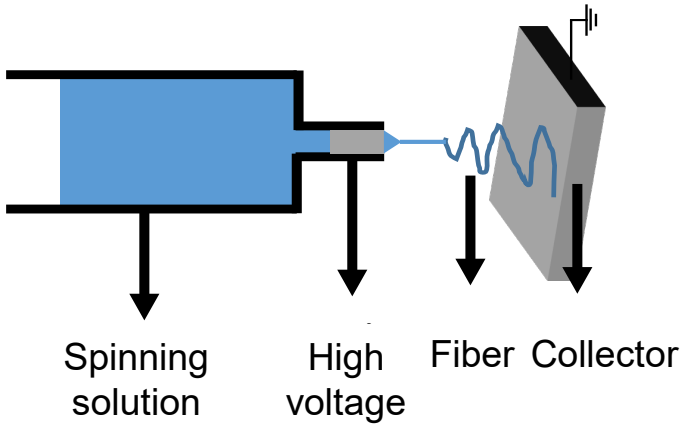

Highly porous fibrous morphology of Fe-N-C catalysts via electrospinning synthesis

Fibrous morphology of MOF-derived Fe-N-C catalysts via electrospinning

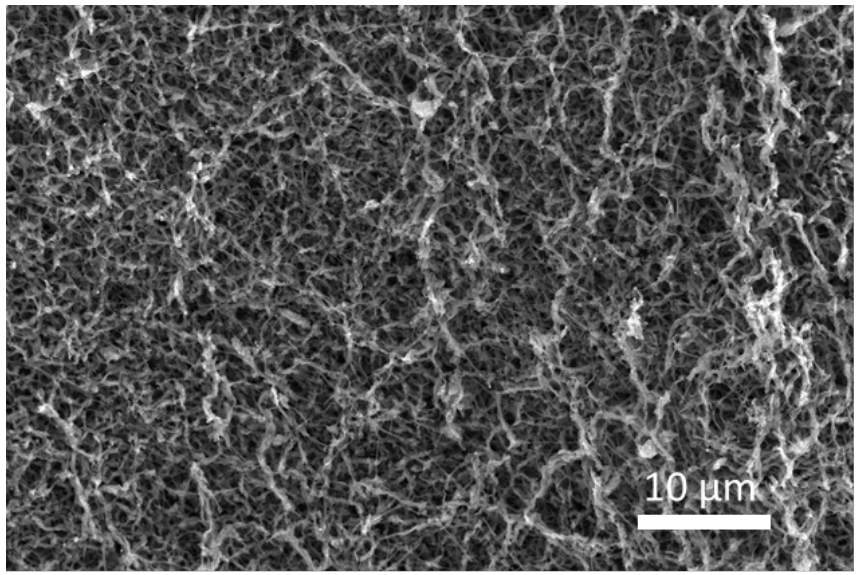

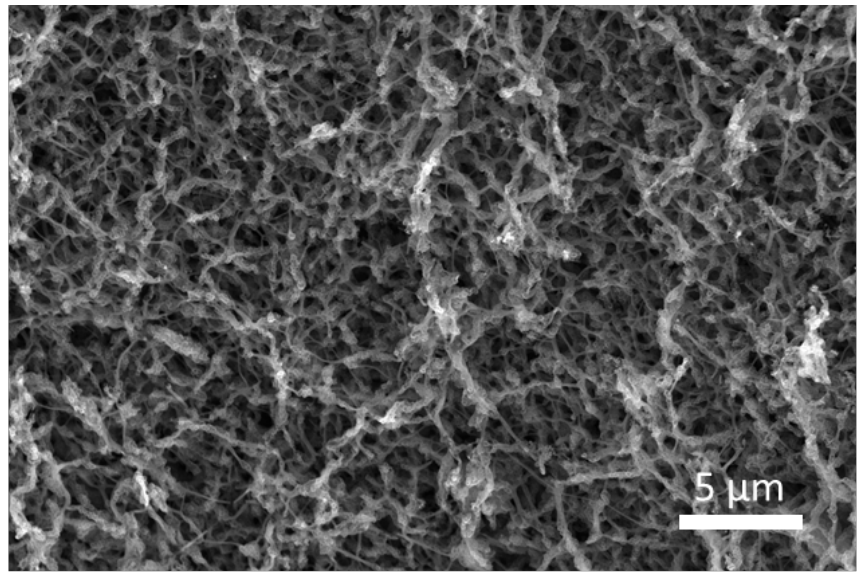

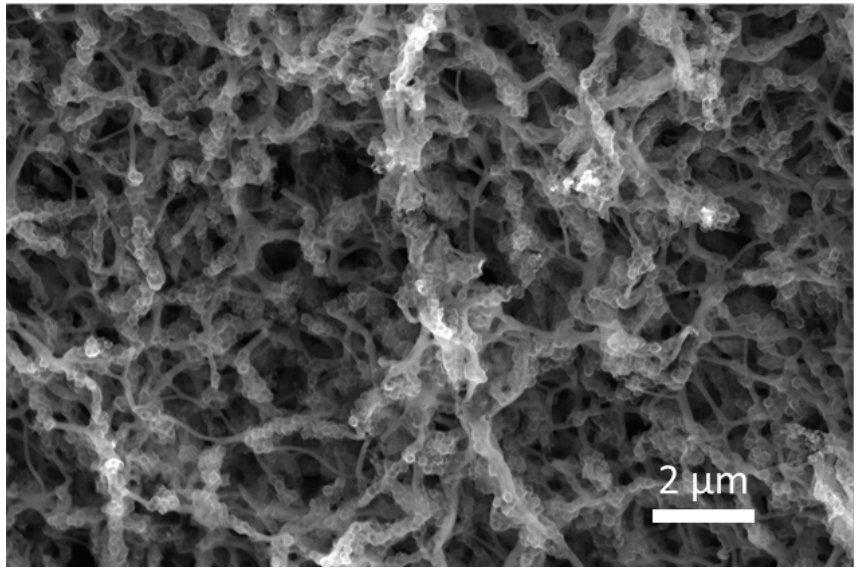

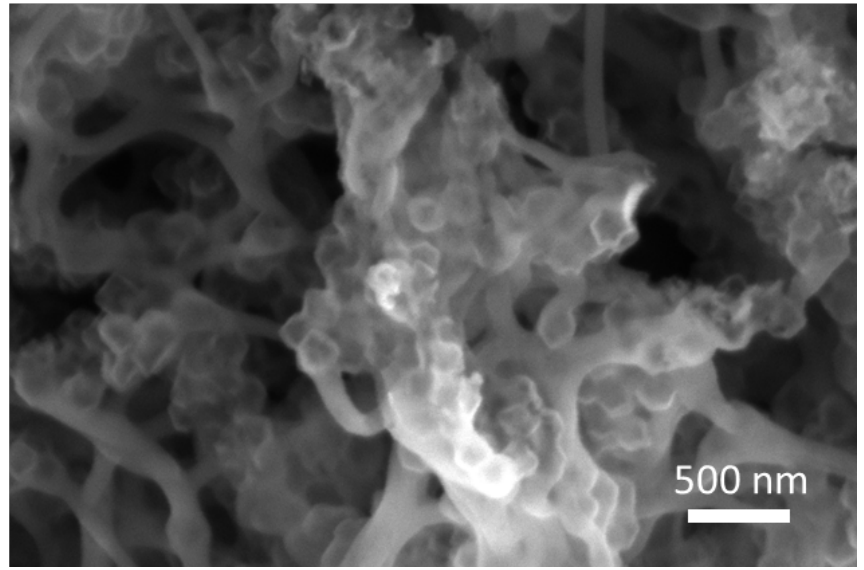

Thioacetamide (H_3CCSNH_2) Probe Poisoning of 'Single Zone' *vs.* 'Dual Zone' Catalysts

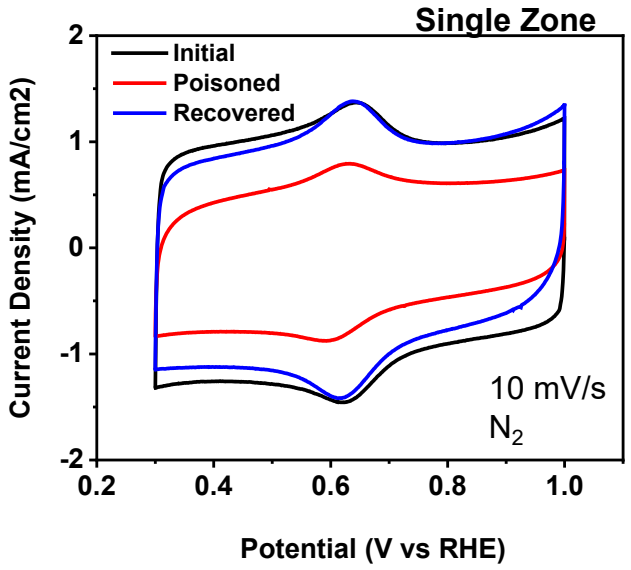

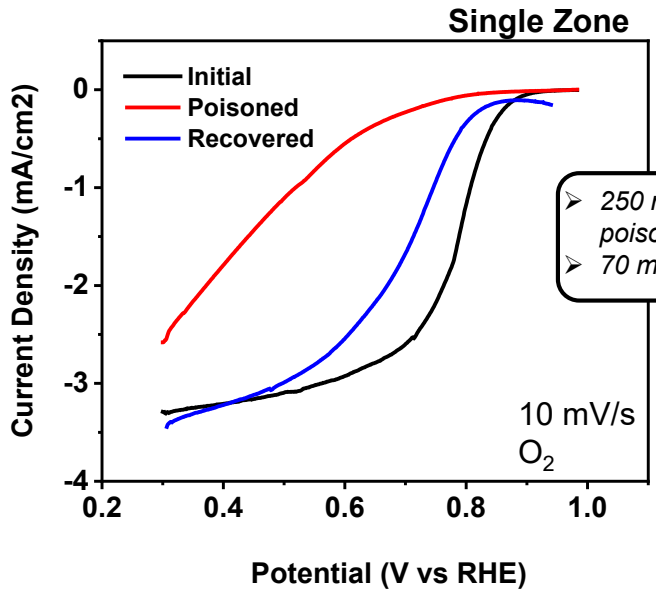

- *250 mV shift after poisoning*
- *70 mV unrecovered*

Ink preparation: 5 mg catalyst, 500 µL IPA, 20 µl 1-5 wt% Disp 30 **Catalyst Loading:** 0.6 mg cm^{-2} **Electrochemical Conditions:** 0.5 M H_2SO_4, 1600 rpm, O_2 **Poisoning:** 1. wash electrode in water, 10 min, 300 rpm 2. soak electrode in 0.25 M H_2SO_4, 0.01 M TAA overnight 3. wash electrode in water, 10 min, 300 rpm **Cycling:** 0.6 V to -0.3 V vs RHE at 10 mV/s, under N_2 (6 total cycles)

Single Zone	$E_{1/2}$ (V *vs.* RHE)
Initial	0.79
Poisoned	0.54
Recovered	0.72

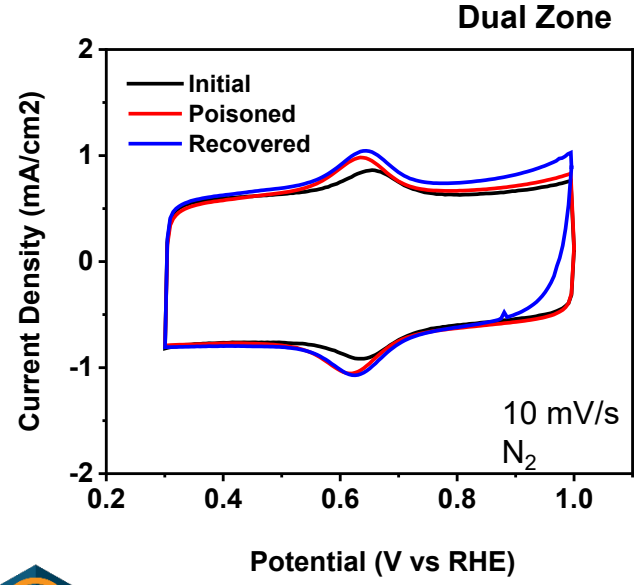

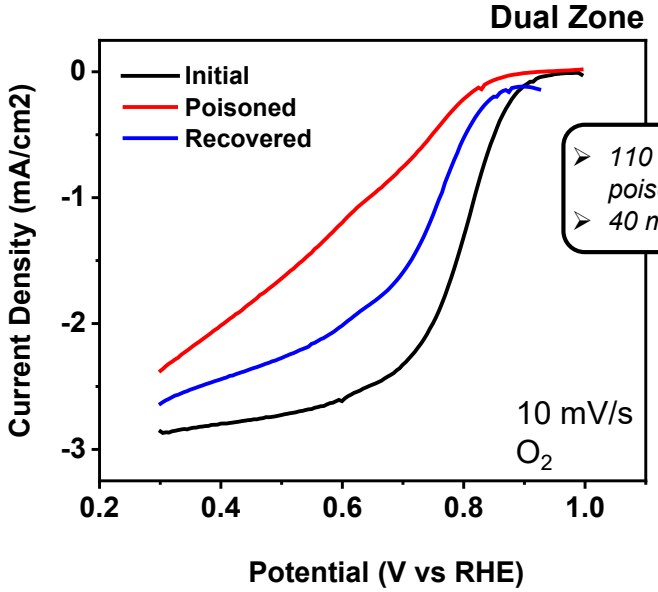

- *110 mV shift after poisoning*
- *40 mV unrecovered*

Dual Zone	$E_{1/2}$ (V *vs.* RHE)
Initial	0.80
Poisoned	0.69
Recovered	0.76

- ORR activity of both catalysts decreases after treatment with thiol-probe
- 'Single zone' catalyst has stronger interaction with thiol-probe than 'dual zone' catalyst'
- **Highlight:** Thiol probe remains strongly bound to active sites after recovery cycling; remaining blocked active sites account for ca 90% ORR activity

Thioacetamide (H_3CCSNH_2) Probe Poisoning of 'Single Zone' *vs.* 'Dual Zone' Catalysts

Angelica Benavidez

CENTER FOR MICRO-ENGINEERED MATERIALS

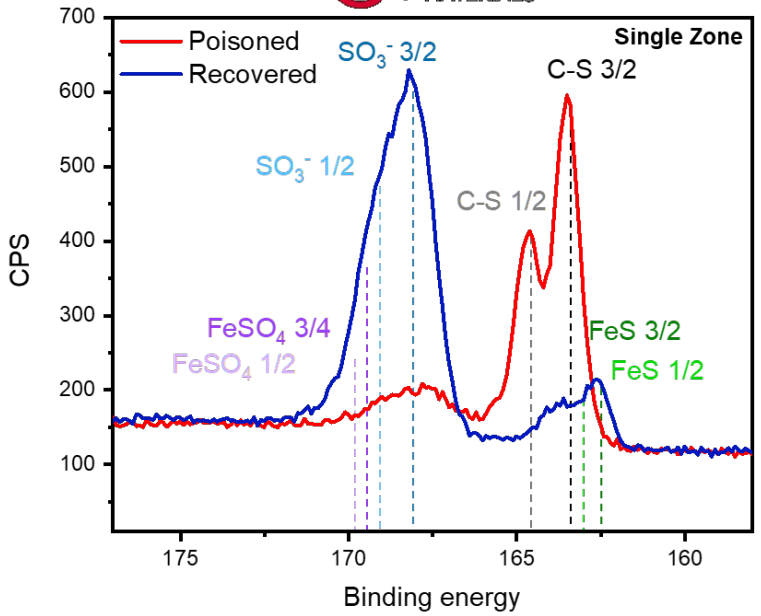

Proposed surface interactions:

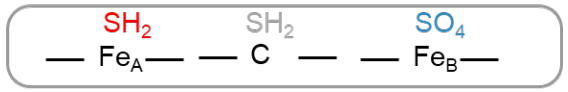

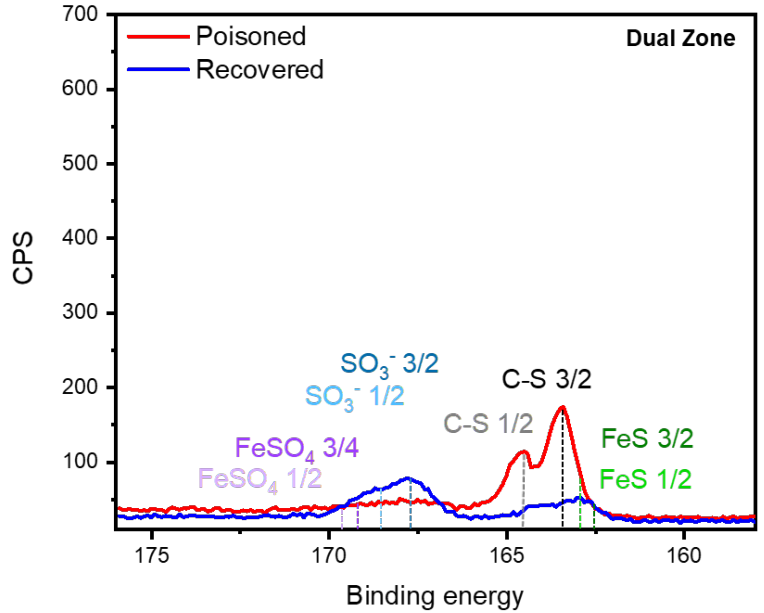

Proposed surface interactions:

'Single zone' catalyst:

- *Recovered ORR activity correlates with loss of probe at carbon (C) sites*
- *Fe sites have a strong interaction with the S-probe (no probe loss at Fe, increase at FeS)*

'Dual zone' catalyst:

- *Recovered ORR activity correlates with loss of probe at C and Fe sites*
- *Fe sites are a mixture sites with varying strength of interaction with the S-probe*

- Recovered sites at "single ' and 'dual zone' catalysts correlate well with the loss of C-S interactions; remaining poisoned sites at both catalysts are Fe-containing
- Both catalysts have Fe-sites that interact differently with the thiol probe; Fe sites in 'single zone' catalyst interact strongly with the S-probe; 'dual zone' catalyst contains one Fe site (Fe_A) that binds strongly and a second site (Fe_c) that can be recovered via stripping; both catalysts have Fe sites (Fe_B) that do not interact with the thiol probe
- **Conclusion:** Thioacetamide is not site specific; Fe-containing sites are likely responsible for observed high ORR activity of both catalysts

Performance in AEMWE – Effect of PTL

- **Sintered Ti: thickness ~275 µm, less porous**
- **Ni foam: thickness ~290 µm, highly porous**

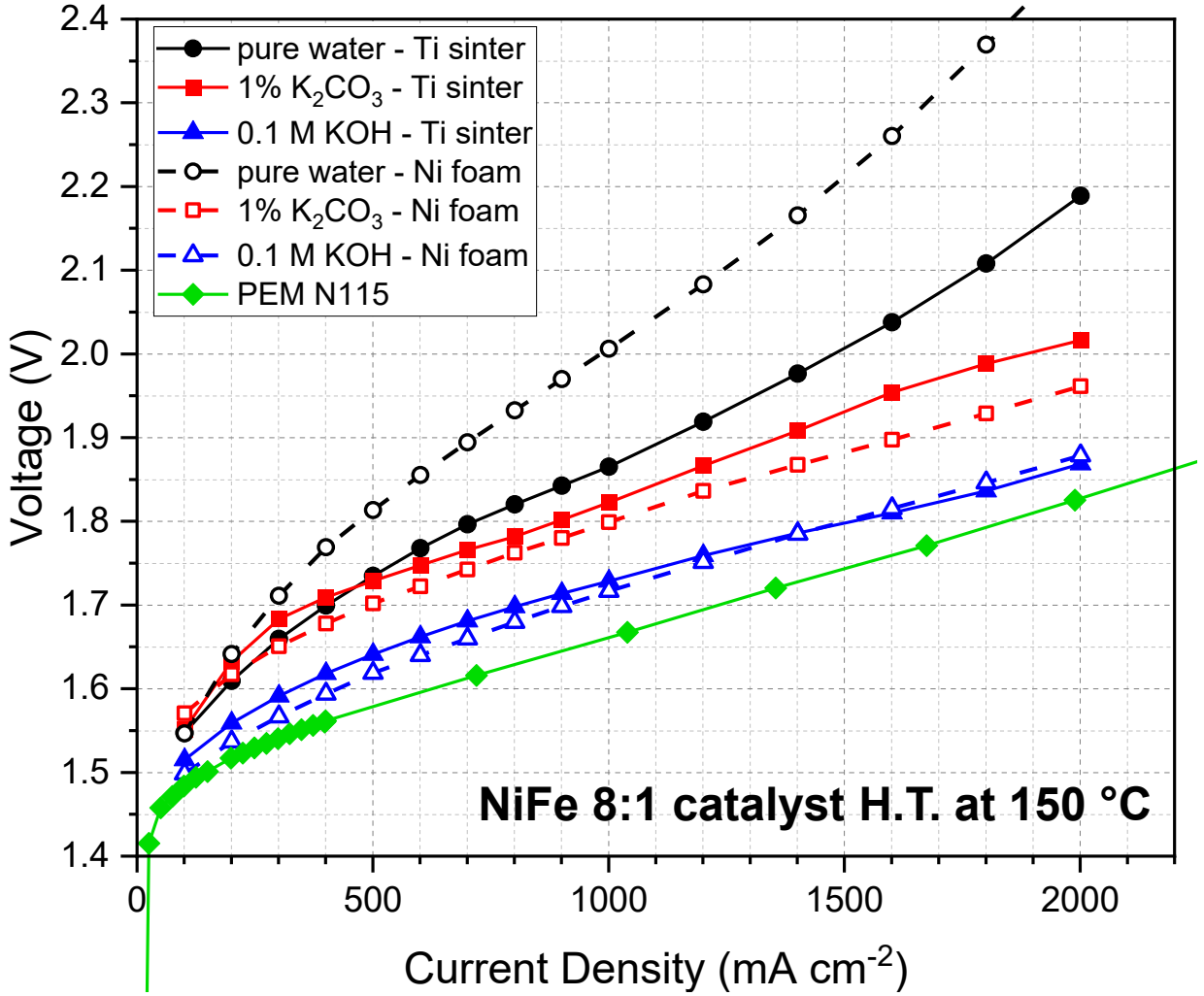

With 0.1 M KOH, only ~50 mV gap vs. PEM (N115) at 2 A cm^{-2}

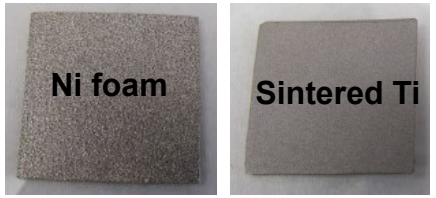

- **Sintered Ti PTL is better in pure water.**
- **Ni Foam is slightly better with supporting electrolyte** (Ni may be oxidized to NiOOH and doped with some Fe, contributing to OER as well).

- In pure water OH^- ion transport in the CL depends on the catalyst-ionomer interface.
- Distribution of catalyst + ionomer on the PTL may also play an important role.

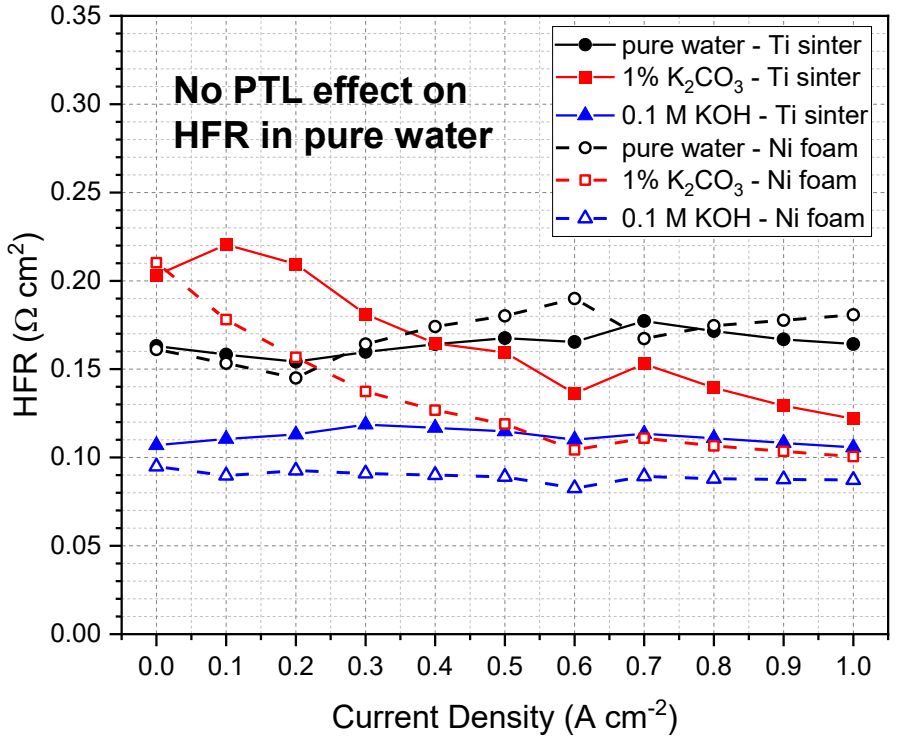

Catalyst Characterization Before and After Testing

EDS mapping: uniform distribution of Fe on the Ni oxide matrix.

NiFe 8:1 aerogel precursor

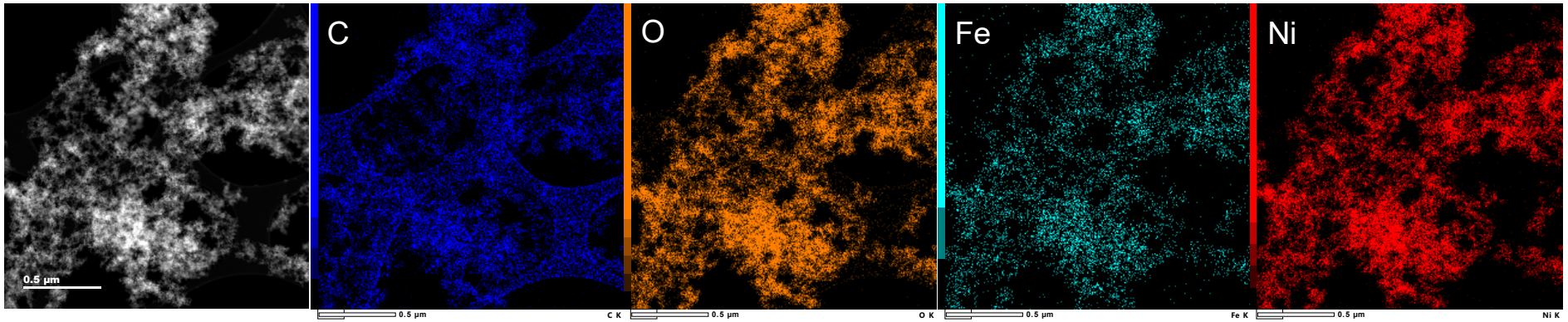

Catalyst heat treated at 150 °C in air before testing

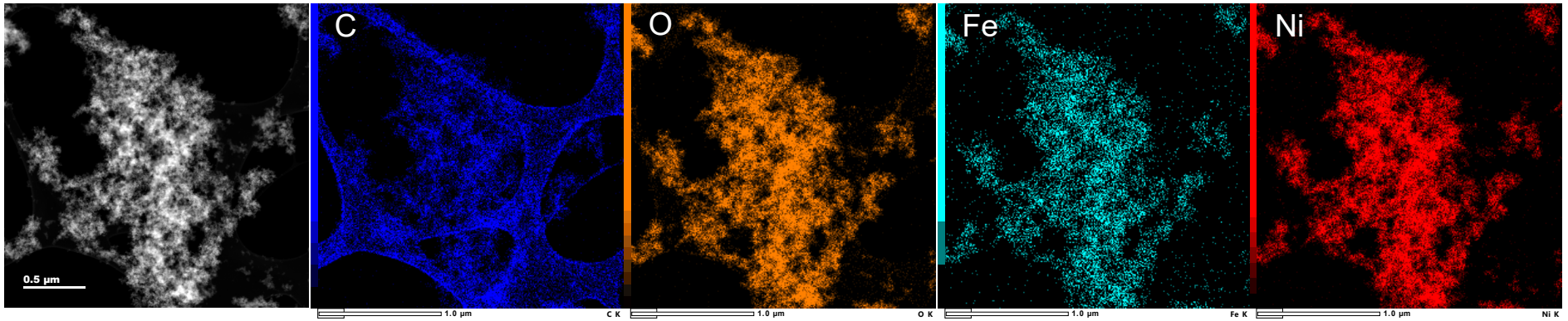

Catalyst heat treated at 150 °C in air after testing (on electrode)

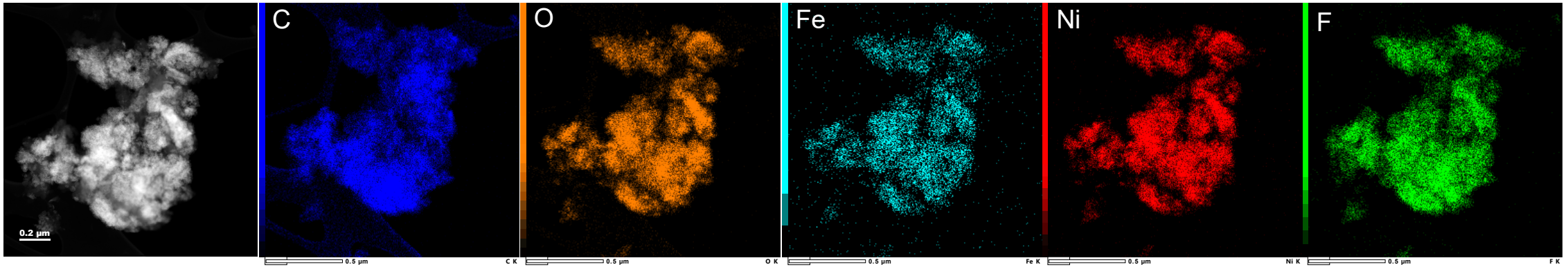

F is detected because catalyst after testing is mixed with AEM ionomer and binder

FY21 LTE Annual Milestone: Summary

WSU NiFe Oxide Catalyst

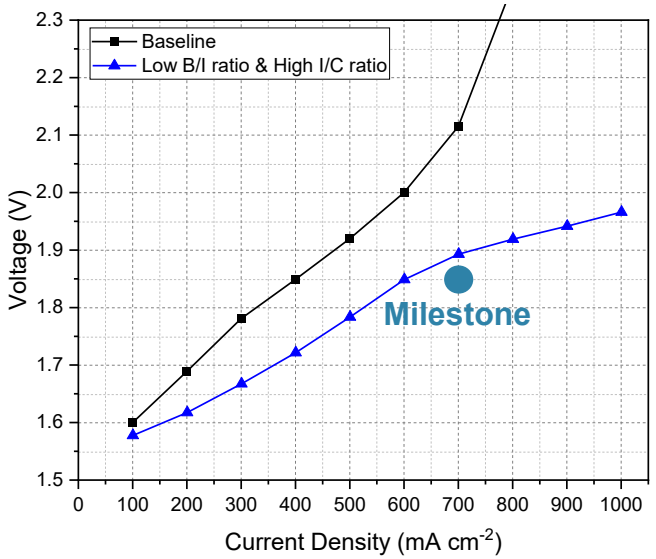

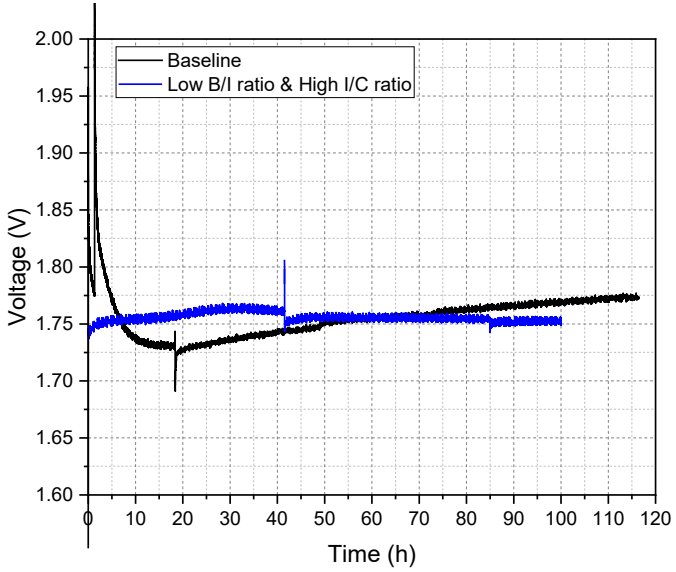

LANL-Pajarito Powder $La_xSr_{1-x}CoO_{3-\delta}$ (LSC) OER49B Catalyst

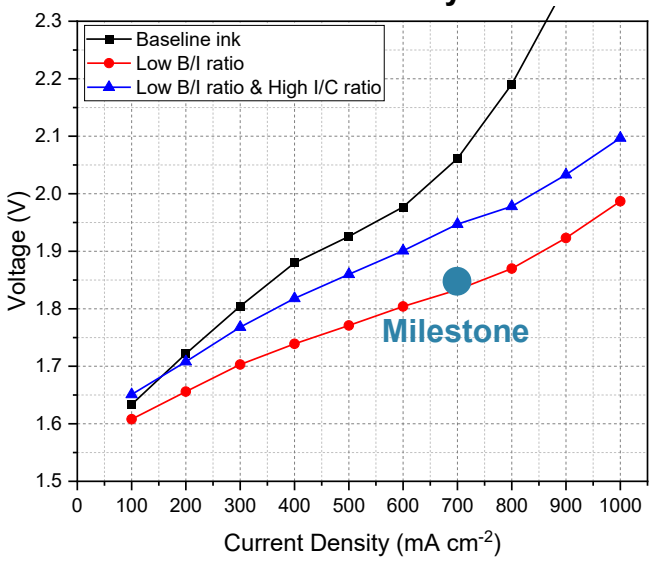

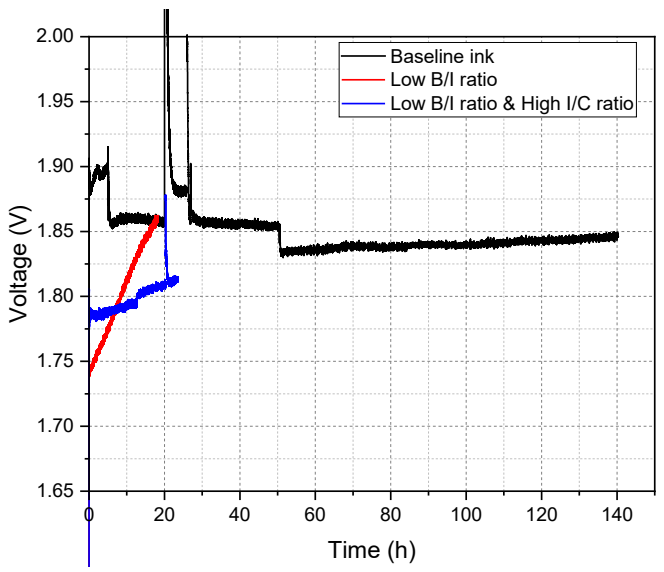

GDE fabrication method: Anode: ~3.5 mg cm^{-2} PGM-free catalyst, spray-coating onto sintered Ti PTL; **Cathode**: Pt 40% Ru 20% on C, ca. 1 mg_{Pt}/cm^2, spray-coating onto MGL370 GDL; **Cell:** 5 cm^2 electrode area; **Membrane:** Versogen Piper-Ion (40 μm); **Temperature:** 80 °C

B/I = binder-to-ionomer ratio
I/C = ionomer-to-catalyst ratio

- WSU NiFe oxide catalyst activity only *ca.* 40 mV away from the activity milestone in the anode with optimized ink; the catalyst **meets durability target of FY21 annual milestone** with both ink formulations over > 100 h testing
- LSC OER49B catalyst **meets activity target of FY21 milestone** with low B/I ratio ink and **durability target of the milestone** with baseline ink

Publications (since 2021 AMR presentation submission)

1. "Standardized protocols for evaluating durability and performance of platinum group metal-free oxygen reduction reaction electrocatalysts in polymer electrolyte fuel cells;" H. Zhang, L. Osmieri, J. H. Park, H. T. Chung, D. A. Cullen, K. C. Neyerlin, D. J. Myers, and P. Zelenay, *Nat. Catal.*, https://doi.org/10.1038/s41929-022-00778-3 (2022).
2. "Quantifying the electrochemical active site density of precious metal-free catalysts in situ in fuel cells;" R. Z. Snitkoff, A. Friedman, Y. Yurko, A. Kozhushner, M. J. Zachman, P. Zelenay, A. M. Bond, and L. Elbaz, *Nat. Catal.*, **5**, 163-170 (2022).
3. "Electrocatalysis in Alkaline Media and Alkaline Membrane-Based Energy Technologies;" Y. Yang, C. R. Peltier, R. Zeng, R. Schimmenti, Q. Li, Xin Huang, Z. Yan, G. Potsi, R. Selhorst, X. Lu, W. Xu, M. Tader, A. V. Soudackov, Ha. Zhang, M. Krumov, E. Murray, P. Xu, J. Hitt, L. Xu, H.-Y. Ko, B. G. Ernst, C. Bundschu, A. Luo, D. Markovich, M. Hu, C. He, H. Wang, J. Fang, R. A. DiStasio Jr., L. F. Kourkoutis, A. Singer, K. J. T. Noonan, L. Xiao, L. Zhuang, B. S. Pivovar, P. Zelenay, E. Herrero, J. M. Feliu, J. Suntivich, E. P. Giannelis, S. Hammes-Schiffer, T. Arias, M. Mavrikakis, T. E. Mallouk, J. D. Brock, D. A. Muller, F. J. DiSalvo, G. W. Coates, and H D. Abruña, *Chem. Rev.*, **122**, 6117-6321 (2022).
4. "Mesoporous textured Fe-NC electrocatalysts as highly efficient cathodes for proton exchange membrane fuel cells;" S. Akula, M. Mooste, B. Zulevi, S. McKinney, A. Kikas, H.-M. Piirsoo, M. Rähn, A. Tamm, V. Kisand, A. Serov, E.B Creel, D. A. Cullen, K. C. Neyerlin, H. Wang, M. Odgaard, T. Reshetenko, and K. Tammeveski, *J. Power Sources* **520**, 230819 (2022).
5. "Elucidating fuel cell catalyst degradation mechanisms by identical-location transmission electron microscopy;" H. Yu, M. Zachman, D. Myers, R. Mukundan, H. Zhang, P. Zelenay, K. Neyerlin, and D. Cullen, *Microsc. Microanal.*, **27**, 974-976 (2021).
6. "Effects of Ink Formulation on the Structure and Performance of PGM-Free Catalyst Layer in PEMFCs;" C. Li, L. Shengwen, Y. Zeng, Y. Liu, G. Wu, D.A. Cullen, and J. Xie, *ECS Trans.,* **104**, 327, (2021).
7. "Single Atomic Iron Site Catalysts via Benign Aqueous Synthesis for Durability Improvement in Proton Exchange Membrane Fuels Cells;" M. Chen, D.A. Cullen, S. Karakalos, X. Lu, J. Cui, K. Jeremy, H. Mistry, K. He, D.J. Myers, and G. Wu, *J. Electrochem. Soc.*, **168**, 044501 (2021).

Publications II & Patent Application (since 2021 AMR presentation submission)

8. “Chemical vapour deposition of Fe–N–C oxygen reduction catalysts with full utilization of dense Fe–N4 sites;” L. Jiao, J. Li, L. LaRochelle Richard, Q. Sun, T. Stracensky, E. Liu, M. Tahar Sougrati, Z. Zhao, F. Yang, S. Zhong, H. Xu, S. Mukerjee, Y. Huang, D. A. Cullen, J. H. Park, M. Ferrandon, D. J. Myers, F. Jaouen, and Q. Jia. *Nat. Mater.,* **20**, 1385-1391 (2021).
9. “Promoting Atomically Dispersed MnN4 Sites via Sulfur Doping for Oxygen Reduction: Unveiling Intrinsic Activity and Degradation in Fuel Cells;” L. Guo, S. Hwang, B. Li, F. Yang, M. Wang, M. Chen, X. Yang, S. G. Karakalos, D. A. Cullen, Z. Feng, G. Wang, G. Wu, and H. Xu, *ACS Nano*, **15**, 6886-6899 (2021).

Patent Application

1. B.-Z. Zhan, Z. He, H. T. Chung, P. Zelenay; “Metal nanoparticle-deposited, nitrogen-doped carbon adsorbents for removal sulfur impurities in fuels;” Application No. 17/533,838; Pub. No. US 2022/0080382 A1; Pub. Date March 17, 2022.

Presentations (since 2021 AMR presentation submission)

1. SUNCAT Symposium, Stanford University, Virtual, March 16, 2022. Title: "In Search of the Active Site in Fe-N-C and Evolution of the Active Site in Pt alloy PEMFC Cathode Catalysts", D. Myers (**invited**).
2. 2021 MRM Materials Research Meeting, Virtual, December 15, 2021. Title: "Synchrotron X-ray Spectroscopy, Scattering, and Tomography of Proton Exchange Membrane Fuel Cell Catalysts and Electrodes" D. J. Myers, A. J. Kropf, E. C. Wegener, J. Wright, J. Park, N. N. Kariuki, C. F. Cetinbas, R. Ahluwalia (**invited**).
3. Materials Research Society Meeting, Virtual, December 7, 2021. Title: "Iron-based Proton Exchange Membrane Fuel Cell Cathode Catalysts," D. J. Myers, M. Ferrandon, J. H. Park, X. Wang, A. J. Kropf, and E. Wegener (**invited**).
4. 240th Meeting of the Electrochemical Society, Orlando, Florida, October 10-14, 2021 (held remotely, talk presented live). Title: "PGM-free Catalyst Durability: Evaluation, Validation, and Progress (summary of abstracts I01D-1022, I01D-1144 & I01D-1149);" P. Zelenay, H. Zhang, J. H. Park, and D. Myers (**invited**).
5. 240th Meeting of the Electrochemical Society, Orlando, Florida, October 10-14, 2021 (held remotely, talk presented live). Title: "Enhancements in PGM-free Catalyst Performance via High-Throughput Synthesis and Machine Learning (summary of abstracts I01D-1145 & I01D-1147);" D. Myers, T. Ahmed, and P. Zelenay (**invited**).
6. 240th Meeting of the Electrochemical Society, Orlando, Florida, October 10-14, 2021 (held remotely). Title: "Multi-Lab Round Robin Evaluation of PGM-Free Catalyst Durability;" J. H. Park, H. Zhang, L. Osmieri, H. T. Chung, D. A. Cullen, P. Zelenay, K. C. Neyerlin, and D. J. Myers.
7. 240th Meeting of the Electrochemical Society, Orlando, Florida, October 10-14, 2021 (remote). Title: "A Durable Platinum Group Metal-Free Oxygen Reduction Catalyst for Polymer Electrolyte Fuel Cells;" H. Zhang, H. T. Chung, U. Martinez, E. F. Holby, and P. Zelenay.
8. 240th Meeting of the Electrochemical Society, Orlando, Florida, October 10-14, 2021 (held remotely). Title: "Optimizing High-Throughput Synthesis of PGM-Free ORR Electrocatalyst Using Machine Learning Approach;" T. Ahmed, M. Karim, M. Ferrandon, E. F. Holby, D. J. Myers, and P. Zelenay.

Presentations (since 2021 AMR presentation submission)

9. 240th Meeting of the Electrochemical Society, Orlando, Florida, October 10-14, 2021 (held remotely). Title: “Standardized Protocols for Platinum Group Metal-Free Fuel Cell Catalysts for Oxygen Reduction Reaction;” P. Zelenay, H. Zhang, L. Osmieri, J. H. Park, A. A. Farghaly, H. T. Chung, D. A. Cullen, K. C. Neyerlin, and D. J. Myers.
10. 240th Meeting of the Electrochemical Society, Orlando, Florida, October 10-14, 2021 (held remotely). Title: “Identical Location Scanning Transmission Electron Microscopy Study of Fuel Cell Catalyst Degradation;” H. Yu, M. J. Zachman, D. J. Myers, R. Mukundan, H. Zhang, P. Zelenay, K. C. Neyerlin, and D. A. Cullen.
11. 240th Meeting of the Electrochemical Society, Orlando, Florida, October 10-14, 2021 (held remotely). Title: “Quantifying and Understanding PGM-Free ORR Active Sites by in Situ Molecular Probes;” B. M. Ceballos and P. Zelenay.
12. 240th Meeting of the Electrochemical Society, Orlando, Florida, October 10-14, 2021 (held remotely, talk presented live). Title: “ElectroCat 2.0: Accelerating PGM-Free Catalyst and Electrode Development;” D. Peterson, D. Papageorgopoulos, P. Zelenay, and D. J. Myers (**invited**).
13. XXVII Congresso Nationale della Società Chimica Italiana, September 14-23, 2021 (held remotely). Title: “Oxygen Reduction at Platinum Group Metal-Free Fuel Cell Catalysts: Recent Progress;” P. Zelenay (**invited keynote lecture**).
14. Microscopy & Microanalysis, August 2021. Title: “Atomic-scale Imaging of Intact PGM-free Catalyst Active Sites at 30 keV by 4D-STEM;” M. J. Zachman, C. O’Leary, D. Y. Chung, H. Hafiz, E. F. Holby, V. Stamenkovic, and D. A. Cullen.
15. 2021 World Fuel Cell Conference (WFCC2021), Waterloo, Ontario, Canada, August 16-20, 2021. Title: “Durability of PGM-Free ORR Catalysts: Recent Progress;” H. Zhang and P. Zelenay (**invited plenary lecture**).
16. PEGASUS Technical Workshop/Webinar, Platinum Group Metal-free Catalysts for Oxygen Reduction Reaction, June 14-15, 2021. Title: “ElectroCat: Recent Progress in PGM-free Electrocatalysis;” P. Zelenay (**invited**).
17. 239th Electrochemical Society Meeting, Honolulu, Hawaii, June 2, 2021 (held remotely, talk presented live), Title: “In Situ and Operando Synchrotron X-Ray Spectroscopy and Scattering Characterization of PEFC Cathode Catalysts”, D. Myers, A. J. Kropf, E. Wegener, and J. H. Park (**invited**).